Canadian Bathymetric Gap Analysis and the Comparison of Barometric Pressure Enhanced Predicted Tides to Ellipsoid Referenced Hydrographic Surveys

by

Andrew Richard Forbes

A thesis submitted in conformity with the requirements
for the degree of Master of Science

Department of Geography, Geomatics, and the Environment
University of Toronto

Canadian Bathymetric Gap Analysis and Comparison of Barometric Enhanced Predicted Tides to Ellipsoid Referenced Hydrographic Surveys

Andrew Richard Forbes

Master of Science

Department of Geography, Geomatics, and the Environment
University of Toronto

2023

Abstract

Highly accurate bathymetric models are paramount for building an understanding within many research fields including climate change, tsunamis and wave propagation, marine and benthic habitat management and marine navigation studies among others. Developing highly accurate bathymetric models begins with nations understanding their bathymetric holdings and identifying where gaps exist which will assist survey planning and policy making. This study investigates the extent of bathymetric coverage within Canada's Exclusive Economic Zone; additionally, to reduce the uncertainty in hydrographic surveys, this study investigates the influence of the inclusion ERA5 mean sea level pressure (barometric pressure) on harmonic analysis predicted tide for the vertical reduction of hydrographic surveys, comparing the results to ellipsoid referenced surveys to quantify the uncertainty. Using the Canadian Hydrographic Service's digital bathymetric data, we show that the bathymetry within Canada's exclusive economic zone is largely unknown with results indicating 84.89% (4,991,873 km^2) are void of soundings and 13.45% (790,690 km^2) have full bottom coverage. Implications for Lakebed 2030, which is concerned with the Great Lakes region, show 74.31% (67,482 km^2) are void of soundings and 14.16% (12,863 km^2) have full

bottom coverage. At a hydrographic surveying rate of 1.5% increase in seafloor coverage per year (74,873 km^2), Canada can achieve full bottom coverage within their exclusive economic zone by 2079; however, seafloor coverage acquired during Ocean's Protection Plan increased on average of 22,380 km^2 per year. Taking this rate of seafloor coverage change, Canada will obtain full seafloor coverage of their Exclusive Economic Zone by 2246. Furthermore, we show that applying barometric pressure data to predicted tide time-series has the potential to improve the vertical reduction and lower the uncertainty. This is especially significant ($p < 0.01$) in < 2 meter tidal areas. We show that in the Canadian Arctic where Global Navigation Satellite Systems (GNSS) are susceptible to signal drop out or degradation, the addition of barometric pressure to predicted tide will provide a slightly improved result then using predicted tide only; however, the results seem to be dependent on the geography of the area of study. This study developed a baseline for future seafloor coverage progress comparison, called the Canadian Bathymetric Gap Analysis epoch 2023 (CBGAe2023) and investigated a means to reduce the uncertainty in the vertical component of hydrographic survey solutions, thus increasing the safety to marine navigation.

Acknowledgments

I would like to thank my supervisor Dr. Laura Brown for her guidance during my Master's program at the University of Toronto Mississauga. Dr. Brown has provided me opportunities to expand my knowledge base and challenge me to expand my deep understanding of the topics covered within this thesis. I would also like to thank my wife, Michelle and kids Sloane and Xavier for continued support, encouragement and non-stop attention seeking anytime I sat down behind my computer to work.

Additionally I would like to thank Dana Gallant, Chris Marshall, Jason Bartlett, and John Mercuri of the Canadian Hydrographic Service for supporting my efforts throughout this process. Furthermore, I would like to thank the Canadian Hydrographic Service and Fisheries and Oceans Canada for providing access to data that was used in this study.

Table of Contents

Acknowledgments iv

Table of Contents v

List of Tables viii

List of Figures ix

List of Appendices xii

Chapter 1 General Introduction 13

1 General Introduction 13

1.1 Motivation 13

1.2 Significance 14

1.3 Literature Review 16

1.3.1 Bathymetric Gap Analysis 16

1.3.2 Data Management and Quality 20

1.3.3 Hydrographic Surveys Tidal Reduction 22

1.3.4 Meteorological and Oceanographic Variables of Concern 23

1.4 Objectives and Thesis Structure 27

1.5 References 29

Chapter 2 Canadian Bathymetric Gap Analysis 35

2 Canadian Bathymetric Gap Analysis 35

2.1 Introduction 35

2.1.1 The History and Development of Modern Bathymetric Measurements 36

2.2 Determination of International Seafloor Coverage Amount 37

2.2.1 GEBCO - Method and Results 38

2.2.2 National Oceanic and Atmospheric Administration - Method and Results 40

2.2.3 Instituto Hidrográfico – Method and Results 41

2.2.4 Goals of the Bathymetric Gap Analysis for the Canadian Hydrographic Service....41
2.3 Study Area....42
2.3.1 Coastline....42
2.3.2 Maritime Boundaries and Canada's Exclusive Economic Zone....42
2.3.3 Regional Boundaries....43
2.4 Data and Methodology....45
2.4.1 Canadian Hydrographic Service's Bathymetric Database....45
2.4.2 Terminology....52
2.4.3 Determination of Seafloor Coverage....53
2.5 Results and Discussion....61
2.5.1 Canada....61
2.5.2 Results for Lakebed 2030 Initiative....69
2.6 Conclusions....71
2.7 References....72
CHAPTER 3....82
3 Comparison of Barometric Pressure Enhanced Predicted Tides to Ellipsoid Referenced Hydrographic Surveys....82
3.1 Introduction....82
3.2 Materials and Methods....86
3.2.1 Study Areas....86
3.2.2 Data Sources....88
3.3 Methodology....95
3.4 Results and Discussion....98
3.4.1 Predicted Tides versus Barometric Pressure Enhanced Predicted Tides Time-series Comparison....98
3.4.2 Predicted Tide versus Barometric Pressure Enhanced Predicted Tide Hydrographic Survey Line Influence....100

3.4.3 Full Surface Comparisons 110
3.5 Conclusion 113
3.6 References 115
Chapter 4 122
4 Conclusions 122
4.1 References 124
Appendices 126
Appendix 1 – List of Acronyms 126

List of Tables

Table 1. Recommended depth range with associated grid-cell size resolution. 18

Table 2. Recommended depth range with associated grid-cell size resolution for the assessment of bathymetric gaps. 39

Table 3. Category of Zone of Confidence (CATZOC) 47

Table 4. A breakdown of all contributing data sources used in this analysis. 50

Table 5. Final Reclassify and classification terms 60

Table 6. CBGAe2023 results at both national and regional scales. 65

Table 7. Bathymetric Gap Analysis results for the Great Lakes (Canadian waters only). 70

Table 8. Study site in the Canadian Arctic and the associated spatial extents 87

Table 9. Tidal stations used in this study. The length of observations (in days) to generate the tidal constituents as well as the large tide range to indicate amplitude of the tide at the stations. 91

Table 10. ERA5 mean sea-level pressure data cell location, associated tidal station number and the max, min, mean and range of the barometric pressure over the course of hydrographic survey operations. 95

Table 11. Difference in the time series of the predicted tidal records before and after applying ERA5 mean sea level pressure corrections. The results compared to the Larger Large Tide derives the influence, as a percentage of the height of the Larger Large Tide for each station is calculated. 99

Table 12. Full surface comparisons and the resulting effect of applying ERA5 mean sea level pressure as the vertical reduction technique. 110

List of Figures

Figure 1. Visual depiction of the various regional boundaries as seen within the Canadian Hydrographic Service. 44

Figure 2. Multibeam survey conducted in 2009 classified as CATZOC B existing in the Canadian Hydrographic Service's Bathymetric Database shows large areas in which the bounding polygons misrepresent the data as the software at the time of loading the data into Bathymetric Database could not represent holes in the data. Area A, B, C and D, represent approximately 8000, 9600, 11100, 3700 km^2 respectively, which were not surveyed and are void of soundings, thus an approximate total of 32,400 km^2 of seafloor are misrepresented in CATZOC classification. 48

Figure 3. Random sample bounding polygon vs data. Area A represents 126 km^2. Area B represents 79 km^2. The survey data (Area C) represents 230 km^2. Total area of the bounding polygon is 435 km^2, therefore calculating statistics on the bounding polygon vs the data shows a 47% overestimation. 49

Figure 4. CHS Bathymetric Database displaying multiple data types and varying resolutions and or line spacing. The image on the left is a visualizing of the soundings with the Canadian Hydrographic Services. The image on the right is the classification of the resolution (indicated by RES) or line spacing (indicated by LS). 51

Figure 5. OAT layer conversion. The bin size of 10-meters showing the density of the actual sounding data points contained within (Left). This is converted to cell size based on resolution defined by the user and representative soundings are generated (Middle). Overall representative sounding density within a 100-meter cell for use in ArcGIS in downstream process (Right). 56

Figure 6. Examples of 100-meter resolution cells contain various degrees of coverage acquired from MLV sources. All cells will be considered 'Full Bottom Coverage" classification group 3.58

Figure 7. Pacific region raster where the grey raster is the classified as void of soundings, the green is classified as 300 (MLV) and the black is the data points from the OAT prior to clipping and reclassifying 59

Figure 8. Representative soundings and their associated classification based on sounding density within a 100-meter resolution cell. 60

Figure 9. Sample of the final symbolized raster. Dark purple is full bottom coverage. medium purple is moderate coverage, light purple is minimal coverage, grey is gaps - void of soundings, and white is no-data (i.e. land). 61

Figure 10. Visual representation of the Canadian Bathymetric Gap Analysis epoch 2023 (CBGAe2023). 62

Figure 11. Canada's marine transportation Low Impact Shipping Corridors (Source: (Chénier et al.,2017)) 63

Figure 12. Final CBGAe2023 results at both national and regional scales. Considerable amount of gaps are present in all regions, and are especially evident in the Canadian Arctic. 66

Figure 13. Pacific region bathymetric gap analysis results. Full bottom coverage is achieved in 15.00% and concentrated in the nearshore regions such as the Strait of Georgia, Queen Charlotte Sound and Hecate Strait. Many bathymetric gaps are present (82.55%) but are main offshore due to sparse soundings. 67

Figure 14. Overview of A) Quebec regional bathymetric gap analysis results B) Atlantic regional bathymetric gap analysis results. 68

Figure 15. Canadian Bathymetric Gap Analysis results for the Great Lakes Observing System's Lakebed 2030 initiative. 70

Figure 16. Survey site locations across the Canadian Arctic with the associated tidal zone. The primary tidal station for each zone is shown by the blue circled X. 87

Figure 17. Canadian Hydrographic Service CUBE processing workflow. 89

Figure 18. Site Z008-003 St. Roch and Rasmussen Basin. This figure shows the extent of the hydrographic survey, colour band indicating depth, as well as the location of all the tidal prediction station used for the zone definition file. The zone definition file is an average weighted mean of the predicted tide time-series based on distance between stations. 90

Figure 19. CANNORTHv1HyVSEP_ITRF08_CD. The colour scale depicts the separation between the International Terrestrial Reference Frame, epoch 2008 ellipsoid and chart datum in meters. 93

Figure 20. Time-series of Z008-007 (Paulatuk) showing the predicted tide (red) to the barometric pressure corrected predicted tide (blue) along with the residual (green). This record indicates good agreement in the first half of the record (101.430 kPa) and a gradual separation occurring during the second half as barometric pressure began to rise (101.880 kPa). 97

Figure 21. Single line investigation from post processed data. Two figures per section, where the bottom figure is the variable signature over the time series of a specific survey line and the top figure is the examined timescale defined by the highlighted yellow box in the bottom box. (A) Heave signature of the vessel, (B) The GPS Tide height referenced to the ellipsoid, (C) GPS Tide solution - post processing using CANNORTH2016v1HyVSEP_ITRF_CD model corrects the GPS Tide height in relation to CD(note the heave signature is still embedded, when viewing the individual line but it is overwritten with either delayed heave or real-time heave during the georeferenced bathymetry processing step in CARIS HIPS), and (D) the predicted tide signature over the course of the line, referenced to CD. This is a smoothed line as it has been interpolated between 3-minute intervals. 101

Figure 22. Site Z008-004 (Cambridge Bay West) - Line ID 2018TR2531845 (A) Fluctuating line (blue) is the GPS Tide solution with Heave embedded and the smooth line (yellow) is predicted tide from station 6240 (the highlighted yellow box is the examined timescale, shown in the top graph), (B) is the GPS Tide solution (blue) compared to the barometric pressure enhanced predicted tide (yellow). This shows good alignment between GPS Tide solution and barometric pressure enhanced predicted tide, shown by the 0.131 m vertical shift in the predicted tide. 103

Figure 23. Site Z004-002 (Hopes Advance Bay) Line ID 0063_20190916_122434_Petrel. (A) GPS Tide (blue) overplotted with PT solution from station 4325. Note GPS tide at tool tip is 8.346 m and Predicted Tide is at 9.442 m. (B) GPS Tide (blue) overplotted with BT solution from station 4325. Note GPS tide at tool tip is 8.345m (slight difference in the time tag between A and B) and BT is at 9.350 m, showing a vertical shift in the predicted tide by -0.092 m..... 105

Figure 24. Site Z003-001 (Clyde River) is located on the northeast coast of Baffin Island, Canada. The survey site averages 18km from Clyde River tidal station 3940. 107

Figure 25. Site Z003-001 (Clyde River) Line ID 4013_20190822_060735_LSSL. This figure depicts a large vertical offset between the GPS Tide solution and the BT solution of approximately 1 meter. The GPS solution is above the predicted Larger Large Tide range of 1.533 meters (station 3940) by ~0.4 meters. 108

Figure 26. Site Z007-001 (Lancaster Sound) (Line ID 4801_20190902_172106_LSSL) shows highly unstable GPS signal (light blue) in comparison to the vessel heave (dark blue). A) Stable GPS signal but above the BT solution (green horizontal line). B) Highly unstable GPS signal on line. C) Stabilized GPS signal but below the tide BT solution. 109

Figure 27. Site locations of Z008-004 (Cambridge Bay West) and Z008-005 (Cambridge Bay East) with a visual display of the ERA5 0.25˚ x 0.25˚ grid (Orange Grid). Final results in the comparison between GPS tidal solutions and the BT solution showed conflicting agreement at both sites. 112

List of Appendices

Appendix 1 – List of Acronyms …….. 126

Chapter 1
General Introduction

1 General Introduction

1.1 Motivation

Seventy-one percent of the Earth's surface is covered by water (Mayer et al., 2018). The world's oceans contribute to 82% of the global water cycle, and the water cycle is critical in tracking global climate change (Charette & Smith, 2010). To estimate the global water cycle, ocean volume is first calculated. A major variable in ocean volume calculation is depth (Charette & Smith, 2010). Developing a high-resolution global bathymetric model will lead to a better estimate of the global water cycle, a better understanding of ocean/atmosphere exchange, climate change, weather forecast modeling, ocean circulation patterns that affect tides and wave action, sediment transport, tsunami wave propagation and underwater geo-hazards, as well as other political and economic applications.

Inspired by the Nippon Foundation and the General Bathymetric Charts of the Ocean's ambitious project to map the world's oceans by 2030, International Hydrographic Organization (IHO) member states are beginning to investigate their digital bathymetric holdings. The investigations are centered on supporting the 'Seabed 2030 initiative' of mapping the world's ocean seafloors by 2030, Blue Economy, and the United Nations Decade of Ocean Science for Sustainable Development. As a member state of the IHO, Canada has yet to analyze its data holdings to determine the extent to which their waters have been mapped. This thesis develops a methodology that classifies and quantifies Canada's territorial waters and determine the extent of bathymetric gaps in their holdings.

Along with knowing the extent of coverage, data quality is of concern. There are several contributing factors that influence the uncertainty in bathymetric data. One of the largest contributors to depth uncertainty is the tidal influence. With the onset of Global Navigation Satellite Systems (GNSS) and the development of Ellipsoid Referenced Surveys (ERS), the uncertainty decreases, (Dodd & Mills, 2014), however in polar regions, where GNSS satellites are low on the horizon, frequent signal dropouts and degradation of signal occur, and it has been recommended that predicted or observed tides are used during GNSS position dropouts (Dodd &

Mills, 2011). Predicted tides can be used in scenarios that are not conducive to obtaining observed tides; however, predicted tides lack the current environmental conditions. Of those, barometric pressure plays a large role (Forrester, 1983; Wolski, et al., 2014; Gregory, et al., 2019). This thesis also compares ERS to barometric pressure-enhanced predicted tides to quantify the effect on uncertainty of the depth measurements.

1.2 Significance

General Bathymetric Chart of the Oceans (GEBCO) Seabed 2030 initiative has an ambitious goal to map 100% of the world's oceans by 2030 (The Nippon Foundation, 2022). GEBCO is responsible for developing global ocean and land terrain models. In June 2022 GEBCO released a high-resolution grid, increasing the resolution from 30-arc-seconds (approximately 1 km resolution) from previous models to 15-arc-seconds (approximately 450 m resolution) (General Bathymetric Chart of the Oceans, 2022). Studies using this new grid estimates that 24.9% of the global seafloor has been mapped, an increase from 23.4% the previous year (Nation, 2022). This indicates an increase of nearly 1.5% from 2022 to 2023 globally, with an overall average increase of 2.5% over the last 4 years (GEBCO, 2023). Other nations such as the United States of America and Portugal are already conducting bathymetric gap analyses within the limits of their Exclusive Economic Zone (EEZ). A country's EEZ is the area of the ocean that extends 200 nautical miles beyond the nation's territorial sea unless impeded by another nations EEZ, in which case the extent of the two meeting boundaries are evenly distributed. A nations' territorial sea is a boundary extending from the coastline to 12 nautical miles seaward. Within the EEZ, the coastal nation has jurisdiction over both living and non-living resources. A study by Westington et al. (2018) considered sounding density as a variable in what they considered mapped. Sounding density is the number of seafloor returns from the source of measurement (e.g. soundwave reflection, leadline observation) in a predefined spatial extent. This study also introduced a fixed grid resolution in ground units (meters) and limited data based on an arbitrary cutoff date, in an attempt to better represent data quality (Westington, et al., 2018). The study concluded that 41% of the United States of America waters were mapped. Since this paper was released, yearly reports have been posted with the most recent in January 2023, whereby, mapping the United States of

America’s waters at 100-meter resolution has progressed to an estimated 50% (National Oceanic and Atmospheric Administration, 2023).

This thesis investigated the previously developed methods for assessing and quantifying bathymetric gaps in order to determine a Canada-specific method, one that enables the current digital holdings within the Canadian Hydrographic Service’s Bathymetric Database to be easily queried allowing for the extraction and manipulation of the data holdings in order to produce a one-dimensional analysis that is repeatable, thus formalizing a baseline to measure year-over-year variability. The study area of this bathymetric gap analysis is nationwide, covering all Canadian waters from the shoreline to Canada’s EEZ. This approach will enable a future joint partnership with Canada’s neighboring nations to create a pan-North American bathymetric gap analysis, providing key information to policymakers and adding an additional tool for prioritizing hydrographic survey operations. A key subset of this analysis will focus on the Laurentian Great Lakes and support non-profit organization's efforts to generate the ‘Great Map’, a continuous digital terrain surface of the Great Lakes under the Lakebed 2030 project initiative. As of 2021, 15% of the Great Lakes have been mapped to a high-resolution (Great Lakes Observing System, 2021).

In addition to providing a baseline of bathymetric coverage in Canadian waters, data quality was also considered in this thesis. Excluding data holdings based on quality would dramatically decrease the overall coverage in the Canadian Arctic, where some locations have not been revisited since the late 1800’s and simple technologies such as lead lines (an outdated physical tool to measure the depth of the water via a graduated line with weighted end) were used to gain depth information. For this reason, the bathymetric gap analysis considers all data in CHS’s digital portfolio in order to better align with GEBCO’s requirements to meet and exceed international hydrographic standards allowing for a more accurate depth measurement, thus leading to higher-resolution global bathymetric terrain model. Identifying sources of uncertainty in the depth measurements and applying techniques to improve the accuracy and lower the uncertainty in the depth solution will benefit the model. This thesis also identifies oceanographic and environmental variables that contribute to the tidal signature, which is the largest vertical uncertainty related to depth measurements.

1.3 Literature Review

1.3.1 Bathymetric Gap Analysis

Although mapping the oceans for navigation has been done for centuries, modern seafloor mapping, or bathymetry, dates back to 1840, when Sir James Clark Ross, a British explorer began to record depth measurements along the United State coast (Dierssen & Theberge Jr., 2014). In Canada, a marine accident initiated and highlighted the need for hydrographic surveys to be conducted on the Great Lakes to ensure safe navigation (Canadian Hydrographic Service, 2022). In 1883, the Georgian Bay Survey was established and then expanded to the Pacific coast around 1891 before moving further east into Quebec by 1901. The Canadian Hydrographic Service was officially created in 1928 (Canadian Hydrographic Service, 2022). The hydrographic mapping efforts in Canada became a truly national organization in the 1950's as there was a national need to map the Canadian Arctic to support the Distant Early Warning (DEW line) System (Canadian Hydrographic Service, 2022).

Depth measurements began with physical measurements by means of sounding poles with weights attached; however, this method was very susceptible to errors. Sources of the errors included the slope of the line due to currents and/or vessel drift, as well as human error. In soft substrate, it was often difficult to know exactly when a weight touched the seafloor. Investigations into acquiring more accurate depth measurements began shortly after, which was the precursor to data quality assessment. New technologies were introduced to improve depth measurements. First was the introduction of the piano wire for lead-lines as opposed to the hemp ropes since the strength and relative thinness of the piano wire was not as susceptible to currents, thus reducing the angle of the measurement as the wire would remain on a more vertical plane (Dierssen & Theberge Jr., 2014). Triangulation and range bearing techniques were introduced to improve positioning. In the Early 1900's acoustic methods were developed to help ships navigate in poor visibility conditions whereby an acoustic pulse was deployed from navigational buoys and received by hydrophones aboard approaching vessels. Changing the path of the horizontal transmitting and receiving acoustic pulse to a vertical path, led to the first acoustic depth measuring devices used to profile the seafloor. In 1922 the U.S.S Stewart collected over 900 soundings on a trans-Atlantic voyage (Dierssen & Theberge Jr., 2014).

Determining how much of the Earth's seafloor has been mapped is a complex question, where the term 'mapped' has been interpreted differently between studies. There are many variables that can alter the definition and lead to interpretation inconsistencies from researchers. Some of these variables include spatial and temporal resolution, data quality, and technique used to acquire the depth measurement. Over the last several years, there have been a limited number of studies to determine how much of the global oceans have been mapped; however, due to inconsistent methodologies, the results vary based on input variables. A study conducted in 2017 indicated that 15% of the oceans had been directly mapped (Wölfl et al., 2017). This study defined the spatial resolution which it considered mapped as 1 kilometer grid cells, and the input data considered only soundings that were directly measured. Direct measurements occur from either ship-based surveys utilizing echo sounders, side scan sonar or lead lines, or airborne surveys using light detection and ranging (LiDAR) techniques. Indirect methods of measuring the seafloor are derived from gravity measurements using satellite altimetry. Altimetric vertical gravity gradient anomalies are used to develop global bathymetric models where voids exist from direct measurements (Sepúlveda et al., 2020; Hu, et al., 2022). Recent studies are attempting to improve the accuracies of the predicted depth measurements by using ship-based multibeam surveys to 'ground truth' the results; however, current models still result in a relatively large uncertainly (Hu, et al., 2022; Wang et al., 2022).

Developing a high-resolution bathymetric model at a global scale falls under the responsibility of General Bathymetric Chart of the Oceans (GEBCO). In 2009, GEBCO released a global compilation of the ocean bathymetry at a resolution of 30-arc seconds (approximately 926 meters at the equator), the GEBCO_08 model, and was derived mainly from Shuttle Radar Topography Mission (SRTM30) data (GEBCO, 2008). The model was refined in 2014 when GEBCO released GEBCO_2014 grid, whereby multiple data sources were used, such as Bathymetry of North American Great Lakes and International Bathymetric Chart of the Arctic Ocean (IBCAO v3), to improve the model. Mayer et al. (2018) investigated GEBCO_2014 grid and found that roughly 82 percent of the grid cells were void of directly measured soundings. This study went on to introduce the notion of depth-dependent resolution. Unlike mapping land topography where a fixed resolution can be achieved, the propagation of electromagnetic waves needs to be considered in waterbodies. In shallow waters, remote sensing techniques such as Light Detection and Ranging (LiDAR) use optical instruments to measure the seafloor but are limited based on water clarity. Ship-based echo sounders propagate a soundwave to the seafloor. The further the distance the

soundwave travels through the water column, the larger the footprint size is on the seafloor (Galway, 2000). Furthermore, the angle away from nadir of the transmission face of the echo sounder will increase the oblique footprint of the soundwave as it comes into contact with the seafloor. The slant range of the soundwave transmission is a function of the beam angle and water depth (Galway, 2000). At an average ocean depth of approximately 3,900 meters (Weatherall, et al., 2015) and assuming a flat seafloor, the footprint size would be approximately 157.21 m along track by 181.55 m across track at 30° grazing angle from nadir of the transmission face. The dimensions of the area on the seafloor receiving the sonar expand with depth. Depth-dependent resolution and gridding is a concept worth investigating; however, until there is a model that can define the depth areas, it is difficult to divide the seafloor into these categories.

The depth-dependent resolution grid cell size to account for the relative footprint size on the seafloor suggested by Mayer et al. (2018) are presented in (Table 1).

Table 1. Recommended depth range with associated grid-cell size resolution.

Depth	***Grid-cell Size***
0 – 1,500 m	100 x 100 m
1,500 – 3,000 m	200 x 200 m
3,000 – 5,750 m	400 x 400 m
5,750 – 11,000 m	800 x 800 m

In 2019, a newly developed global bathymetry and topography grid at 15 arc-seconds, the SRTM15+, was released. Using the new grid, it was calculated that 10.84% of the seafloor has been mapped by direct measurements (Tozer, et al., 2019). The SRTM15+ has a resolution of approximately 500 m X 500 m at the equator. Although the sounding count (contributing data) remained the same, the change in resolution meant an increase in the total number of cells, so the ratio of cells to soundings decreased; hence a lower percentage of the seafloor was considered mapped.

GEBCO has recently released a new grid, GEBCO_2022 Grid. This grid resolution is still 15 arc-seconds, similar to SRTM15+ however it uses predicted depths based on the V31.1 gravity model (GEBCO, 2022). With the latest grid, GEBCO reports that 23.4% of the world's oceans have been mapped, an increase from 20.6% in 2021 (GEBCO, 2022). GEBECO has set an ambitious goal of mapping the world's oceans seafloor by 2030. The project has been named Seabed 2030 and has gained international recognition; the goal of Seabed 2030 is

> *"A collaborative project between Nippon Foundation of Japan and GEBCO aims to bring together all available bathymetric data to produce the definitive map of the world ocean floor by 2030 and make it available to all"*
>
> (Nippon Foundation and GEBCO, 2022).

Since this Seabed 2030 project was initiated, several Hydrographic Offices around the world have begun to investigate their data holdings and derive their own way of calculating the percentage of their nations EEZ that has been mapped.

In the United States, this responsibility falls to the National Oceanic and Atmospheric Administration (NOAA). To prepare for Seabed 2030 initiative, a study by Westington et al. (2018) was undertaken at NOAA to investigate the digital bathymetric holdings and develop a methodology to set a baseline for seafloor mapping progression. This study was substantially different than previous studies for multiple reasons. Firstly, this was the first study to be done on a national scale as opposed to a global scale. The geographical limits were defined so that the extent of data included in the study was from the shoreline to the United States' EEZ. Secondly, this study excluded data prior to 1960 as a means of narrowing the coverage to 'modern' survey standards. Thirdly, the resolution moved away from arc seconds to ground measurements of 100 meters. The fourth important change in methodology introduced sounding density as a variable for seafloor gridding classification, whereby data from multiple sources were merged into gridded 100 meter cells. Suppression rules were applied during the merging based on the relative sounding densities of the bathymetry layers ensuring that higher-density soundings (Multibeam Echo sounders [MBES]) outweighed lower-density soundings (Singlebeam Echo sounders [SBES]). This study found that 41% of the U.S EEZ is 'mapped' (Westington, et al., 2018). Since this study was published, NOAA releases annual updates whereby the most recent update in January 2023 revealed 50% of U.S. EEZ has been mapped to 100 meter resolution (National Oceanic and

Atmospheric Administration, 2023). Current trends indicate a 3% increase per year of additional seafloor mapping in the U.S.; therefore, it can be predicted that if the same level of effort continues, the U.S. EEZ will be fully 'mapped' by 2041 (Integrated Ocean & Coastal Mapping, 2022); however, more realistic predictions considered the US level of mapping to be 1.4% increase, therefore 100% 'mapped' can be achieved by 2060 (GEBCO, 2023).

Another Hydrographic Office entity is the Instituto Hidrográfico (IH) which is a body within the Portuguese Navy who have committed to mapping, observing and forecasting the oceans (Dias, 2021). The IH aims to contribute to global knowledge of seabed morphology by acquiring high-resolution bathymetry within the Portuguese EEZ and has committed to supporting the Seabed 2030 project. The bathymetric resolution standards the IH are seeking to achieve are based on both sounding density and ensuring the acquisition equipment is capable of acquiring the angular resolution required to produce high-resolution models (Dias, 2021). The IH produces two bathymetric models, one for object detection and one for full bottom coverage (Dias, 2021). The object detection model aims to produce a grid surface at a resolution of 2.5% of the depth; whereas, the full bottom coverage model generates gridded surfaces at a resolution of 5% of the depth. Comparisons to the earlier study by Mayer et al. (2018) and the suggested depth-dependent resolution variability, show that setting the standards as a percentage of depth creates a significantly higher resolution model. Introducing this into data processing has recently become much easier to manage with the introduction of Variable Resolution Surfaces in popular bathymetric processing software such as Teledyne CARIS HIPS/SIPS. Variable Resolutions (VR) surfaces can adequately demonstrate the concept of "full seafloor coverage" (Foster et al., 2017).

1.3.2 Data Management and Quality

Variable resolution surfaces become problematic at the data management stage within national hydrographic office repositories. The current capabilities of the data management tools used in the Canadian Hydrographic Service's data management framework do not support variable resolution surfaces (Beach, 2022). Although VR surfaces can be generated through post-processing procedures, and the resulting gridded surfaces can be loaded into the CHS bathymetric database, VR surfaces will have negative downstream effects on internal processes and product generation, such as the integration of the different data sources, and complications in the resampling to a standard resolution. The CHS is moving toward a Continuous Maintenance (CM) model for all

digital source products. The intent of the CM model will allow for newly acquired bathymetric surfaces to be ingested in the database, compared to other overlapping bathymetric sources through a process called Comparative Validation (CV) and then pushed to a nautical product on-the-fly with minimal human oversight. The CV process interrogates overlapping sources and applies pre-established rules to make decisions on which source data will 'win' over other source data. The filtering rules take into consideration several attributes such as survey dates, sounding accuracies, positional accuracies and the acquisition technique. All winning sources are then combined at a specified resolution prior to export (Beach, 2022).

To ensure the CHS achieves automation of the workflow from ingestion of source data through the incorporation of the data on the nautical product, all while maintaining the goal of highly accurate products to support safe navigation in Canadian waters, the CHS stresses the importance of metadata and attributions. As a member state of the International Hydrographic Organizations (IHO), the CHS adopts the standards and specifications published by the IHO, in particular *IHO Special Publication S-44* which is the standard for Hydrographic Surveys and *IHO Special Publication S-57* which the standard for Transfer Standard for Digital Hydrographic Data. The CHS modifies the S-44 making them more stringent. The CHS promotes those standards in a publication *Standards for Hydrographic Surveys* where the aim of this publication is two-fold. Firstly, to specify the requirements for hydrographic surveys in Canada, ensuring data acquired meet sufficient accuracies, and secondly, to ensure that the spatial uncertainty of data is adequately quantified (Canadian Hydrographic Service, 2021).

Data quality is documented through data attribution, known as metadata. The CHS requires metadata related to several categories of hydrographic survey data: general survey information (survey start and end dates, acquisition hardware, survey vessel name, position hardware, technique of sounding measurement, the agency who acquired the data), the vertical and horizontal datums of the data, the calibration procedures and results, sound velocity, tidal datum and reduction method, and horizontal (position) and vertical (sounding) accuracies (Canadian Hdyrographic Service, 2021).

Not only do the overall gridded surfaces contain metadata attribution, known as surface attribution level, but the soundings themselves are attributed with an uncertainty level, known as point data attribution level. All soundings should be attributed with a 95% statistical error estimate in the

horizontal and vertical planes (Canadian Hdyrographic Service, 2021). The depth accuracy is the accuracy of the depth measure after it has been reduced to a defined datum (discussed further in the next section), most notably Chart Datum. Sources of all contributing uncertainties need to be quantified, and the sum of the contributing uncertainties is referred to as the Total Propagated Uncertainty (TPU). Among the contributors to the TPU is the tidal measurement, modelling errors, and measurement system errors.

1.3.3 Hydrographic Surveys Tidal Reduction

Hydrographic surveying provides information regarding the depth of the seafloor by using remote sensing techniques such as MBES. Ship-mounted MBES reflect a soundwave pulse off the seafloor and record the timing of the return signal at the transducer face. On-board computers convert the timing of the return signal to depth range information. To derive a highly accurate depth range, a sophisticated combination of Cartesian coordinate system measured offsets and angular offsets between the physical survey components (i.e. Inertial Motion Unit [IMU], primary and secondary Global Navigation Satellite System [GNSS] antennas, MBES transducer, center of rotation of the vessel, and the vessels waterline) and high-frequency vessel motion data, high-frequency GNSS signal positioning and timing data, and environmental data, such as water column sound velocity profiles (SVP), are systematically applied. The resulting depth range is relative to the water level height at the time of collection; however, a reduction to a zero reference is required to ensure all depths are relative to the same vertical datum. The vertical datum, known as Chart Datum (CD), in Canada, is Lower Low Water Large Tide (LLWLT) and is defined as ‘a plane so low that water but seldom falls below it’ (Forrester, 1983). To reduce to CD, tidal influences are removed from the equation. Tidal signatures, amplitude and frequency, have traditionally been applied through either observed tidal records, using in-situ data loggers, or predicted tidal records. Predicted tidal records use harmonic analysis to decompose a tidal signature into individualized components that facilitate predictions to be generated. Tidal predictions lack the capability to account for some environmental effects that influence sea surface heights (SSH), such as inverse barometer, sea water density, and wind set-up. SSH are the sea surface height measured from satellite altimetry in relation to the reference ellipsoid. Wind-driven SSH, known as wind set-up, refers to the slope of the water surface in the direction of the wind stress (Forrester, 1983).

New vertical reduction techniques consider GNSS. High-accuracy GNSS data are used to reference bathymetric data to a reference ellipsoid such as the World Geodetic System 1984 (WGS84). Translating the ellipsoid-referenced bathymetry to CD is done using modelling. The model, known as a Hydrographic Vertical Separation Model (HyVSEP) (Robin, et al., 2016) is a gridded surface that defines the vertical separation between the ellipsoid and CD. This technique of using models to reduce bathymetry to CD is known as Ellipsoidal Referenced Surveys (ERS) (Dodd & Mills, 2014).

In the process of hydrographic surveying, high-accuracy data recorded by on-board instruments inadvertently capture tidal signatures within the GNSS signal itself. Influenced by the motion of the vessel on the water surface, the GNSS antenna move in line with the ebb and flow of the tides. Furthermore, because the vessel is floating on the surface of the water, localized meteorological variables and the density of the water play a role in the vertical positioning of the vessel, which then relates to the vertical positioning of the GNSS antennas. Therefore, in the ERS methodology of vertically reducing bathymetry, localized meteorological and oceanographic variables are inadvertently accounted for; however, when using predicted tide vertical reduction techniques, these variables are unaccounted for.

Although it has been noted that several environmental and oceanographic variables influence the finalized bathymetric surface, this research will focus on a single variable, that being barometric pressure.

1.3.4 Meteorological and Oceanographic Variables of Concern

There is a significant reduction in Arctic sea ice due to climate change (Moore & McNeil, 2018; Plank et al., 2019). Over the past 33 years (1985-2018), sea ice loss has increased, and as a result, extreme wave heights have increased in the Arctic (IPCC, 2019). Extreme wave heights pose a threat to Arctic coastal communities as these Arctic communities rely heavily on sea-based transportation to support the local economy, and extreme wave heights could accelerate coastal erosion threatening shoreline infrastructure (Schädel, 2022). The reduction of sea ice also increases the potential for a rise in polar transiting maritime vessels (Pizzolato, et al., 2016). According to the Intergovernmental Panel on Climate Change's Special Report on the Ocean and Cryosphere,

summertime Arctic ship-based transportation has increased over the past two decades, which has implications for global trade that use traditional shipping corridors in the Arctic. Arctic transiting vessels have an increased exposure to navigational hazards due to poor weather conditions, poor communications, and poor navigational charts (Tulaktarvik Inc., 2014). Developing navigational charts and surveying Canada's waters is the responsibility of the Canadian Hydrographic Service (CHS) (Canadian Hydrographic Service, 2017). The motto of CHS is '*Nautical charts protect lives, property and the marine environment*' (Canadian Hydrographic Service, 2019). The development of nautical charts relies on the accuracy and precision of hydrographic surveys, in particular bathymetry.

In order to achieve the best possible vertical accuracies of hydrographic surveys, meteorological and oceanographic variables that influence sea level heights should be included in predicted tide vertical reduction methods. Meteorological variables such as barometric pressure influence sea level heights (LINZ, 2015;Smith, 2016). Tidal prediction algorithms use a standard barometric pressure of 1013.25 hectopascals (hPa) (LINZ, 2015); however, it has been well documented that ± 1 hPa can influence water level heights by ± 1 cm (Forrester, 1983; Wolski, et al., 2014; Gregory, et al., 2019). This effect is known as the inverse barometric pressure effect (IBE). The direct relationship of an increase (decrease) of 1 hPa to the decrease (increase) of 1 cm of water level is only true in the absence of other forces (Forrester, 1983). In fair weather conditions, IBE is difficult to separate from wind set-up influences.

With the advances of satellite radar altimetry technology, studies on the IBE could be conducted on a global scale. In a study by van Dam and Wahr (1993) a comparison between satellite radar altimetry-derived SSH and a mathematical barometric pressure gradient model resulted in 60-70% deviation from the IBE theoretical response. In another study by Fu and Pihos (1994), a similar comparative analysis was conducted differentiated only by the satellites used in the study. Using the TOPEX/Poseidon satellite, deviation from the IBE theoretical response was 110%, equating to 1.11 cm/hPa. This led the authors to conclude that the disagreement was the result of other environmental variables and suggested wind-driven sea surface variability as the source. However, it has been noticed that the influence of wind-driven sea surface fluctuation is relatively small in comparison to IBE (Hamon, 1966; Ponte, 1994). Studies compared the atmospheric pressure forcing and wind set-up and concluded that there is a negative correlation between the

two variables in that as one increased the other decreased and vice versa. (van Dam & Wahr, 1993; Ponte, 1994).

Since IBE and wind set-up are meteorological effects, they are non-periodic phenomena and thus can be separated from tidal predictions (Miller, 1958). A simple relationship between wind stress fluctuation and tidal energetics is difficult to determine (Kurapov, Allen, & Egbert, 2010). This is because the slope of the water surface is dependent on the topography of the study area (LINZ, 2015) as well as the speed and duration of wind forcing and fetch, which is the length of omnidirectional winds across open water. Ocean topography can be accounted for by high resolution bathymetry, and wind speed and the duration of wind forcing is easily obtainable through reanalysis models and/or downloaded from Environment and Climate Change Canada (ECCC) historical data collected from airports with proximity to the investigative site. On the other hand, fetch is difficult to determine because it is not data that are directly observed by instruments.

Persistent winds can lower or raise water level heights over several days, but shorter duration effects over hours can be noted as well (Miller, 1958). The water surface will rise in the direction of wind stress and lower in the opposite direction (LINZ, 2015). Strong offshore winds can exaggerate low-tide exposure along shorelines; conversely, strong onshore winds can virtually eliminate low-tide (NOAA, 2017).

Fetch plays an important role in wind driven sea surface heights, thus forcing a deviation from predicted tide models. In several studies aimed at modelling wave predictions and storm surges, fetch was calculated and used as an input variable (Fagherazzi & Wiberg, 2009; Rusu & Soares, 2015). These studies used the Simulating Waves Nearshore (SWAN) model (Booij, Holtuijsen, & Ris, 1997) to determine direction and height of waves. The authors used input data from the National Climate Environmental Prediction's (NCEP) Climate Forecast System Reanalysis version 2 (CFSRv2) (Saha, et al., 2014) model for inputs of surface wind direction and speed, as well as SSH. Using these models, fetch was calculated as an intermediate step. A process described by Forrester (1983), allows for a direct calculation of the change in sea level height based on wind speed, length of fetch and average depth of a cross section of bathymetry (Forrester, 1983).

SSH variability is broken into two fundamental components. The first is barotropic which is changes in mass of a water column namely due to gravitational forces, and the second is baroclinic, stemming from steric changes in the water column (Baker-et al., 2009). A study by Nagano &

Wakita (2019) use a Rossby wave model forced by wind stress to determine variations in SSH on a decadal scale. The authors suggest that the SSH over the subpolar North Pacific is primarily caused by barotropic Rossby wave response to an Aleutian Low in the North Pacific northwest of Japan. These decadal changes are on the scale of centimeters in the variation of SSH (Nagano & Wakita 2019).

Fluctuation in SSH, forced by wind stress, will not affect hydrographic ellipsoidal referenced surveyed depth measurements; however, this cannot be said for the predicted tide methodology to vertically reduce bathymetry to CD. Large fluctuations in SSH stemming from wind stress and storm surges can cause diversions from predicted tides in the magnitude of several meters; however, hydrographic surveys will not conduct operations in these types of conditions. Therefore, the influence of wind set-up is expected to be minimal. The largest meteorological variable on SSH will be atmospheric pressure forcing. As mentioned previously, predicted tides do not consider variations in these meteorological variables nor do they consider water column density.

The influence of the water column density on water level heights is regionally dependent. Steric heating was shown to an account for 30% of SSH variability between 30°S and 30°N and nearly 70% in equatorial regions between 10°N and 10°S (Vivier et al.,1999). In polar regions where water temperature is more consistent, influence of water column density is shown to be less (Armitage et al.,2016); however, the influx of freshwater from the melting of polar ice sheets and glaciers may offset and possibly exaggerate the water column density effect. A study by Postlethwaite et al. (2011) was conducted to determine the influence that sea ice has on tides and particularly the influence of sea ice melt or formation for the purpose of determining influx of freshwater that disrupts the salinity in the water column. The stratified water column impacts tidal heights shown by the tidal constituent M2, the semidiurnal lunar constituent (Postlethwaite et al., 2011). When studying the interaction between ocean tides and sea ice, it was found that the salt budget model was regionally dependent when tide was included in the model. It is also noted that discrepancies in the model may be a result of anomalous atmospheric forcing (Postlethwaite et al., 2011). In another study by Chuang and Wang (1981), it was shown that density fronts have strong effects on the generation and propagation of internal tides, and that tides at continental margins are affected by surface tide and topographic features, such as steep slopes. These slopes facilitate the transport of dense water, thus affecting the water level height above. For seaward-inclined density fronts, the tidal frequency increases towards the continental shelf (Chuang & Wang 1981).

One could hypothesize that since water column density is regionally and seasonally unique due to variables such as seafloor topography, sea ice melting, and freshwater influx, a comparison between sea surface height corrected for water column density will deviate from predicted tides.

In studies conducted by hydrographic offices around the world such as CHS, United Kingdom Hydrographic Office, and US naval Oceanographic Office, and summarized in the Federation of International Surveyors Publication No. 62, GNSS tides were compared to observed tides, resulting in a direct comparison between vertical reductions techniques involved with Ellipsoidal Referenced Surveys (ERS) and traditional reduction methods. A recommendation was made by Dodd and Mills (2014) to ensure validation checks remain common practice. The authors recommended that validation checks include the installation of tide gauges at the survey sites in that they serve two purposes, i) to validate the GNSS observations, the inherently recorded tidal signature, and ii) to validate the HyVSEP models being used (Dodd & Mills, 2014). The downside of that recommendation is that in-situ tide gauges increase the cost and effort to conduct hydrographic surveys. Validating observed tides against GNSS tides adds confidence to the finalized bathymetry; however, meteorological-enhanced predicted tides can offer a less expensive alternative as it eliminates the time required to deploy, retrieve, and calibrate in-situ tide gauges. After examining and reviewing literature, not a single case comparing meteorologically enhanced predicted tides and Ellipsoidal Referenced Surveys could be found. It is hypothesized that the reason for this lack of comparisons is twofold. First, Ellipsoidal Referenced Surveys techniques are relatively new (2009). Second, hydrographic offices have followed the recommendations of the FIG publication No. 62 and have used observed tides as validation. The hydrographic survey case studies have been conducted in areas where permanent tide gauges exist, making comparisons between observed tides and GNSS tides easier. Comparisons between Ellipsoidal Referenced Surveys and meteorologically enhanced predicated tides, especially in the Canadian Arctic, could not be located.

1.4 Objectives and Thesis Structure

The main gaps that have been identified in the literature review are that although hydrographic organizations are beginning to assess their digital data holdings to identify and quantify bathymetric gaps, there has been little computational analysis completed specifically reviewing

Canada's EEZ. There has been a consorted effort by non-profit organizations such as GEBCO to gather various bathymetric data from a wide range of data providers so that a global estimate on bathymetric data gaps can be quantified. Although the data gaps can be quantified, the definition of what is considered a gap varies. Additionally, as organizations ingest data, assessing the data quality becomes increasingly important so that important information can be conveyed to those who need it, whether that is for navigation safety, marine engineering applications, benthic habitat mapping or other applications.

The overall goal of this work is to derive a methodology for defining and quantifying bathymetric gaps in Canadian waters and to investigate efforts to increase data quality of newly acquired hydrographic data. This was achieved through two main objectives: 1) investigating the Canadian Hydrographic Service's digital bathymetric holdings and on a national scale, classifying those data holdings and quantifying the output to identify the extent of bathymetric gaps and 2) focusing on a specific environmental variable (barometric pressure) obtained from ECWMF ERA5 reanalysis data and applying that variable to predicted tides to compare to Ellipsoid Referenced Surveys to see if data quality increases.

To address objectives 1 and 2, this manuscript-based thesis has been structured into two primary content chapters. Chapter 1 serves as an introduction, while Chapter 2 addresses objective 1 by identifying differences in bathymetric gap analyses, defining terminology, detailing the approach to classifying and quantifying bathymetric gaps within Canada. Preliminary results of Chapter 2 were presented at the Canadian Hydrographic Conference 2022 in Gatineau, Quebec as a poster presentation. Furthermore, a concentrated analysis centered on the Great Lakes was presented at Lakebed 2030. This work is planned for publication in the journal 'International Hydrographic Review'.

Chapter 3 focuses on the data quality of newly acquired hydrographic surveys bathymetry, primarily on the tidal portion of uncertainty. Comparison between two vertical reduction methods, namely Ellipsoid Referenced Surveys and Predicted Tidal Surveys was carried out at 10 Canadian Arctic sites where GNSS signal loss increases the uncertainty associated with the depth measurement, thus decreasing data quality. This work is also planned for publication in the journal 'International Hydrographic Review'.

Finally, Chapter 4 provides an overall conclusion of the research findings and suggests future steps to improve both the Canadian Bathymetric Gap Analysis and data quality by examining additional environmental variables that can be applied to predicted tides.

1.5 References

Baker-Yeboah, S., Watts, D. R., & Byrne, D. A. (2009, December). Measurements of Sea Surface Height Variability in the Eastern South Atlantic from Pressure Sensor–Equipped Inverted Echo Sounders: Baroclinic and Barotropic Components. *Journal of Atmospheric and Oceanic Technology*, *26*(12), 2593-2609. doi:10.1175/2009JTECHO659.1

Beach, M. (2022, November 11). Canadian Hydrographic Service Data Management Processes. (A. Forbes, Interviewer)

Booij, N., Holtuijsen, L. H., & Ris, R. C. (1997). The "Swan" Wave Model for Shallow Water. *Coastal Engineering 1996-1997.*

Canadian Hdyrographic Service. (2021, March 10). *Standards for Hydrographic Surveys*. Retrieved from Fisheries and Oceans Canada: Canadian Hydrographic Service: https://www.charts.gc.ca/data-gestion/standards-normes/pre-eng.html

Canadian Hydrographic Service. (2012, January 1). *Defining Canada's Maritime Zones.* Retrieved April 26, 2022, from Government of Canada Publications: https://publications.gc.ca/collections/collection_2012/mpo-dfo/Fs23-571-2011-eng.pdf

Canadian Hydrographic Service. (2017, December 08). *About the Canadian Hydrographic Service*. Retrieved from Department of Fisheries and Oceans Canada: https://www.dfo-mpo.gc.ca/career-carriere/science/chs-shc/index-eng.html

Canadian Hydrographic Service. (2019, November 21). *Why hydrography matters*. Retrieved from Fisheries and Oceans Canada: http://charts.gc.ca/help-aide/about-apropos/index-eng.html

Canadian Hydrographic Service. (2022, 10 12). *About the Canadian Hydrographic Service*. Retrieved 11 02, 2022, from Nautical Charts and Services: https://www.charts.gc.ca/help-aide/about-apropos/index-eng.html

Charette, M. A., & Smith, W. H. (2010, June). The Volume of Earth's Ocean. *Oceanography, 23*(2), 112-114.

Chuang, W.-S., & Wang, D.-P. (1981, October). Effects of Density Front on the Generation and Propagation of Internal Tides. *American Meteorological Society, II*, 1357-1374.

Dias, T. G. (2021, May 31). Program Seamap 2030 - 100% of the Portuguese maritime spaces mapped by 2030. *International Hydrographic Review, 27*. Retrieved from https://ihr.iho.int/articles/program-seamap-2030-100-of-the-portuguese-maritime-spaces-mapof-the-portuguese-maritime-spaces-mapped-by-2030/

Dierssen, H. M., & Theberge Jr., A. E. (2014). Bathymetry: History of Seafloor Mapping. *Encylopedia of Natural Resources*. doi:10.1081/E-ENRW-120047531

Dodd, D., & Mills, J. (2011, November). Elliposidally Referenced Surveys: Issues and Solutions. *International Hydrographic Review*, 20-30.

Dodd, D., & Mills, J. (2014, May). *FIG Publication No. 62 - Ellipsoidally Referenced Surveying for Hydrography.* Retrieved from International Federation of Surveyors (FIG): https://www.fig.net/resources/publications/figpub/pub62/Figpub62.pdf

Forrester, W. D. (1983). *Canadian Tidal Manual.* Ottawa: Department of Fisheries and Oceans.

Foster, B., Hart, K., & Beduhn, T. (2017, March 6). *What Can Variable Resolution Do For You?* Retrieved from Teleydne CARIS HIPS/SIPS: https://www.teledynecaris.com/en/products/hips-and-sips/

Galway, R. S. (2000). *Comparision of Target Detection Capablilities of the Reson Seabat 8101 and Reason Seabat 9001 Multibeam Sonars.* Univsersity of New Brunswick, Department of Geodesy and Geomatics Engineering. Fredricton: University of New Brunswick. Retrieved November 5, 2022, from http://www.omg.unb.ca/omg/papers/MBSS_TermPaper.pdf

GEBCO. (2008). *General Bahtymetric Chart of the Oceans (GEBCO): The GEBCO_08 Grid.* Retrieved from General Bahtymetric Chart of the Oceans:

https://www.gebco.net/data_and_products/gridded_bathymetry_data/documents/gebco_08.pdf

GEBCO. (2022). *Mapping Progress*. Retrieved from General Bathymetric Chart of the Oceans: https://seabed2030.org/mapping-progress

GEBCO. (2022). *The GEBCO_2022 Grid*. Retrieved from General Bathymetric Chart of the Oceans: https://www.gebco.net/data_and_products/gridded_bathymetry_data/gebco_2022/

GEBCO Complilation Group . (2021). *GEBCO 2021 Grid*. Retrieved from The Nippon Foundation - Gebco-Seabed 2030 Project: https://www.gebco.net/data_and_products/gridded_bathymetry_data/gebco_2021/

General Bathymetric Chart of the Oceans. (2022, January 1). *The GEBC_2022 Grid*. Retrieved from GEBCO: https://www.gebco.net/data_and_products/gridded_bathymetry_data/gebco_2022/

Great Lakes Observing System. (2021, January 1). *Great Lakes Observing System - Lakebed 2030*. Retrieved from Great Lakes Observing System: https://glos.org/priorities/lakebed-2030/

Hu, M., Jin, T., Jiang, W., Chu, Y., Wen, H., & Li, J. (2022). Bathymetry Model in the Northwestern Pacific Ocean Predicted from Satellite Altimetric Vertical Gravity Gradient Anomalies and Ship-Board Depths. *Marine Geodesy, 45*(1), 24-46. doi: 10.1080/01490419.2021.1943576

Integrated Ocean & Coastal Mapping. (2022). *Status of Seafloor Mapping Within U.S. Waters*. Retrieved November 10, 2022, from Integrated Ocean & Coastal Mapping: https://iocm.noaa.gov/seabed-2030-status.html

IPCC. (2019). *IPCC Special Report on the Ocean and Cryosphere in a Changing Climate.* In Press: Intergovernmental Panel on Climate Change.

Kurapov, A. L., Allen, J. S., & Egbert, G. D. (2010, April). Combined Effects of Wind-Driven Upwelling and Internal Tide on the Continental Shelf. *American Meteorolgical Society, 40*, 737-756. doi:10.1175/2009JPO4183.1

LINZ. (2015, December 21). *Meteorological effects on tides*. Retrieved from Land Information New Zealand: https://www.linz.govt.nz/sea/tides/introduction-tides/meteorological-effects-tides

Louvart, P., Cook, H., Smithers, C., & Laporte, J. (2022). A New Approach to Satellite-Derived Bathymetry: An Exercise in Seabed 2030 Coastal Surveys. *Remote Sensing, 14*. doi:10.3390/rs14184484

Mayer, L., Jakobsson, M., Allen, G., Dorschel, B., Falconer, R., Ferrini, V., . . . Weatherall, P. (2018, February 8). The Nippon Foundation - GEBCO Seabed 2030 Project: The Quest to See the World's Oceans Completely Mapped by 2030. *Geosciences, 8*(2). doi:10.3390/geosciences8020063

Miller, A. R. (1958, January). The effects of winds on water levels on the New England Coast. *Limnology and Oceanography, 3*(1), 1-14.

Nagano, A., & Wakita, M. (2019, August 30). Wind-driven decadal sea surface height and main pycnocline depth changes in the western subarctic North Pacific. *Progress in Earth and Planetary Science, 6*(59). doi:10.1186/s40645-019-0303-0

Nation, J. (2022). NOAA NCEI Bathymetry Team: Data Contribution, Sharing, Accessibility and Archive Overview. *Lakebed 2030 Conference.* Traverse City, Michigan: National Oceanic and Atmospheric Administration. Retrieved September 29, 2022

National Oceanic and Atmospheric Administration. (2022). *Progress Report: Unmapped U.S. Waters.* NOAA. Retrieved April 6, 2022, from https://iocm.noaa.gov/documents/mapping-progress-report2022.pdf

Nippon Foundation and GEBCO. (2022). *About the Seabed 2030 Project*. Retrieved November 2, 2022, from The Nippon Foundation - GEBCO Seabed 2030 Project: https://seabed2030.org/about-us

NOAA. (2017, August 13). *Tides and Water Levels*. Retrieved from National Ocean Service: https://oceanservice.noaa.gov/education/tutorial_tides/tides08_othereffects.html

Postlethwaite, C. F., Morales Maqueda, M. A., le Fouest, V., Tattersall, G. R., Holt, J., & Willmott, A. J. (2011). The effect of tides on dense water formation in Arctic shelf seas. *Ocean Science, 7*, 203-217. doi:10.5194/os-7-203-2011

Robin, C., Nudds, S., MacAulay, P., Godin, A., De Lang Boom, B., & Bartlett, J. (2016). Hydrographic Vertical Separation Surfaces (HyVSEPs) for the Tidal Waters of Canada. *Marine Geodesy, 39*(2). doi:10.1080/01490419.2016.1160011

Saha, S., Moorthi, S., Wu, X., Wang, J., Nadiga, S., Tripp, P., . . . Becker, E. (2014). The NCEP Climate Forecast System Version 2. *Journal of Climate*, *27*, 2185-2208.

Sepúlveda, I., Tozer, B., Haase, J. S., Liu, P. L.-F., & Grigoriu, M. (2020, September 9). Modeling Uncertanties of Bahtymetry Predicted with Satellite Altimery Data and Application to Tsunami Hazard Assessment. *Journal of Geophysical Research: Solid Earth*, 25. doi:10.1029/2020JB019735

The Nippon Foundation. (2022, January 1). *The Nippon Foundation - GEBCO Seabed 2030 Project*. Retrieved from Seabed 2030 Project: https://seabed2030.org/

Tozer, B., Sandwell, D. T., Smith, W. H., Olson, C., Beale, J. R., & Wessel, P. (2019, August 8). Global Bathymetry and Topography at 15 Arc Sec: SRTM15+. *Earth and Space Science, 6*. Retrieved from https://doi.org/10.1029/2019EA000658

Tulaktarvik Inc. (2014, May 14). *Tulaktarvik: Submission to the Tanker Safety Expert Panel (Phase II - 'North of 60').* Retrieved from Transport Canada: https://www.tc.gc.ca/media/documents/mosprr/Tulaktarvik_and_Ocean_Group.pdf

United Nations Convention on the Law of the Sea. (2022, February 11). *United Nations Convention on the Law of the Sea of 10 December 1982.* Retrieved April 26, 2022, from United Nations: https://www.un.org/Depts/los/convention_agreements/texts/unclos/unclos_e.pdf

USACE. (1984). *Shore protection manual.* Vicksburg, Mississipi: Coastal Engineering Research Cener. Retrieved from http://ft-sipil.unila.ac.id/dbooks/S%20P%20M%201984%20volume%201-1.pdf

Vivier, F., Kelly, K. A., & Thompson, L. (1999, September 15). Contributions of wind forcing, waves, and surface heating to sea surface height observations in the Pacific Ocean. *Journal of Geophysical Research, 104*(C9).

Wang, F., Wan, X., & Annan, R. F. (2022). Accuracy requirement for altimetry observations for bathymetry inversion using gravity anomaly and gravity gradients. *Arabian Journal of Geosciences, 15*(627). doi:https://doi.org/10.1007/s12517-022-09901-x

Weatherall, P., Marks, K. M., Jakobsson, M., Schmitt, T., Tani, S., Arndt, E., . . . Wigley, R. (2015, June 29). A new digital bathymetric model of the world's oceans. *Earth and Space Science*. doi:https://doi.org/10.1002/2015EA000107

Westington, M., Varner, J., Johnson, P., Sutherland, M., Armstrong, A., & Jencks, J. (2018). Assessing Sounding Density for a Seabed 2030 Initiative. *2018 Joint Canadian Hydrographic and National Surveyors' Conference.* Victoria, British Columbia. Retrieved from https://www.eiseverywhere.com/ehome/chc-nsc2018/711593/

Wölfl, A.-C., Jencks, J., Johnston, G., Varner, J., & Devey, C. (2017). Identifying deep-sea target areas for a pilot Atlantic seabed mapping project using GIS techniques. *Journal of Ocean Technology, 12*(4), 28-42.

Wölfl, A.-C., Snaith, H., Amirebrahimi, S., Devey, C. W., Dorschel, B., Ferrini, V., . . . Wigley, R. (2019, June). Seafloor Mapping - The Challenge of a Truly Global Ocean Bathymetry. *Frontiers in Marine Science, 6*(283). doi:10.3389/fmars.2019.00283

Chapter 2
Canadian Bathymetric Gap Analysis

2 Canadian Bathymetric Gap Analysis

2.1 Introduction

Seventy-one percent of the Earth's surface is covered by water (Mayer et al., 2018). The world's oceans contribute to 82% of the global water cycle, and the water cycle is critical in tracking global climate change (Charette & Smith, 2010). To estimate the global water cycle, ocean volume is first calculated. A major variable in ocean volume calculation is accurate depth measurements (Charette & Smith, 2010) which are obtained from bathymetric digital elevation models (DEMs). Current global bathymetric DEMs incorporate data sources from multiple contributors; however, much of these contributing sources are not direct measurements (Mayer et al., 2018). To compensate for the lack of directly measured depths, indirect measurements from satellite sensors such as the Shuttle Radar Topography Mission are used to augment and interpolate the gaps. The Shuttle Radar Topography Mission 30-meter resolution (SRTM30) DEM's vertical uncertainty is around 16 m with a root mean square error (RSME) of 8.28 m (Santillan & Makinano-Santillan, 2016). Direct measured depths from multibeam echosounders (MBES) can achieve a much lower uncertainty with correctly configured systems. It is important to understand the extent of the differences of the direct measured depths versus interpolated depths as this will assist in communicating the uncertainty of the model.

Developing global bathymetric models will lead to a better estimate of the global water cycle (Khazaei et al., 2022), a better understanding of ocean/atmosphere exchange (Cubukcu et al., 2000), climate change (Kitchel et al., 2022), weather forecast modeling (Xie et al., 2002), ocean circulation patterns (Gille et al., 2004) that affect tides and wave action (Xie et al, 2018), sediment transport (Kanari et al., 2020), tsunami wave propagation (Satake, 1988) and underwater geo-hazards (Lecours et al., 2015), increase knowledge of marine habitat (Yesson et al., 2020) and biological communities (Rattray et al., 2009) as well as other political and economic applications of marine spatial planning initiatives (Evagorou et al., 2018; Guinan et al., 2021; Contarinis &

Kastrisos, 2022). To achieve more accurate global bathymetric models, sovereign nations need to assess the extent of their data holdings that contribute to the bathymetric DEM in their territory. Currently, celestial bodies such as Earth's moon, Mars and Mercury's surfaces are 100% mapped (Costello, 2019). This is in drastic contrast to the knowledge of Earth's surface where only 23.4% of Earth's oceans have been mapped (GEBCO, 2022).

The objective of this paper is to quantify the bathymetric gaps in Canada's EEZ by analyzing all digital soundings in possession of the CHS, which has been quality controlled and verified for use on Canadian navigational products, major gaps in data are identified supporting hydrographic survey planning operations and improved nautical charting. Although there are other sources of sounding data publicly available (e.g. the International Hydrographic Organization's Data Centre for Digital Bathymetry (https://www.ngdc.noaa.gov/iho/), National Centers for Environmental Information's Great Lakes Bathymetry products (Great Lakes Bathymetry | National Centers for Environmental Information (NCEI) (noaa.gov))), this study will only investigate CHS' data holding to ensure accurate representation of verified data that can be used on Canadian navigational products. All of this can lead to improved future planning for marine protection, safe navigation, and eventual development of enhanced tools to support studies in topics such as climate change and water cycles.

2.1.1 The History and Development of Modern Bathymetric Measurements

Although mapping the oceans for navigation has been done for centuries, modern seafloor mapping, or bathymetry, dates back to 1840, when Sir James Clark Ross, a British explorer began to record depth measurements along the United States coast (Dierssen & Theberge Jr., 2014). In Canada, a marine accident initiated and highlighted the need for hydrographic surveys to be conducted on the Great Lakes to ensure safe navigation (CHS, 2022). In 1883, the Georgian Bay Survey was established and then expanded to the Pacific coast around 1891 before moving further east into Quebec by 1901. The Canadian Hydrographic Service was officially formed in 1928 (CHS, 2022). The hydrographic mapping efforts in Canada became a truly national organization in the 1950's as there was a national need to map the Canadian Arctic to support the Distant Early Warning (DEW line) System (CHS, 2022).

Depth measurements began with physical measurements by means of sounding poles with weights attached; however, this method was very susceptible to errors such as the slope of the line due to

currents and/or vessel drift, as well as human error. In soft substrate, it was often difficult to know exactly when a weight touched the seafloor. Investigations into acquiring more accurate depth measurements began shortly after, which was the precursor to data quality assessment. New technologies were introduced throughout history to improve depth measurements. First was the introduction of the piano wire for lead-lines as opposed to the hemp ropes since the strength and relative thinness of the piano wire was not as susceptible to currents, thus reducing the angle of the measurement and increasing the accuracy in the true depth directly below the deployment location (Dierssen & Theberge Jr., 2014). Triangulation and range bearing techniques were introduced to improve positioning. In the Early 1900's acoustic methods were developed to help ships navigate in poor visibility conditions whereby an acoustic pulse was deployed from navigational buoys and received by hydrophones aboard approaching vessels. Changing the path of the horizontal transmitting and receiving acoustic pulse to a vertical path, led to the first acoustic depth measuring devices used to profile the seafloor, when in 1922 the U.S.S Stewart collected over 900 soundings on a trans-Atlantic voyage (Dierssen & Theberge Jr., 2014).

2.2 Determination of International Seafloor Coverage Amount

Determining how much of the Earth's seafloor has been mapped is a complex question, where the term 'mapped' has been interpreted differently between studies. There are many variables that can alter the definition and lead to interpretation differences between researchers. Some of these variables include spatial and temporal resolution, data quality, and technique used to acquire the depth measurement. Over the last several years, there have been a limited number of studies to determine how much of the global oceans have been mapped; however, due to inconsistent methodologies, the results vary based on input variables. A study conducted in 2017 indicated that 15% of the oceans had been directly mapped (Wölfl et al., 2017). Defining the term mapped was based on two factors, the spatial resolution and the method of measurement. The spatial resolution which they considered mapped was 1 km X 1 km grid cells, and the input data considered only soundings that were directly measured (with direct measurements defined as those that occur from either ship-based surveys utilizing echo sounders, side scan sonar or lead lines, or airborne surveys using light detection and ranging (LiDAR) techniques). Indirect methods of measuring the seafloor, not considered in the 2017 study by Wölfl et al. are derived from gravity measurements using satellite altimetry. Altimetric vertical gravity gradient anomalies are used to develop global bathymetric models where voids exist from direct measurements (Sepúlveda et al., 2020; Hu et

al., 2022). Recent studies are attempting to improve the accuracies of the predicted depth measurements by using ship based MBES surveys to ‘ground truth’ the results; however, current models still result in a relatively large uncertainly (Hu et al., 2022; Wang et al., 2022).

2.2.1 GEBCO - Method and Results

Developing a high-resolution bathymetric model at a global scale falls under the responsibility of General Bathymetric Chart of the Oceans (GEBCO). In 2009, GEBCO released a global compilation of the ocean bathymetry at a resolution of 30-arc seconds (approximately 926 meters at the equator), the GEBCO_08 model, and was derived mainly from Shuttle Radar Topography Mission (SRTM30) data (GEBCO, 2008). The model was refined in 2014 when GEBCO released GECO_2014 grid, whereby multiple data sources were used to improve the model. The model was improved by increasing the source density compared to the previous version and supplementing the grid with a Source Identifier (SID) grid which provides metadata (containing the source contributor of the data) related to each particular grid cell (Weatherall et al., 2015). A study in 2018 investigated the GEBCO_2014 grid and found that roughly 82% of the grid cells were void of soundings (Mayer et al., 2018). This study went on to introduce the notion of depth-dependent resolution. Unlike mapping land topography where a fixed resolution can be achieved, the propagation of electromagnetic waves needs to be considered in waterbodies. In shallow waters, remote sensing techniques such as Light Detection and Ranging (LiDAR) use optical instruments to measure the seafloor but are limited based on water clarity. Ship-based echosounders propagate a soundwave to the seafloor. The further the distance the soundwave travels through the water column, the larger the footprint size is on the seafloor (Galway, 2000). Furthermore, the angle away from nadir of the transmission face of the echo sounder will increase the oblique footprint of the soundwave as it comes into contact with the seafloor. The slant range of the soundwave transmission is a function of the beam angle and water depth (Galway, 2000). At an average ocean depth of approximately 3,900 meters (Weatherall et al., 2015) and assuming a flat seafloor, using the equations described by Galway (Galway, 2000) the footprint size would be approximately 157.21 m along track by 181.55 m across track at 30° grazing angle from nadir of the transmission face.

The dimensions of the area on the seafloor receiving the sonar signal expand with depth. Depth-dependent resolution and gridding is a concept worth investigating; however, until there is a model that can define the depth areas, it is difficult to divide the seafloor into these categories.

Mayer et al., (2018) suggested using depth dependent resolution grid-cell sizes (**Table 2**).

Table 2. Recommended depth range with associated grid-cell size resolution for the assessment of bathymetric gaps.

Depth	Grid-cell Size
0 – 1,500 m	100 x 100 m
1,500 – 3,000 m	200 x 200 m
3,000 – 5,750 m	400 x 400 m
5,750 – 11,000 m	800 x 800 m

With the release of a global bathymetry and topography grid at 15-arc seconds, the SRTM15+, it was calculated that 10.84% of the seafloor has been mapped by direct measurements (Tozer et al.,2019). The SRTM15+ has a resolution of approximately 500 m X 500 m at the equator. Although the sounding count (contributing data) remained the same, the change in resolution meant an increase in the total number of cells, so the ratio of cells to soundings decreased, hence a lower percentage of the seafloor was considered mapped.

GEBCO has recently released a new grid, GEBCO_2022 Grid. This grid resolution is still 15-arc seconds, similar to SRTM15+ however it uses predicted depths based on V31.1 gravity model (GEBCO 2022). With the latest grid, GEBCO reports that 23.4% of the world's oceans have been mapped, an increase from 20.6% in 2021 (GEBCO 2022). GEBECO has set an ambitious goal of mapping the world's oceans seafloor by 2030. The project has been named Seabed 2030 and has gained international recognition; the goal of Seabed 2030 is

> *"A collaborative project between Nippon Foundation of Japan and GEBCO aims to bring together all available bathymetric data to produce the definitive map of the world ocean floor by 2030 and make it available to all"*

(Nippon Foundation and GEBCO 2022).

Since this Seabed 2030 project was initiated, several Hydrographic Offices (HO) around the world have begun to investigate their data holdings and derive their own way of calculating the percentage of their nations EEZ that has been mapped.

2.2.2 National Oceanic and Atmospheric Administration - Method and Results

In the United States, the responsibility of determining and tracking the amount of seafloor coverage that has been mapped falls to the National Oceanic and Atmospheric Administration (NOAA). To prepare for Seabed 2030 initiative, a study by Westington et al., (2018) was undertaken at NOAA to investigate the digital bathymetric holdings and develop a methodology to set a baseline for seafloor mapping progression. This study was significantly different than previous studies for multiple reasons. Firstly, this was the first study to be done at a national scale as opposed to global scale. The geographical limits were defined so that the extent of data included in the study was from the shoreline to the United States' EEZ. Secondly, this study excluded data prior to 1960 as a means of narrowing the coverage to 'modern' survey standards. Thirdly, the resolution moved away from arc seconds to ground measurements of 100-meters. The fourth significant change in methodology introduced sounding density as variable for seafloor gridding classification, whereby data from multiple sources were merged and gridded into 100-meter cells. Suppression rules were applied during the merging based on the relative sounding densities of the bathymetry layers ensuring that higher density soundings (Multibeam Echosounders [MBES]) outweighed lower density soundings (Singlebeam Echosounders [SBES]). Using this new methodology, Westington et al., (2018) found at that 41% of the U.S. EEZ is 'mapped'. Since this study was published, NOAA releases annual updates whereby the most recent update in January 2023 revealed 50% of U.S. EEZ has been mapped to 100-meter resolution (Integrated Ocean & Coastal Mapping, 2022). Current progress indicates a 3% increase per year of additional seafloor mapping in the U.S. This increase is similar to the global trends calculated at 2.8% increase between GEBCO 2021 gird and GEBCO 2022 grid (Nation, 2022). Using the rate of 4% per year, it can be predicted that if the same level of effort continues, the U.S. EEZ will be fully 'mapped' by 2033 (Integrated Ocean & Coastal Mapping, 2023); however, more conservative predictions considered the U.S level to increase by 1% per year and therefore 100% 'mapped' of the U.S can be achieved by 2041 (Integrated Ocean & Coastal Mapping, 2023).

2.2.3 Instituto Hidrográfico – Method and Results

Another Hydrographic Office entity is the Instituto Hidrográfico (IH) which is a body within the Portuguese Navy who have committed to mapping, observing and forecasting the oceans (Dias, 2021). The IH aims to contribute to global knowledge of seabed morphology by acquiring high-resolution bathymetry within the Portuguese EEZ. Additionally, the IH has committed to supporting the Seabed 2030 project. As of 2021, 55% of the Portuguese EEZ has been mapped (Dias, 2021). The bathymetric resolution standards the IH are seeking to achieve are based on both sounding density and ensuring the acquisition equipment is capable of acquiring the angular resolution required for producing high resolution models (Dias, 2021). The IH produces two bathymetric models, one for object detection and one for full bottom coverage (Dias, 2021). The object detection model requires higher resolution and therefore the gridded surfaces are generated at a resolution of 2.5% of the depth, whereas, the full bottom coverage model generates gridded surfaces at a resolution of 5% of depth. Comparisons to the earlier study by Mayer et al.,(2018) and the suggested depth dependent resolution variability, indicate that setting the standards as a percentage of depth creates a significantly higher resolution model. Introducing this into data processing has recently become much easier to manage with the introduction of Variable Resolution Surfaces in in popular bathymetric processing software such as Teledyne CARIS HIPS/SIPS. Variable Resolutions (VR) surfaces can adequately demonstrate the concept of "full seafloor coverage" (Foster et al.,2017). As of

2.2.4 Goals of the Bathymetric Gap Analysis for the Canadian Hydrographic Service

The CHS is under mandate to provide bathymetric information to ensure safe navigation within Canadian waters. Knowing the extent of the bathymetric coverage will highlight key areas which should be prioritized for survey planning purposes. Additionally, knowledge and understanding of the bathymetry within Canada's EEZ will support the broader science communities in a wide range of studies. The goal of the CHS is to assess all digital bathymetric holdings and set a baseline for year-over-year comparisons on data acquisition progress. This will provide a starting point to better understand CHS's data holdings, inform planning for data collection, and perhaps also communicate with policy makers, external partners, and IHO member states. A key objective of

this study is to align the methodology with NOAA's bathymetric gap analysis study so that shared waters between the two sovereign nations can align and report on progress, which can lead to a pan-North American bathymetric gap analysis.

2.3 Study Area

2.3.1 Coastline

Measuring at 243,042 kms, Canada's coastline is the world's longest (Statistics Canada 2016). For this study, CanCoast Shoreline 2.0 data, which is derived from open-source data, was used to spatially define the interior extents of the data (Natural Resources Canada, 2019). This data was derived from CanVec 9.0 at a 1:50,000 for the majority of the product. In a small number of areas in the Canadian Arctic, shoreline data were not available in CanVec 9.0. To compensate for the gap in data, shoreline data was extracted from national topographic database maps (NRCan 2011b) at a scale of 1:250,000 (Manson et al., 2019).

2.3.2 Maritime Boundaries and Canada's Exclusive Economic Zone

In Canada, Lower Low Water Large Tide (LLWLT) is recognized as chart datum on nautical charts. Chart datum is defined as 'a plane so low that water but seldom falls below it' (Forrester, 1983). Where this reference plane intersects with the coastline is known as the 'normal baseline' and is the line from which each maritime zone is measured. Canada shares maritime boundaries with three nations, the United States of America, Demark and France (St. Pierre and Miquelon) (Byers & Østhagen, 2017). The international agreements that established these boundaries are justified by the use of maritime zones which are recognized by the United Nations Laws of the Seas Convention of 1982. Among the recognized maritime zones are the Territorial Sea and the Exclusive Economic Zone. The territorial sea baseline is derived from the "low-water line along the coast as marked on large-scale charts officially recognized by the coastal State" (United Nations Convention on the Law of the Sea, 2022) and is located 12 nautical miles from the country's shoreline. From the territorial sea baseline, other maritime limits are defined including the Economic Exclusive Zone (EEZ). The EEZ is the region of water extending beyond the sovereign state's territorial sea to a maximum of 200 nautical miles from the territorial sea baseline. The Exclusive Economic Zone is an area where sovereign states have jurisdiction over "exploration, exploitation, management, and conservation of resources in the water, on the seabed

and under the seafloor" (CHS, 2012). The Canadian EEZ delineates the outer limit of the study area.

2.3.3 Regional Boundaries

The Canadian Hydrographic Service resides in the Department of Fisheries and Oceans Canada's science division. Canada's Department of Fisheries is subdivided into five regions, Pacific, Ontario and Prairies, Quebec, Atlantic and Arctic Regions (**Figure 1a**). Although departmentally these boundaries are well established and the CHS respects the departmental boundaries in organizational governance, alternative boundaries were created to suit internal requirements that support functional unit responsibilities. These include the data management and data integration units, whose responsibility it is to ingest bathymetric data into regional databases. Internally, the CHS defines the regional boundaries in one of three ways, Departmental Organization Governance (**Figure 1a**), Navigational Charting (**Figure 1b**), or CHS Bathymetric Database limits (**Figure 1c**). The boundaries associated with navigational charting are derived from natural geographic boundaries, those being the Atlantic Coast, the Pacific Coast, Ontario and Manitoba including the Great Lakes, and the Arctic. The CHS's bathymetric database is divided in a such a way that it does not conform to the same boundaries as navigational charting as Quebec does not have a specified chart catalogue (**Figure 1c**)**.** Finally, the CHS Bathymetric Gap Analysis has been further divided for the sole purpose of subdividing the Ontario & Prairies and Arctic region into Eastern Arctic and Western Arctic and Great Lakes and St. Lawrence River regions (**Figure 1d**) to allow for faster computer processing time and better data management practices.

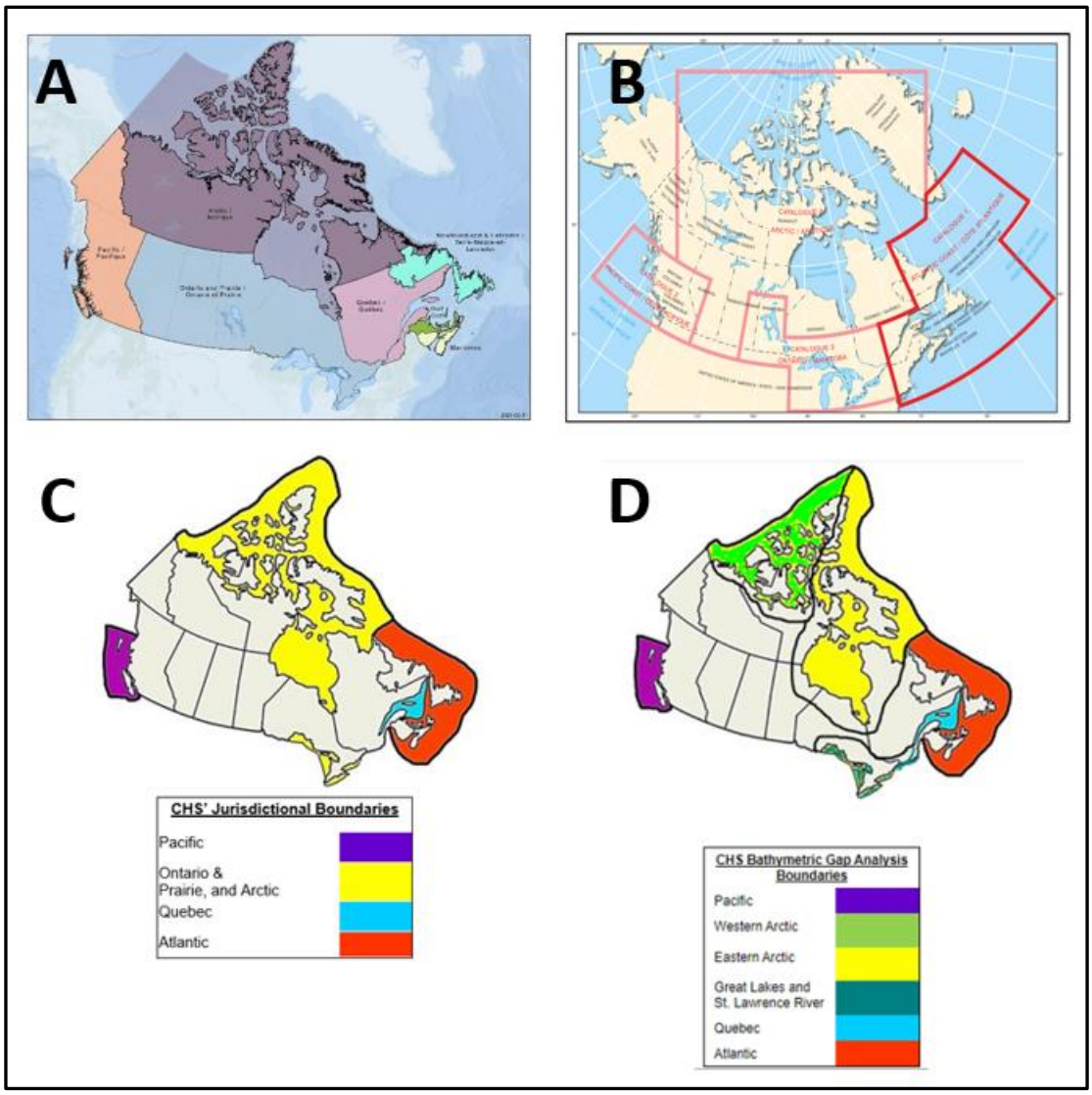

Figure 1. Visual depiction of the various regional boundaries as seen within the Canadian Hydrographic Service.

A) Department of Fisheries and Ocean Canada regional boundaries.

B) The Canadian Hydrographic Service's nautical charting catalogue boundaries.

C) The Canadian Hydrographic Service's regional bathymetric database boundaries.

D) The Canadian Hydrographic Service's bathymetric gap analysis boundaries.

2.4 Data and Methodology

2.4.1 Canadian Hydrographic Service's Bathymetric Database

2.4.1.1 History and Legacy Issues

In 2011, the CHS began a digital transformation initiative whereby the organization committed to integrating all source data into a consolidated digital sounding database, using the software CARIS (Computer Aided Resource Information System) Bathymetric Database (BDB). BDB is a robust scalable solution to store bathymetric data (Teledyne CARIS, 2023), capable of storing and maintaining low-density and geographically sparse data (lead line for example) to high-density data (MBES or Light Detection and Ranging (LiDAR) for example). The CHS began to convert soundings from numerous sources including nautical paper charts, analogue sounding rolls, field sheets, and digital archives among others to digital format and attributed the soundings with key metadata. In the early stages of the migration, it became apparent that there were significant differences in the regional procedures in aspects from data acquisition, data attribution and coding and data archiving and storage procedures. The CHS Hydrographic Data Working Group was formed, which included members from the regional offices in an attempt to introduce national consistency in the attribution, coding and best data management practices of the CHS' holdings.

In 2018, the Canadian Hydrographic Service developed a geospatial approach to prioritizing hydrographic surveying and charting priorities on a national scale. Known as the CHS Priority Planning Tool (CPPT), this GIS based analysis was comprised of multiple GIS layers including marine transportation corridors, water depth ranges, seafloor complexity, ice concentrations, tidal windows, among others (Chénier et al, 2018). At its root, the CPPT interrogates the national level bathymetric database and extracts the geometric bounding polygons of the hydrographic surveys, which represent the survey extents and are coded with metadata about the survey. The CPPT uses specific metadata attribution in its analysis, specifically the Category Zone of Confidence (CATZOC). The CATZOC classification is divided into six groups (A1, A2, B, C, D, U), where A1 and A2 contain high accuracy depth and positional information, B is medium accuracy depth and positional information, C and D are low accuracy depth and positional information, and U is unassessed accuracy depth information (International Hydrographic Organization, 2020).

Along with water depth, a description of the extent of seafloor coverage expected within a Zone of Confidence (ZOC) classification is also considered in calculating the CATZOC. This can be deduced by the method of which soundings were acquired, and therefore another variable that should be considered is the technique of soundings (TECSOU). Although technique cannot be used for as a proxy for data quality, it does assist in describing the seafloor coverage, a component of the CATZOC. By design, MBES, Light Detection and Ranging (LiDAR) technologies and vertically swept acoustic sounding systems are designed to ensonify the seafloor to 100% coverage. Hydrographic survey planning selects the appropriate sounding technique for each particular use case. LiDAR technology has limitations in the depth of water that the light can reach and varies depending on water clarity. Vertically swept acoustic sounding systems are an array of singlebeam echo sounders (SBES) mounted on a fixed across-track arm on a vessel, whereby the distribution of the transmit and receive arrays are evenly spaced so that the footprint of each beam overlaps with its neighboring beams on the seafloor. This technology has been historically used in shallow water scenarios. MBES are similar in that each beam creates overlapping footprint on the seafloor, thus generating 100% coverage of the seafloor; however, all beams are generated from a single transmit array.

All three conditions (positional accuracy, vertical accuracy, and seafloor coverage) must be met to be classified as a specific ZOC (**Table 3**). CATZOC classification is a great tool to quickly assess areas of varying accuracies of sounding measurements. As a GIS layer, the CPPT root layer depicting CATZOC allows one to calculate coverage statistics of Canadian waters; however, there are some fundamental issues of assessing gaps in Canadian bathymetry based on the bounding polygons alone.

Table 3. Category of Zone of Confidence (CATZOC)

ZOC		Position accuracy	Depth accuracy		Seafloor coverage	Typical survey characteristics
	A1	± 5 m + 5% depth	= 0.50 + 1%d		Full area search undertaken. Significant seafloor features detected and depths measured.	Controlled, systematic survey high position and depth accuracy achieved using DGPS or a minimum three high quality lines of position (LOP) and a multibeam, channel or mechanical sweep system.
			Depth (m)	Accuracy(m)		
			5	0.55		
			10	0.6		
			15	0.65		
			20	0.7		
			25	0.75		
	A2	± 20 m	= 1.00 + 2%d		Full area search undertaken. Significant seafloor features detected and depths measured.	Controlled, systematic survey achieving position and depth accuracy less than ZOC A1 and using a modern survey echosounder and a sonar or mechanical sweep system.
			Depth (m)	Accuracy(m)		
			5	1.1		
			10	1.2		
			15	1.3		
			20	1.4		
			25	1.5		
	B	± 50 m	= 1.00 + 2%d		Full area search not achieved; uncharted features, hazardous to surface navigation are not expected but may exist.	Controlled, systematic survey achieving similar depth but lesser position accuracies than ZOC A2, using a modern survey echosounder, but no sonar or mechanical sweep system.
			Depth (m)	Accuracy(m)		
			5	1.1		
			10	1.2		
			15	1.3		
			20	1.4		
			25	1.5		
	C	± 500 m	= 2.0 + 5%d		Full area search not achieved, depth anomalies may be expected.	Low accuracy survey or data collected on an opportunity basis such as soundings on passage.
			Depth (m)	Accuracy(m)		
			5	2.3		
			10	2.5		
			15	2.8		
			20	3.0		
			25	3.3		
	D	Worse than ZOC C			Full search not achieved, large depth anomalies expected.	Poor quality data or data that cannot be quality assessed due to lack of information.
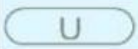	U	**Unassessed** - The quality of the bathymetric data has yet to be assessed				

Although the bounding polygons will approximate the data contained within, they are not an accurate representation of the data. The intent of the bounding polygons is to contain metadata about the survey, not to be used for complex analysis on the data for several reasons. First, the bounding polygons were, for a long period of time, incapable of depicting holes within the data as a result of software limitations. This causes vastly overestimated CATZOC coverage (**Figure 2**).

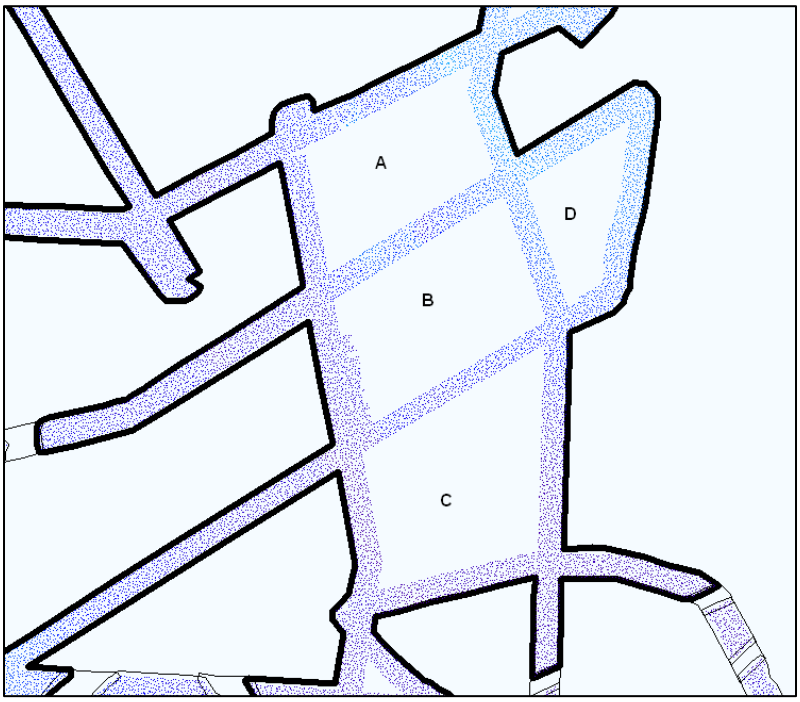

Figure 2. Multibeam survey conducted in 2009 classified as CATZOC B existing in the Canadian Hydrographic Service's Bathymetric Database shows large areas in which the bounding polygons misrepresent the data as the software at the time of loading the data into Bathymetric Database could not represent holes in the data. Area A, B, C and D, represent approximately 8000, 9600, 11100, 3700 km^2 respectively, which were not surveyed and are void of soundings, thus an approximate total of 32,400 km^2 of seafloor are misrepresented in CATZOC classification.

Secondly, there are limitations to the number of vertices that can be created to represent the bounding polygon. This was done by design so that the software would not lag during redraws, thus increasing user experience. The downside to the limitations of the number of vertices imposes generalization on the bounding polygons. The generalization affects large transit style surveys (surveys that transit from the east or west coast of Canada to/from the Canadian Arctic). To overcome the negative impact of generalization, a solution would be to cut the transit surveys into smaller sections; however, there is a great level of effort required to correct the legacy data that exists in the BDB.

Thirdly, there are no defined standards at which the distance from the data to the vertices of the polygon are drawn. In large scale areas (harbours / ports) the hydrographic surveys are generally high resolution, covering a small geographic area. This allows for tight representation of bounding polygons, in most cases the vertices are less than 2 meters from the data. At small scale hydrographic surveys (transit surveys / marine corridors) the geographic areas are vast, thus greatly increasing the number of vertices required, resulting in generalization. Vertices on these types of bounding polygons can be greater than 5 kms from the data. Representation of generalized bounding polygons inflates the total amount of coverage. A random sample from BDB on a transit survey indicates that if the bounding polygon is used instead of the data itself, the total coverage would be inflated 47% (**Figure 3**). This inflated rate is not consistent and can vary depending on the area and complexity of the data. Standards on acceptable limits have not been defined and are a missing component if bounding polygons are to be used for a bathymetric gap analysis.

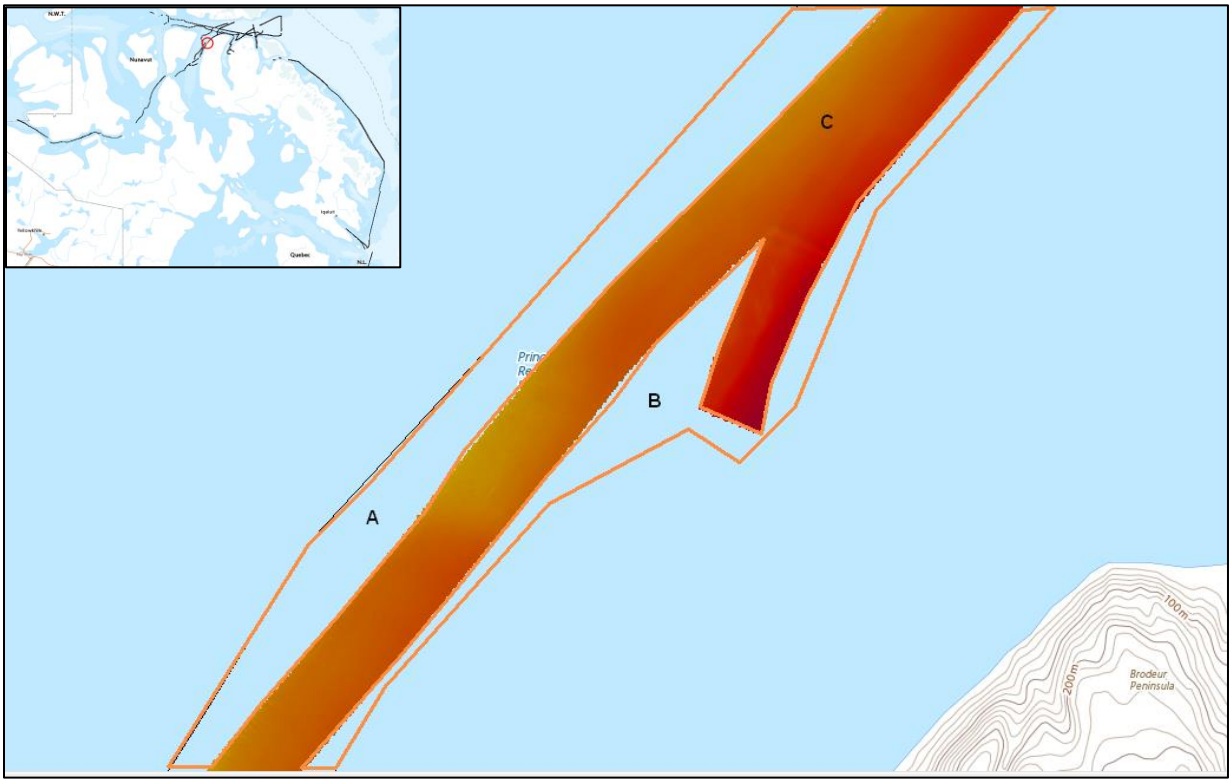

Figure 3. Random sample bounding polygon vs data. Area A represents 126 km^2. Area B represents 79 km^2. The survey data (Area C) represents 230 km^2. Total area of the bounding polygon is 435 km^2, therefore calculating statistics on the bounding polygon vs the data shows a 47% overestimation.

Finally, historical field survey operations often used multiple platforms to acquire soundings. The variety of platforms each utilized various positioning equipment, tidal reductions techniques, sounding hardware and occasionally spanned multiple years. Data management practices at the time were to concatenate all source data into a single product by performing a sounding selection. The resulting product, known as a field sheet, would satisfy charting purposes of the time; however, the final field sheets became problematic when a digital database was introduced. The field sheets were digitized and loaded into the database under a single bounding polygon. Many attribution fields only allowed for a single entry leading to data sets being misrepresented in both vertical and horizontal accuracies, typically tending to the lowest common denominator of accuracies. Multiple attribute profiles were added to the Technique of Sounding attribute (TECSOU), therefore a field sheet would have sections that had full area search undertaken and significant seafloor features detected and other areas were full areas search was not achieved, and anomalies on the seafloor may be expected.

2.4.1.2 Data Types

Data is stored in two formats with CHS' Bathymetric Data base, those being either point cloud data (simple representation of XYZ data points) or gridded data. Each have unique attributes that can add value to the end-user. We have extracted 17,169 sources from the CHS BDB, with 10,093 being gridded data and 7,076 being point cloud data (**Table 4**).

Table 4. A breakdown of all contributing data sources used in this analysis.

	Data Layer	MLV Layer						OAT Layer		Region Total
	ACQUISTION TECHNIQUE	MBES		LiDAR		SWEEP		OTHER		
	VALIDATION STATUS	Validated	Non-Validated	Validated	Non-Validated	Validated	Non-Validated	Validated	Non-Validated	
REGION	PACIFIC	1216	130	155	30	12	0	718	199	2460
	OP&A	5153	374	150	40	0	2	1276	698	7693
	QUE	1485	4	72	0	313	0	1601	1	3476
	ATL	1097	60	126	1	351	1	1830	74	3540
SUBTOTALS	Validation Total	8951	568	503	71	676	3	5425	972	
	Technique Total	9519		574		679		6397		**17169**
	Layer Total	10772						6397		

The advantage of point cloud of data is that the file size is relatively small and the data is easy to handle and manipulate. Point cloud data does not have a resolution but is defined by the density which stems from the line spacing during the data acquisition (the horizontal distance between parallel along-track transits of the vessel as it navigates across the area of interest during survey operations). Conversely, gridded data are typically larger files sizes, have a fixed resolution, and

are harder to manipulate because of the deconfliction that needs to occur when combining sources to make downstream products. The fixed resolution is sufficient enough that gaps in the data are non-existent at resolutions that meet IHO standards. In the CHS BDB, these datatypes are overlaid and complex (**Figure 4**).

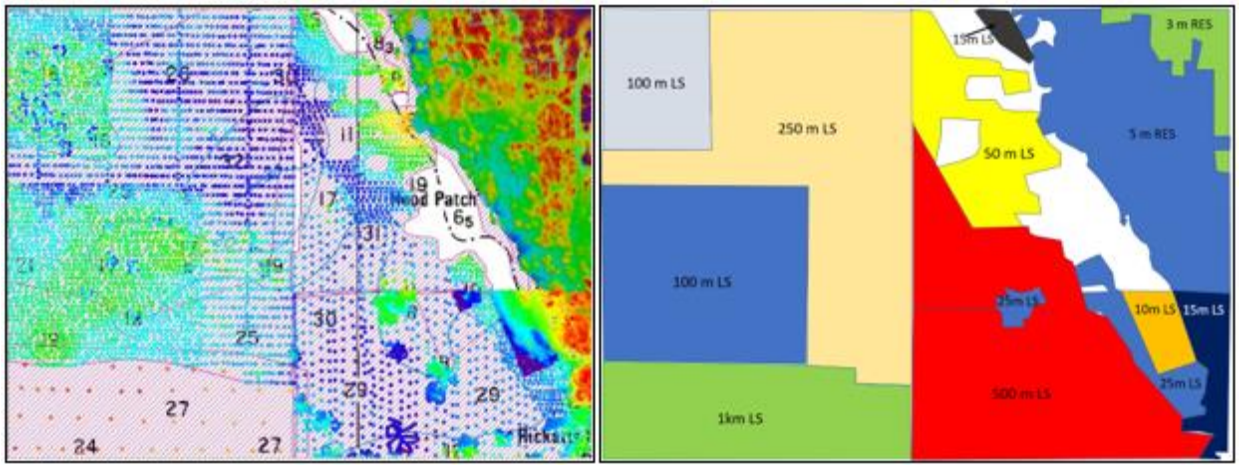

Figure 4. CHS Bathymetric Database displaying multiple data types and varying resolutions and or line spacing. The image on the left is a visualizing of the soundings with the Canadian Hydrographic Services. The image on the right is the classification of the resolution (indicated by RES) or line spacing (indicated by LS).

Classifying the data strictly on storage type (point cloud or gridded data) could not be accurately accomplished because of historical data management practices. When MBES data was first investigated and introduced within the CHS data acquisition techniques arsenal, the data points were drastically denser than previous data acquisition types, which significantly increased the file size. This quickly became a data management concern. To mitigate the risk of compiling, storing and manipulating large volumes of data, decisions were made to convert gridded data to point cloud at a scale appropriate for navigational charts in the area. Thus, data was collected, gridded at a high resolution, cleaned for outliers or noise in the data, and then resampled by conducting a sounding selection to meet the necessary charting scale. The resulting point cloud data was ingested into BDB, so although this data can be considered full bottom coverage, it resides in the database as point cloud data, requiring an alternative method of classifying this data.

2.4.1.3 Horizontal Reference System

The CHS's bathymetric database contains source data in various horizontal reference coordinate systems. Although the database is intended to be a non-projected representation of data, where the soundings can be projected upon export, populating the database from legacy archives maintains the original horizontal datum as recorded upon acquisition. As of February 2023, 64% of CHS BDB is in World Geodetic System 1984 (WGS84) non-projected. The remaining 36% is of various projections.

To align with the CPPT, Canada Albers Equal Area Conic (EPSG 102001) was chosen as the projection to conduct this analysis, as Albers Equal Area Conic Projections have properties in ground units making them ideal to calculate areas. Canada Albers Equal Area Conic is based on the geodetic reference system 1980 (GRS 80) with a semi-major axis of 6378137 and a semi-minor axis of 298.25722101. This was chosen as it has two standard parallels (50˚ N and 70 ˚ N) and a central meridian of 40˚ N, lessening the distortion along those parallels. As we are looking at a national product, a projection that supported less distortion in both Southern waters and Arctic waters was required. Unfortunately, CARIS suite of software does not include this projection type, and therefore an intermediate transformation was needed to extract the data from the BDB. All source data in the BDB were exported using WGS 84 / World Mercator (EPSG:3395) and later transformed to Canada Albers Equal Area Conic in ESRI ArcMap.

2.4.2 Terminology

Defining the terms for each classification group is important to note the differentiation between other bathymetric gap analyses. Both the NOAA and Nippon Foundation-GEBCO's Seabed 2030 project have termed their classification groups as 'mapped', although there are competing definitions from the use of that term. There are many variables to consider such as resolution, technique of soundings, water depth, data quality among others (Westington et al., 2018). Unlike Seabed 2030's definition whereby a cell is considered 'mapped' if it contains a single sounding, NOAA's method aligns with our current analysis in that sounding density is considered. The IHO Standards for Hydrographic Surveys publication S-44 defines the term Bathymetric Coverage as:

> *"Extent to which an area has been surveyed using a systematic method of measuring the depth and is based on the combination of the survey pattern and the theoretical area of detection of the survey instrumentation".*
>
> (International Hydrographic Organization, 2020)

For this study we introduce fundamental definitions while considering IHO definitions of bathymetric coverage as well as attempting to align with NOAA so that a possible future collaboration on a pan-North America Bathymetric Gap Analysis can be conducted:

- ***A cell*** – a 100 m X 100 m area on the seafloor
- ***Representative Sounding*** – a derived value to represent the depth in a 10 m resolution grid as a result of combining of all source data contained within the 10 m grid cell.
- ***Minimal Coverage*** – Classification Level 1 = 1-2 representative soundings in a cell.
- ***Moderate Coverage*** – Classification Level 2 = ≥ 3 representative soundings in a cell.
- ***Full Bottom Coverage*** – Classification Level 3 = a cell that contains representative soundings from either Multibeam, LiDAR or Swept by Vertical Acoustic System.
- ***Gap – Void of Soundings*** – Classification Level 0 = the cell does not contain a representative sounding.

2.4.3 Determination of Seafloor Coverage

As described in the S-57 Appendix B.1 Annex A – Use of the Object Catalogue for ENC edition 4.1.0, the International Hydrographic Organization has stated the purpose of the attribution that describes the technique of sounding measurement (TECSOU). Although TECSOU cannot be encoded on the metadata object responsible for communicating the overall quality of the data, which is reserved for the M-QUAL, (metadata on the quality of data) (International Hydrographic Organization, 2018), the TECSOU has been applied to all source data within the CHS's BDB to describe how the particular data set was acquired. Analysis of the CHS's BDB indicated that data preparation was required prior to undertaking a bathymetric gap analysis.

2.4.3.1 Data Preparation

Data preparation involved interrogating the regional databases for objects coded with multiple TECSOU attributions. A total of 122 files were identified as containing multiple TECSOU, the majority of those being a combination of SBES and MBES, and were split into separate unique files by investigating the sounding level attribution. At the sounding level, extended flag attribution identified the platform by which the sounding was acquired, and a lookup table was used to correlate the platform to the sounding acquisition hardware. This enabled soundings collected by MBES hardware to be exported separately from those acquired by SBES data. Once exported, new metadata records and feature objects were created and then uploaded in to the CHS BDB.

For this study, all data were filtered into two distinct groups, 1) Multibeam, LiDAR, Vertically Swept Acoustic System (MLV) and 2) Other Acquisition Types (OAT).

Data attributed with TECSOU of MBES, Light Detection and Ranging (LiDAR) or Vertically Swept Acoustic System were selected from the regional bathymetric databases for file conversion and analysis. Careful consideration was done to exclude elevation data collected by LiDAR surveys, which are stored in the bathymetric database for ease of access for further assessment. This significantly decreased the number of files and introduced efficiency in the overarching processing time.

MLV Filter Parameters:

> *(TECSOU CONTAINS { 'found by multi-beam' } OR TECSOU CONTAINS { 'found by laser' } OR TECSOU IS { 'swept by vertical acoustic system' }) AND NOT valsta IS { 'Validated elevation data/Données d''élévation validées' }*

Other Acquisition Technique(s) (OAT) Layer is all other digital holdings within CHS' bathymetric database acquired through data acquisition techniques outside of those covered by the MLV layer. Much of this data is in point cloud format. To handle overlapping data points, a simple rule was applied to the deconfliction of data during combines, where survey start date was the newest.

OAT Filter Parameters:

NOT[(TECSOU CONTAINS { 'found by multi-beam' } OR TECSOU CONTAINS { 'found by laser' } OR TECSOU IS { 'swept by vertical acoustic system' }) AND NOT valsta IS { 'Validated elevation data/Données d''élévation validées' }]

A total of 17,169 sources were used in this analysis.

2.4.3.2 Data Combining

To combine the various data types and to deal with the multiple resolutions, all sources contributing to the MLV layer were combined at a 10 m resolution. The resulting CARIS Spatial Archive Raster (CSAR) files were then converted to 32-bit GeoTIFF format, projected to WGS84/World Mercator (EPSG:3395) and export from CARIS BDB.

As the OAT layer is all point cloud data, the data were combined at a 10 m resolution. Although point cloud data does not have a resolution, tools within CARIS Base Editor allow users to define a resolution during the 'combine' process, which set the node spacing for the output coverage. Each node, which can be conceptualized as a bin, contain all data that geographically fall within the limits of the node (**Figure 5**). Since point cloud data uses the true position of the sounding, it is seldom that two or more soundings will exhibit the exact same latitude and longitude coordinates. For soundings that are less than 10 m apart in any horizontal direction, deconfliction must occur so that the algorithm selects the desired contributor. To accomplish this, a deconfliction rule that interrogates the temporal frame in which the survey was conducted and chooses the most recent survey is assigned during the combine process to ensure more modern data would be selected for the resulting node value. At this point, the data was projected to WGS84/World Mercator and exported to ASCII, parsed into simple latitude, longitude, and depth (XYZ) files.

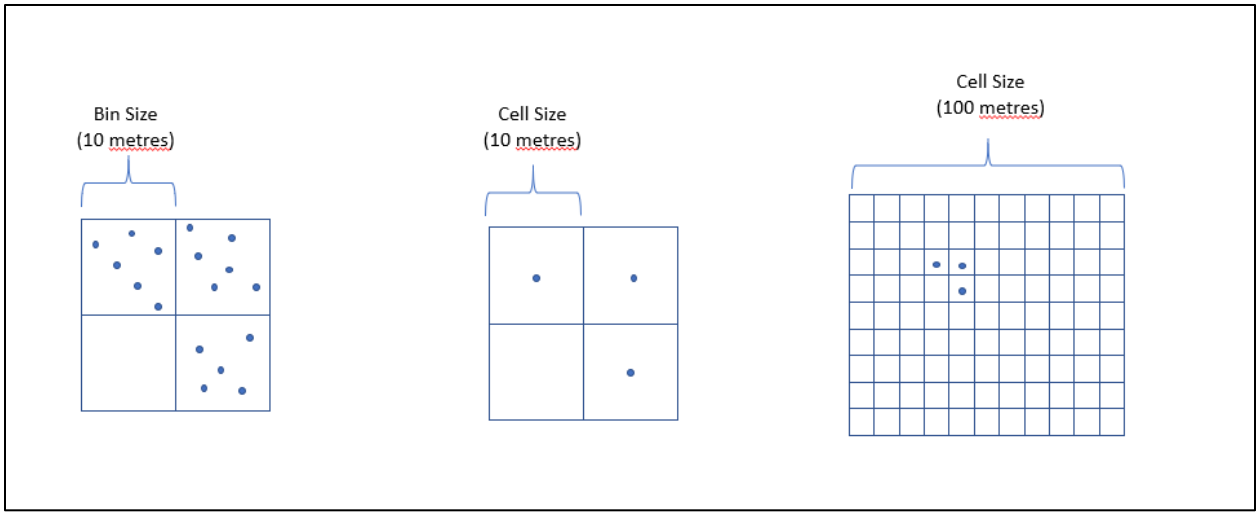

Figure 5. OAT layer conversion. The bin size of 10-meters showing the density of the actual sounding data points contained within (Left). This is converted to cell size based on resolution defined by the user and representative soundings are generated (Middle). Overall representative sounding density within a 100-meter cell for use in ArcGIS in downstream process (Right).

2.4.3.3 Data Integration

A base raster was required to set the framework for this analysis and created by importing the coastline, shoreline, and EEZ limits shapefiles into ArcGIS, projected at Canada Albers Equal Area Conic (CAEAC) (EPSG:102001). Vector polygons were then generated to fill in between the limits of the three intersecting boundaries, and then dissolved to create the fewest number of polygons possible. Following the dissolve, the polygons were rasterized at 100 m resolution and each cell was classified to separate cells between the shoreline and the EEZ from any cells that fell on land. Cells within the area of interest were then extracted, resulting in a single raster extending from shoreline to the EEZ with all 100 m resolution. This base raster was then split at the Gap Analysis Regional Boundaries (**Figure 1d**) for ease of processing.

With the base raster generated, the MLV layer was integrated. The MLV layer was imported into ArcGIS and then converted to 1-bit (binary) GeoTIFF to increase processing efficiency. The resulting 1-bit GeoTIFFs were then mosaiced and reprojected to CAEAC. During this process, the MLV layer was resampled using nearest neighbor (as this technique does not change the value of the cell from the input layer) at 100 m and snapped to the base raster to ensure resolutions were

consistent across all layers and that the cell limits aligned. Nearest neighbor is simplistic in that it takes the cell center form the input raster to determine the closest cell center of the output raster. The simplicity of this process increases efficiency in processing time. Once the mosaic was generated, the cells were reclassified into two distinct classes to identify the differences between cells that contain data and cells that do not contain data. The classification was exaggerated for data present cells allowing those cells to be easily identifiable in downstream processes. At this step we are left with a MLV layer that is 100 m resolution in CAEAC projection and classified as 300 (data) and 1 = void of soundings. The mosaiced MLV layer does not extend to the limits of Canada's EEZ, and therefore the two rasters, the base raster and the MLV raster, were combined. Considerations were made to ensure areas of no-data were removed from this analysis by utilizing the Condition Is Null argument. The map algebra expression used was:

Con(IsNull("MLV_layer"), 0, "MLV_layer")+Con(IsNull("BaseLayer"), 0 "BaseLayer")

The end result has these cells classified as class 3 which is Full Bottom Coverage. It is important to note that regardless of the extent of MLV coverage within a 100-meter cell, the cell will be classified as the highest level (3) and will be regarded as full bottom coverage (**Figure 6**).

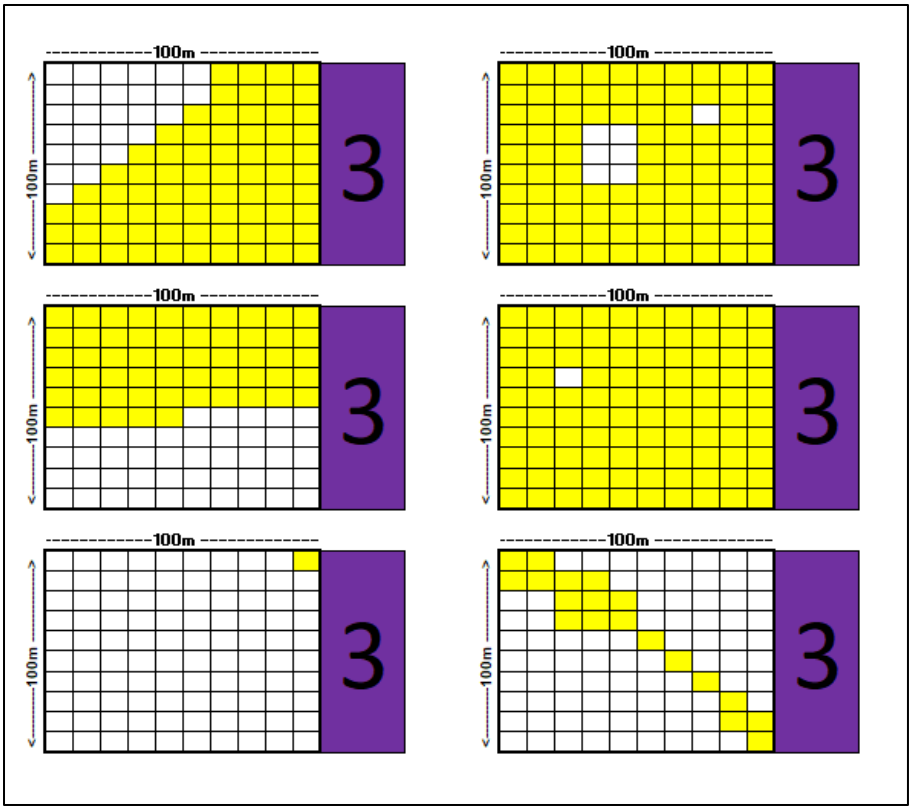

Figure 6. Examples of 100-meter resolution cells contain various degrees of coverage acquired from MLV sources. All cells will be considered 'Full Bottom Coverage" classification group 3.

The point data stemming from the OAT layer was imported into ArcGIS and projected to CAEAC and then converted to raster using the Point to Raster tool where the cell size was set to 100-meters and the cell assignment type was set to Count, which resulted in cells attributed with a value from 1 to 100 (**Figure 7**).

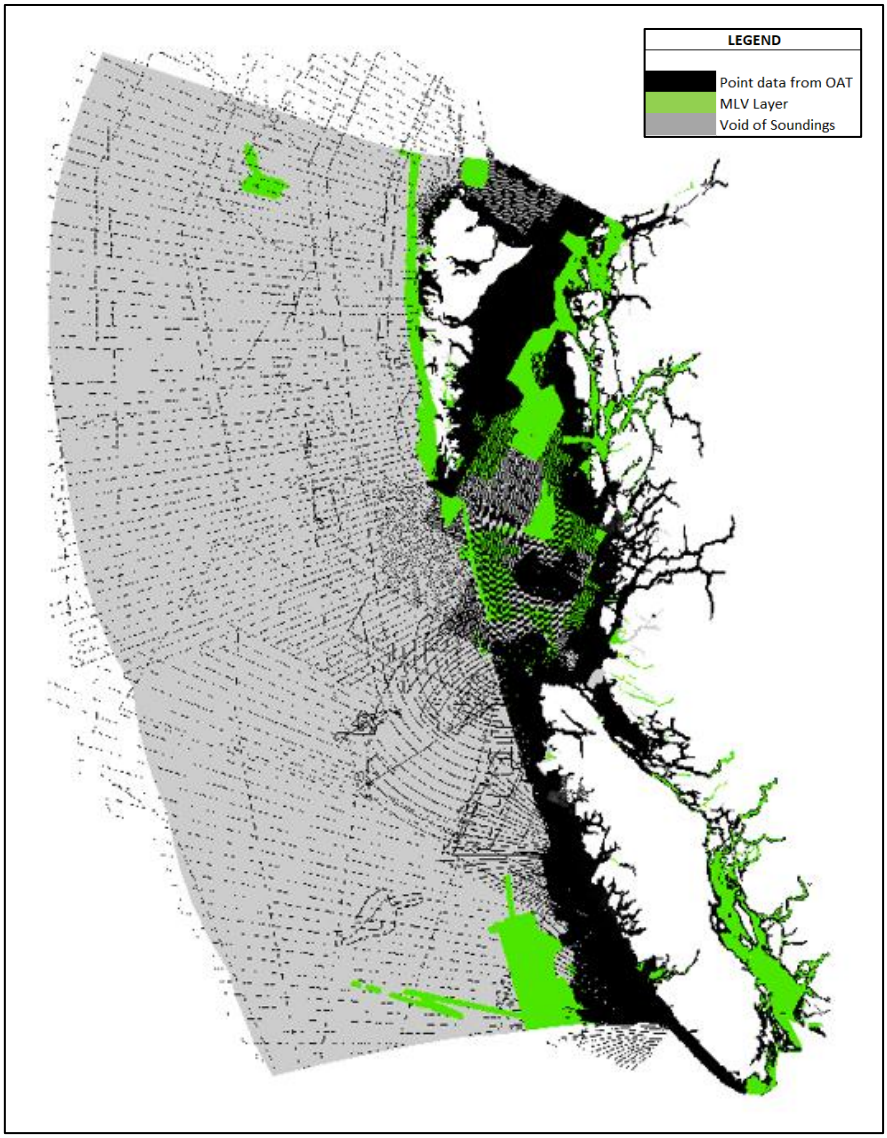

Figure 7. Pacific region raster where the grey raster is the classified as void of soundings, the green is classified as 300 (MLV) and the black is the data points from the OAT prior to clipping and reclassifying

The next step was to reclassify the raster to account for the sounding density to align with NOAA, where 1-2 representative soundings are classified as minimal coverage and greater than 3 representative soundings are classified as moderate coverage. For the reclassification at this stage, once again the cell values are exaggerated to ease downstream processes. The reclass during this step is: 1 – 2 = 1000, 3 – 100 = 2000, NoData = 5000. After reclassifying the OAT layer, the resulting raster was clipped to contain all data with the limits of this study.

The final Canadian Bathymetric Gap Analysis epoch 2023 (CBGAe2023) is then a merge of the MLV classification raster and OAT classification raster using the Raster Calculator which is simply the MLV + OAT followed by a reclassify (**Table 5**), visualized in **Figure 8**.

Table 5. Final Reclassify and classification terms

Output classification	Reclassify	Terms
1001	1	Minimal Coverage
1300	3	Full Bottom Coverage
2001	2	Moderate Coverage
2300	3	Full Bottom Coverage
5001	0	Gap – Void of Soundings
5300	3	Full Bottom Coverage

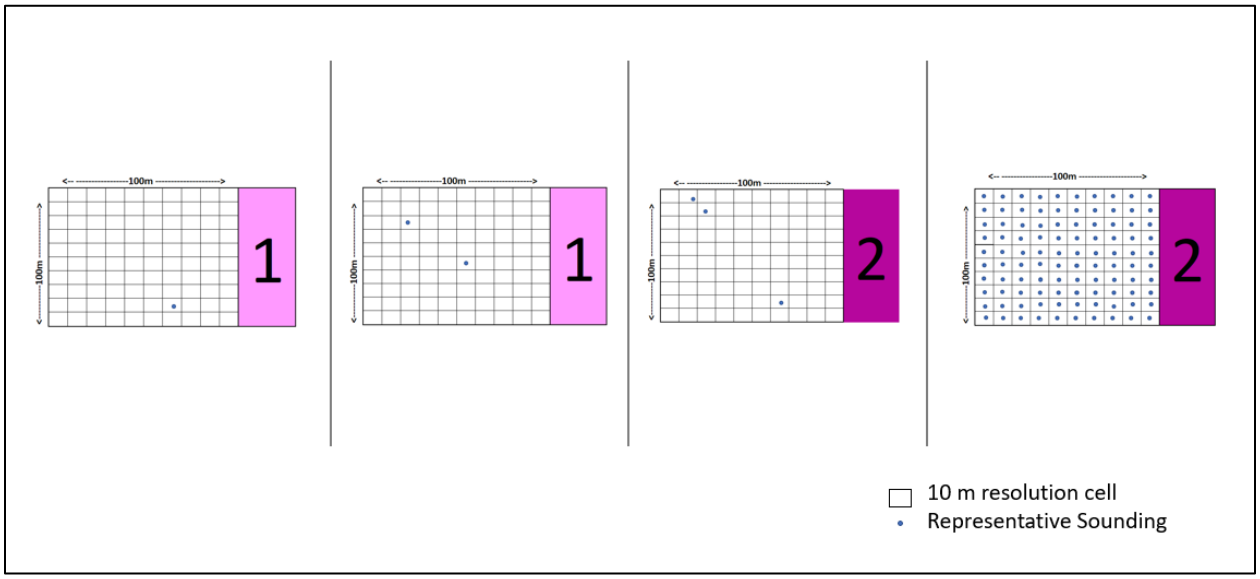

Figure 8. Representative soundings and their associated classification based on sounding density within a 100-meter resolution cell.

The output raster is clipped to the base layer to ensure all data is contained within Canada's EEZ, symbolized for visual representation (**Figure 9**), and calculated to determine the percentage of each classification group.

Figure 9. Sample of the final symbolized raster. Dark purple is full bottom coverage. medium purple is moderate coverage, light purple is minimal coverage, grey is gaps - void of soundings, and white is no-data (i.e. land).

2.5 Results and Discussion

2.5.1 Canada

A visual representation of CBGAe2023 are presented in **Figure 10**. Nationally, there remains a large gap in direct measurements of the seafloor. Results show that 84.89% of the seafloor has not been investigated by direct measurement. This represents 4.99 million km^2 of the seafloor that remains unobserved. Of the areas where direct measurements have been measured, 15.11% of the seafloor is known. This is where the coverage due to the soundwave footprint on the seafloor achieves full bottom coverage and where full object detection can be confidently stated. This represents 705,879 km^2 of modern techniques in seafloor mapping technologies. Minimal coverage and moderate coverage make up the rest of the gap analysis classifications at 1.34% and 0.24%, respectively.

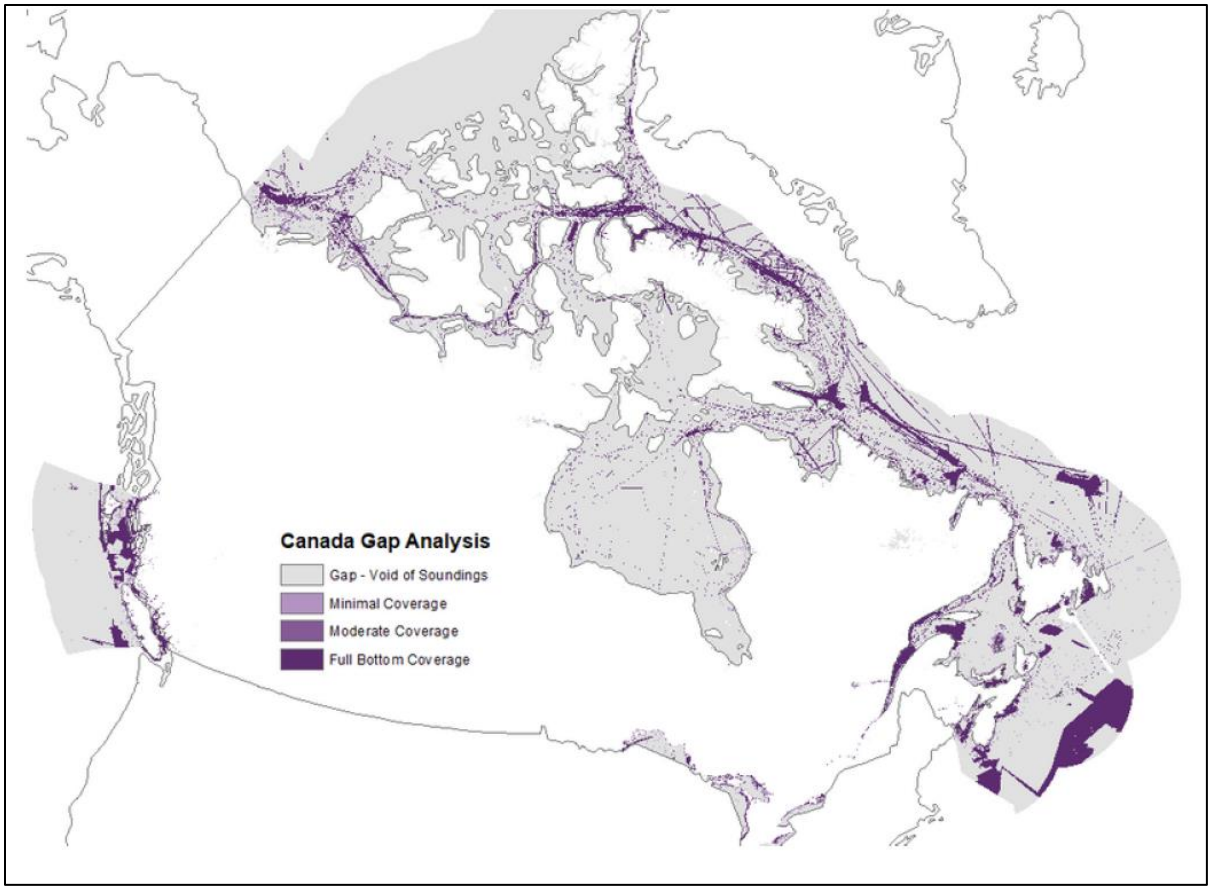

Figure 10. Visual representation of the Canadian Bathymetric Gap Analysis epoch 2023 (CBGAe2023).

The Canadian Arctic shows substantial gaps in bathymetry with 3.248 million km^2 void of soundings. CBGAe2023 results show that Eastern Arctic has 255,021 km^2 with full bottom coverage, which is proportionally higher than the Western Arctic with only 89,818 km^2, a difference of 165,203 km^2 more seafloor directly observed in the Eastern Arctic. This is attributed to the Canadian Arctic accessibility and the Canadian Coast Guard (CCG) deployment sites. Of the eight icebreakers in the CCGs compliment, seven transit to the Arctic via the Labrador Sea, departing from either Quebec City, QC, or St. John's NL (Fisheries, Oceans and the Canadian Coast Gaurd, 2023), acquiring bathymetric information along the way. In general, much of the coverage is along the Northern Low Impact Shipping Corridors (**Figure 11**).

In 2016, Canada committed to a $1.5 billion initiative to protect Canada's oceans, called Ocean Protection Plan (OPP) (Government of Canada, 2020). This initiative is a national strategy to protect Canada's oceans and coastline, improve marine navigation safety, and improve economic

opportunities for Canadians (Arctic Council, 2021). The CHS' role in OPP is to conduct hydrographic surveys to support the safety of marine transportation. Identifying target areas and developing an accompanying prioritization was undertaken by the Department of Fisheries and Oceans between 2016 and 2017. The result of that study was the creation of the Northern Marine Transportation Corridors (NMTC) in Canadian waters (Chénier et al., 2017), now called the Low Impact Shipping Corridor (LISC) (Dawson et al., 2019). Since 2016, Canada has been using the Northern Low Impact Shipping Corridor (**Figure 11**) which has been integrated into the Canadian Priority Planning Tool, as a means to target areas for hydrographic soundings. (Chénier et al., 2020). Currently DFO is reporting that 44.7% of the LISC has been surveyed to modern standards (Canadian Hydrographic Service, 2023). This number was derived from an analysis from the bounding polygons of the hydrographic survey returns.

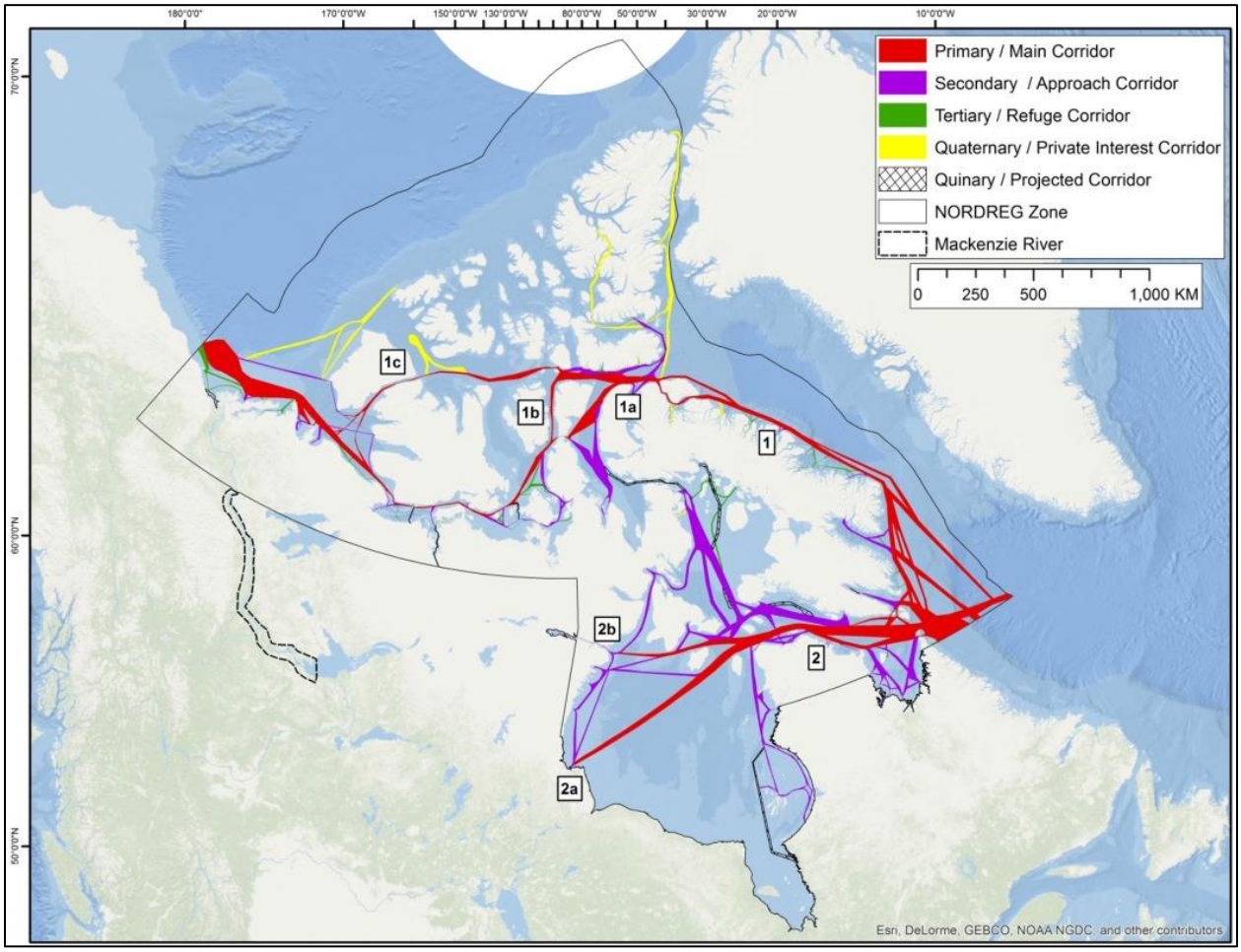

Figure 11. Canada's marine transportation Low Impact Shipping Corridors (Source: (Chénier et al.,2017))

The LISC covers a total of 608,528 km^2 across the Canadian Arctic; however, our study shows that only 29.93% (182,156 km^2) have full bottom coverage, and a total of 193,738 km^2 have a sounding. A total of 414,790 km^2 of the LISC have not been directly observed by modern survey techniques. This is a 14.77% difference from current DFO reporting; although whichever way it calculated, it is evident that there are significant gaps remaining in the Canadian Arctic which can have detrimental risks to safety. This was highlighted by the recent marine incident where on August 24, 2018, the passenger vessel *Akademik Ioffe* struck ground causing extensive damage to the vessel. The vessel was transiting north-northwest of Kugaaruk, Nunavut, through an area not surveyed to modern standards. The location of the grounding was in a remote portion of the Canadian Arctic, which is normally covered in ice for much of the year and seldomly travelled due to the short navigation season (Transportation Safety Board of Canada, 2021); however, due to receding sea ice, the area was accessible at the time of the passenger vessel navigating. Examination by the Transportation Safety Board of Canada described the status of the sounding in the area at the time of the grounding as spot soundings that were acquired between 1984 through 1992 at a spacing of 2 kms (Transportation Safety Board of Canada, 2021). Spot soundings are typically reconnaissance in nature and acquired by helicopter, landing on sea ice and acquiring depth information from through ice echosounder, which acquires a single echo return. At a line spacing of 2 km, significant gaps in the bathymetry are present and unknown hazards are expected to exist.

Canada's Ocean Protection Plan, which ran from 2017-2022 saw an increase in hydrographic surveying efforts in the Canadian Arctic, targeting the main corridors of the LISC. A direct result of the funds invested into increasing navigational safety saw approximately 8,700 km^2 surveyed by contractors and approximately 103,200 km^2 acquired from the CHS lead missions (Béchard, 2023). Over the five-year span of OPP, 111,900 km^2 of seafloor coverage was acquired, averaging 22,380 km^2 per year. The overall effect of OPP improved the total seafloor coverage in the Canadian Arctic by 136.73% above previously known seafloor coverage. Taking CBGAe2023 as the baseline, we can predict that if similar investments and efforts are made to acquiring bathymetry in the Canadian Arctic, it will take another 18.5 years to complete the acquisition of seafloor coverage in the LISC. The Canadian government has since reinvested in the Ocean Protection Plan, coined OPP2, with an additional $3.5B. $84M of this investment will be directly

received by the CHS to expand on the seafloor coverage in Canada, directly contributing to safety to navigation (Fisheries and Oceans Canada, 2022).

The southern regions of Canada show a higher percentage of area with some level of seafloor coverage (**Table 6, Figure 12**). Compared to the national level of gaps in bathymetric coverage, Pacific, the Great Lakes and St. Lawrence River, Quebec and Atlantic all show a greater percentage of seafloor coverage, at 15.00%, 14.08%, 26.46%, and 20.84%, respectively. Pacific region is a self-contained region, geographically separated from connecting boundaries with the other regions. The majority of bathymetry acquired in the Pacific region is concentrated in the nearshore area, such as the Strait of Georgia, Queen Charlotte Sound and Hecate Strait where complex waterways and high population density are present (**Figure 13**). Offshore bathymetry is sparse. Soundings offshore were derived from OAT layer and can be attributed to SBES acquisition efforts of the past.

Table 6. CBGAe2023 results at both national and regional scales.

REGION	CLASS / UNIT	Gap in Coverage	Minimal Coverage	Moderate Coverage	Full Bottom Coverage
CANADA	*km²*	4,991,873	81,420	16,112	790,690
	%	84.89%	1.38%	0.27%	13.45%
PACIFIC	*km²*	375,610	9,281	1,861	68,260
	%	82.55%	2.04%	0.41%	15.00%
WESTERN ARCTIC	*km²*	1,490,709	12,323	2,291	89,818
	%	93.45%	0.77%	0.14%	5.63%
EASTERN ARCTIC	*km²*	1,758,094	11,462	4,608	255,021
	%	86.64%	0.56%	0.23%	12.57%
GREAT LAKES and St. LAWRENCE RIVER	*km²*	66,263	8,464	2,452	12,644
	%	73.77%	9.42%	2.73%	14.08%
QUEBEC	*km²*	99,875	8,216	1,531	39,452
	%	67.00%	5.51%	1.03%	26.46%
ATLANTIC	*km²*	1,201,345	31,674	3,368	325,501
	Percentage	76.92%	2.03%	0.22%	20.84%

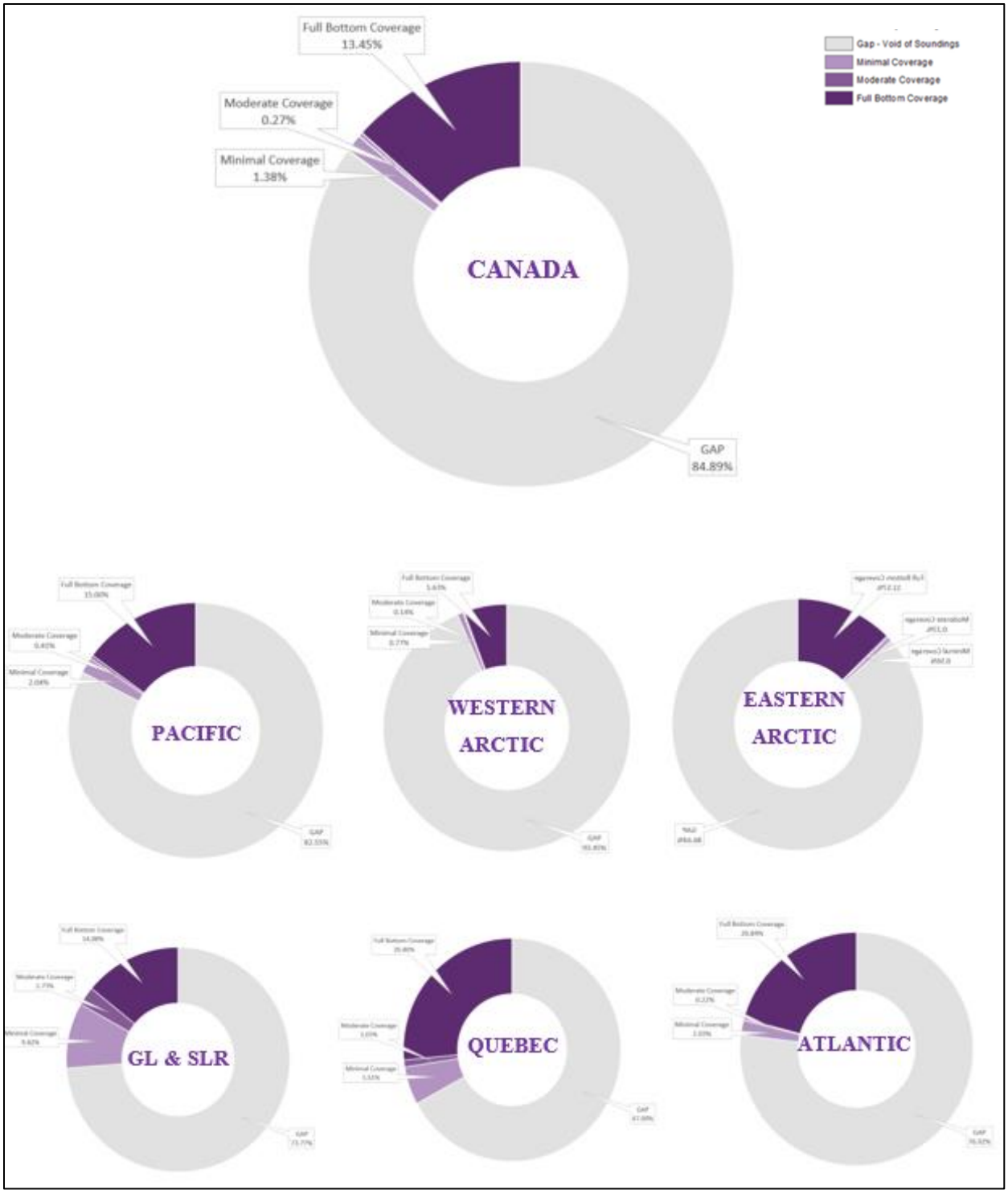

Figure 12. Final CBGAe2023 results at both national and regional scales. Considerable amount of gaps are present in all regions, and are especially evident in the Canadian Arctic.

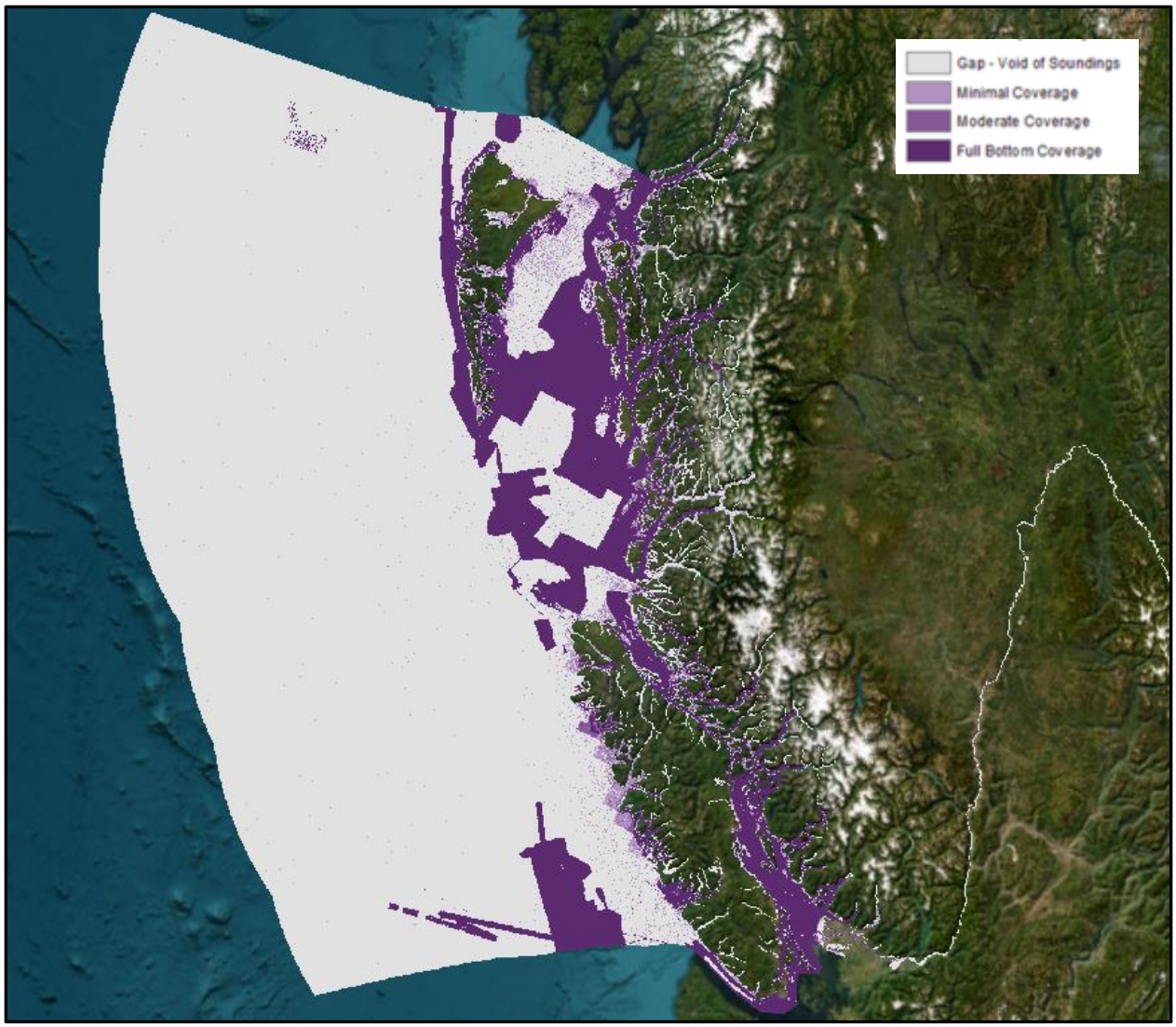

Figure 13. Pacific region bathymetric gap analysis results. Full bottom coverage is achieved in 15.00% and concentrated in the nearshore regions such as the Strait of Georgia, Queen Charlotte Sound and Hecate Strait. Many bathymetric gaps are present (82.55%) but are main offshore due to sparse soundings.

Quebec and Atlantic region have the most complete compliment of seafloor coverage compared to the other regions at 26.46% and 20.84% respectively. Quebec region is substantially smaller in geographic area compared to Atlantic region at approximately 1/10th the size; however, Quebec shows only 67.00% (99,875 km^2) are void of soundings compared to Atlantic region at 76.92% (1,201,345 km^2). Geographically, full bottom coverage has been achieved in the Quebec region for the mouth of the St. Lawrence River through to the Quebec/Ontario boarder. Efforts have been concentrated here due to the narrow marine navigational channels and complex and shallow

waterways (**Figure 14a**). Hydrographic survey efforts in this region are to collect bathymetry on highly dynamic areas where geomorphological phenomena such as silting occur on a regular basis. Pre and post dredge surveys are conducted bi-annually; therefore, the resources are spent ensuring highly dynamic areas are mapped so ensure safety to navigation. Navigational aids mark the channels indicating routes for safe passage. So, although the area is geographically small in comparison to the Atlantic region, resources are not spent on ensuring bathymetry is acquired from shoreline to the international boarder, thus priority of hydrographic survey efforts are not aimed at 'filling the gaps'. Atlantic region on the other hand is geographically more open ocean. There is evidence of heavy seafloor mapping efforts concentrated on the Grand Banks and the continental shelf extending to the Sohm Abyssal Plain in the North Atlantic Ocean. Much of the nearshore bathymetry has been observed by LiDAR missions. Opportunistic MBES surveys track lines are evident as well, indicating the transit from Quebec City, Quebec and St. John's, Newfoundland moving northward towards the eastern Arctic (**Figure 14b**). Over 1.2M km^2 are still void of soundings in the Atlantic region.

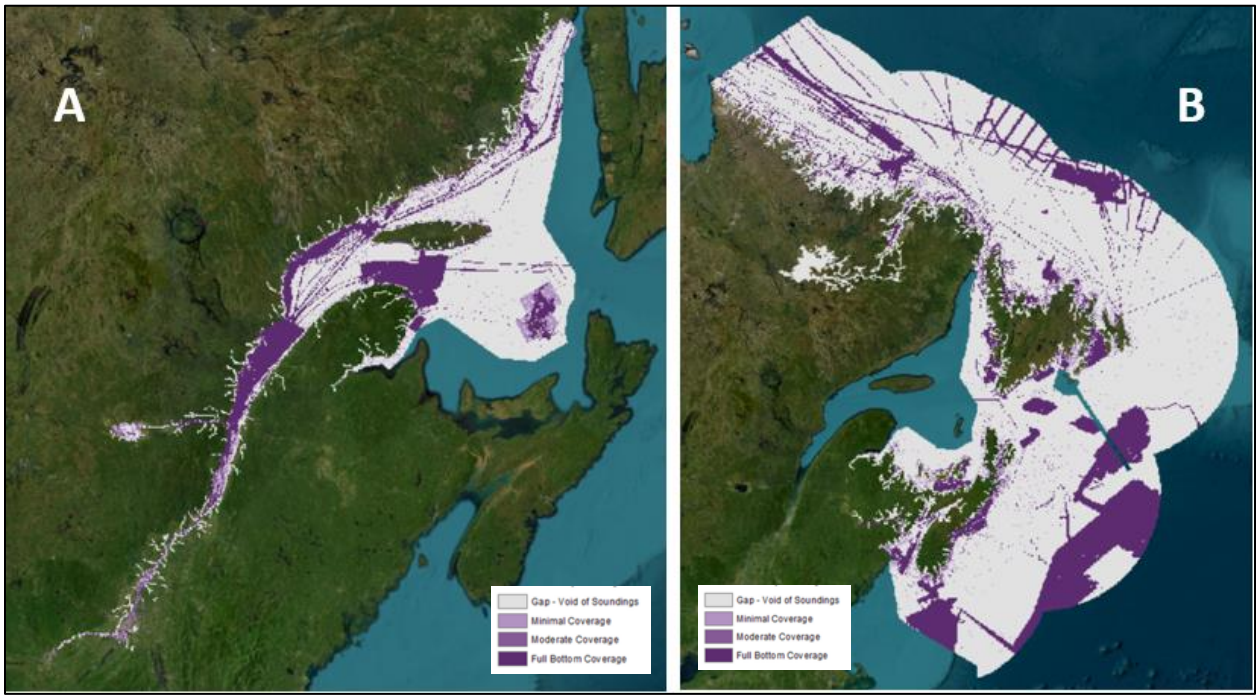

Figure 14. Overview of A) Quebec regional bathymetric gap analysis results B) Atlantic regional bathymetric gap analysis results.

Overall, assuming a similar rate of coverage of 1.5% from GEBCO's 2022 to 2023 reporting, Canada is on pace to obtain fill all bathymetric gaps by 2079. This would equate to approximately 75,000 km^2 per year would need to be surveyed; however, if Canada continues to support bathymetric coverage at a similar rate as those seen during the Oceans Protection Plan at an average of 22,380 km^2 per year, it can be projected to achieve full bottom coverage by 2246. Although Seabed 2030 initiative has the goal of 'mapping' the world's oceans by 2030, the results of this study show that at the current rate, Canada will not be able to obtain that goal. Canada will extend well beyond the 2030 target and bypass NOAA's target date of 2060. Moreover, this study will set a baseline for which comparisons can be kept to monitor rate of change in seafloor mapping for future iterations to redefine the target date as mapping initiatives continue to progress in the following years.

2.5.2 Results for Lakebed 2030 Initiative

The Great Lakes Overserving System (GLOS), is a non-profit organization that provides data services to support scientific communities, policy makers, and industry in both Canada and the United States of America, with the goal of improving marine navigational safety, protecting the nations freshwater environment and enhancing the Great Lakes economy. GLOS has a short list of priorities, one of which is Lakebed 2030. Modelled after Nippon Foundation's Seabed 2030 initiative, Lakebed 2030 aims to 'map' the Great Lakes at a high-density (Great Lakes Observing System, 2021). Current analysis conducted and published by the team at GLOS states that 15% of the Great Lakes have been mapped to a high-density. GLOS's analysis considers both Canadian and U.S. waters.

The results we present in this study are targeted at Canadian territorial waters only, and thus a comparison to GLOS analysis does not encompass the same parameters; however, the results from this study show that 25.69% (23,332 km^2) of Canadian waters contain a sounding at a 100-meter resolution (**Table 7, Figure 15**). It is noted that Lake Erie is vastly void of soundings. 84.08% of cells are void of soundings; however, this is a function of source data not yet being integrated into the CHS' BDB at the time of this study. Recent efforts have been directed at safe navigation of low impact shipping corridors in the Canadian Arctic, so efforts have not been widely applied to seek bathymetric coverage in the Great Lakes. Within the Great Lakes, hydrographic surveying efforts have been prioritized to survey highly dynamic and critical under-keel clearance areas.

Most survey acquisition resources are placed on the interconnecting waterways such as Detroit River, St. Claire River, Lake St. Claire, and St. Mary's River, as the Great Lakes are fairly safe for navigation.

Nautical charts of the Great Lakes show sparse soundings, which are not captured within this analysis, because those sounding are not digital nor have they been integrated in the CHS BDB; however, this is planned to occur in the coming years, thus increasing the density of soundings, which will be reflected in future iterations of this analysis. Lake Erie is a prime example of CHS's legacy data holdings that have not been integrated in the BDB. Although nautical charts of Lake Erie show scale-appropriate level of detail in bathymetry, our results indicate that 84.08% (12,612 km^2) of the lakebed are void of soundings (**Table 7**).

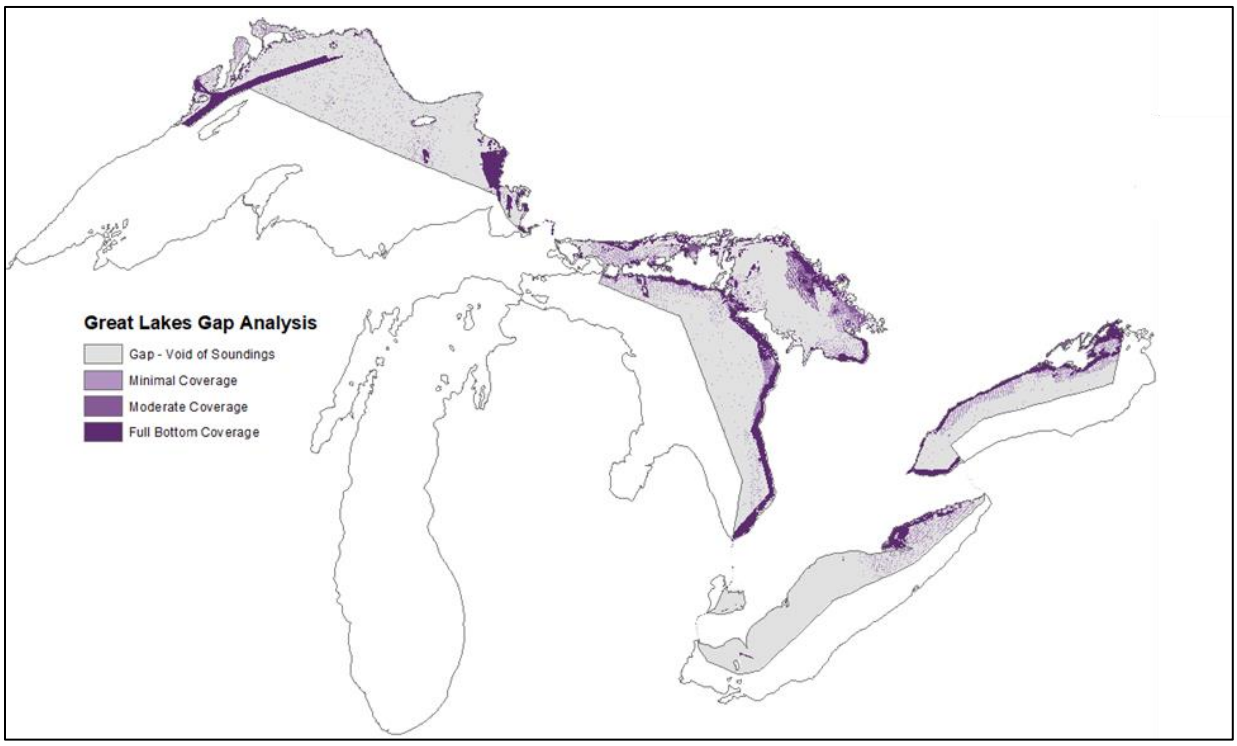

Figure 15. Canadian Bathymetric Gap Analysis results for the Great Lakes Observing System's Lakebed 2030 initiative.

Table 7. Bathymetric Gap Analysis results for the Great Lakes (Canadian waters only).

Lake	Class / Unit	Gap in Coverage	Minimal Coverage	Moderate Coverage	Full Bottom Coverage
	km^2	65,650	8,441	1,933	12,241

Great Lakes (excluding St. Lawrence River)	*%*	74.38%	9.56%	2.19%	13.87%
Lake Superior	*km²*	22,985	1,871	53	3,752
	%	80.20%	6.53%	0.19%	13.09%
Lake Huron	*km²*	24,435	4,505	1,612	5,432
	%	67.91%	12.52%	4.48%	15.10%
Lake Ontario	*km²*	6,546	1,184	206	2,119
	%	65.10%	11.78%	2.05%	21.07%
Lake Erie	*km²*	12,612	916	58	1,415
	%	84.08%	6.11%	0.38%	9.43%

A deep understanding of the geomorphic properties (bathymetry and size) of the Great Lakes will assist scientists in regional and global warming predictions (Zhong et al., 2019) as well as fish distribution, fish habitat (Rudolfsen et al., 2021), and geomorphic studies such as glacial isostatic adjustment (Clark et al., 2007), The Great Lakes prove safe drinking water for over 40 million people (Great Lakes Observing System, 2021) and accounts for 30% of the Canadian population (Office for Coastal Management, 2023). A marine incident within the Great Lakes would have devistating effects. High resolution bathymetry will assist in determinng marine incidnet response plans such as vunerable ecological areas within the Great Lakes basin that would be negativly affected by potential oil spills (The Great Lakes Science Advisory Board's Science Priority Committee, 2018). Canada's bathymetric coverage within the Great Lakes is only at 13.87% (12,241 km^2). More effort is needed to acquire lakebed coverage.

2.6 Conclusions

This is the first paper to conduct a consolidated effort to analyze the bathymetric gaps within Canada's territorial waters. Analysis of more than 17,000 sources were used for this work. This study presents a raster-based analysis where the bathymetric sounding data holdings were converted to raster cells and then classified based on meeting criteria that describe the coverage. This differs from other studies in that it ignores the vector layer bounding polygons and investigates the data holdings, i.e. the point cloud or gridded data itself. Our analysis shows that assessment based on the bounding polygon of hydrographic surveys in Canada overestimate the seafloor coverage within the potential low impact shipping corridors by 14.77% (89,880 km^2). The new methodology presented in this study aligns with NOAA, in that all raster cells are of equal

100-meter resolution and data density is considered for classification. Unlike GEBCO Seabed 2030 initiative and the CPPT, water depth was not considered. This was done by design to ensure alignment with NOAA so that bordering waterbodies, the Great Lakes, for example, can be compared using the same parameters. This study has introduced the classification full bottom coverage, which is an additional classification group from NOAA's bathymetric gap analysis classification groups. This study also moves away from the term 'mapped' as used by NOAA and other Hydrographic Offices, and adopts the terminology of 'coverage' to incorporate terminology accepted by the International Hydrographic Organization and published in Special Publication No. 44 (International Hydrographic Organization, 2020).

The results of this analysis found that Canada has a tremendous amount of their EEZ that is unobserved by direct measurements. Approximately 5 million square kilometers have not been surveyed. Applying a growth rate similar to GEBCO of 1.5% per year, will see all of Canada's EEZ with bathymetric coverage via direct measurement completed by 2079, well beyond the Seabed 2030 target; however, this would equate to approximately 75,000 km^2 per year of hydrographic surveying. At a rate similar to that acquired during the Oceans Protection Plan of 22,380 km^2 per year, complete bathymetric coverage in Canada can be achieved by 2246, an additional 216 years past the target of 2030. More effort and resources must be committed to accomplish full bathymetric seafloor coverage in a reasonable timeframe. Building a digital twin of Earth's ocean will help scientist in a wide range of disciplines increase their knowledge and understanding of critical processes that affect us all, including climate change, policy making, marine and navigational safety among others. High resolution bathymetry is fundamental in gaining this understanding but more effort and resources are required to accomplish .

2.7 References

Arctic Council. (2021). *Overview of Low Impact Shipping Corridors & Other Shipping Managemetn Schemes.* Akureyri - Iceland: Arctic Council.

Béchard, G. (2023). United States-Canada Hydrographic 46th Commission. *US Hydro* (pp. 1-12). Mobile, Alabama: Canadian Hydrographic Service. Retrieved from https://iho.int/uploads/user/Inter-

Regional%20Coordination/RHC/USCHC/USCHC46/USCHC46-3A_2023_EN_CA%20National%20Report%20-presentation-%20final.pdf

Byers, M., & Østhagen, A. (2017). Why does Canada have so many unresolved maritime boundary disputes. *Canadian Yearbook of International Law, 54*, 1-62. doi:10.1017/cyl.2017.14

Canadian Hydrographic Service. (2012, January 1). *Defining Canada's Maritime Zones.* Retrieved April 26, 2022, from Government of Canada Publications: https://publications.gc.ca/collections/collection_2012/mpo-dfo/Fs23-571-2011-eng.pdf

Canadian Hydrographic Service. (2022, October 12). *About the Canadian Hydrographic Service*. Retrieved 11 02, 2022, from Nautical Charts and Services: https://www.charts.gc.ca/help-aide/about-apropos/index-eng.html

Canadian Hydrographic Service. (2023, May 17). *Arctic Charting*. Retrieved from Canadian Hydrographic Service: https://www.charts.gc.ca/arctic-arctique/index-eng.html

Charette, M. A., & Smith, W. H. (2010, June). The Volume of Earth's Ocean. *Oceanography, 23*(2), 112-114.

Chénier, R., Abado, L., & Martin, H. (2018). CHS Priortiy Planning Tool (CPPT) - A GIS Model for Defining Hydrographic Survey and Charting Priorities. *International Journal of Geo-Information, 7*(240). doi:https://doi.org/10.3390/ijgi7070240

Chénier, R., Abado, L., Sabourin, O., & Tardif, L. (2017). Northern marine transportation corridors: Creation. *Transactions in GIS, 21*, 1085-1097. doi:https://doi.org/10.1111/tgis.12295

Chénier, R., Sagram, M., Omari, K., & Jirovec, A. (2020). Earth Observation and Artificial Intelligence for Improving Safety to Navigation in Canada Low-Impact Shipping Corridors. *ISPRS International Journal of Geo-Information, 9*(6), 383. doi:10.3390/ijgi9060383

Clark, J. A., Zylstra, D. J., & Befus, K. M. (2007). Effects of Great Lakes Water Loading upon Glacial Isostatic Adjustment and Lake History. *Journal of Great Lakes Research*, *33*(3), 627-641.

Contarinis, S., & Kastrisios, C. (2022). Marine spatial data infrastructure. The Geographic Information Science & Technology Body of Knowledge (1st Quarter 2022 Edition).

Cubukcu, N., Pfeffer, R. L., & Dietrich, D. E. (2000). Simulation of the Effects of Bathymetry and Land–Sea Contrasts on Hurricane Development Using a Coupled Ocean–Atmosphere Model. Journal of the Atmospheric Sciences, 57(4), 481-492. https://doi.org/10.1175/1520-0469(2000)057<0481:SOTEOB>2.0.CO;2

Dawson, J., Carter, N. A., Reid, M. B., Lalonde, S., Orawiec, A., Pelot, R., & Schmitz, P. (2019, February 4). Development and Management of Low-Impact Shipping Corridors in Nunavut. Retrieved from University of Ottawa: https://ruor.uottawa.ca/bitstream/10393/40068/1/FINAL_Discussion_Paper.pdf

Dias, T. G. (2021, May 31). Program Seamap 2030 - 100% of the Portuguese maritime spaces mapped by 2030. International Hydrographic Review, 27. Retrieved from https://ihr.iho.int/articles/program-seamap-2030-100-of-the-portuguese-maritime-spaces-mapof-the-portuguese-maritime-spaces-mapped-by-2030/

Dierssen, H. M., & Theberge Jr., A. E. (2014). Bathymetry: History of Seafloor Mapping. Encylopedia of Natural Resources. doi:10.1081/E-ENRW-120047531

Evagorou, E., Mettas, C., Agapiou, A., Themistocleous, K., & Hadjimitsis, D. (2018, April). Bathymetry mapping with remote sensing methods for supporting Marine Spatial Planning in Cyprus. In EGU General Assembly Conference Abstracts (p. 3492).

Fisheries and Oceans Canada. (2022, August 10). New Oceans Protection Plan funding will bolster Canadian Coast Guard and Canadian Hydrographic Service in the Arctic. Retrieved from Fisheries and Oceans Canada: https://www.canada.ca/en/fisheries-oceans/news/2022/08/new-oceans-protection-plan-funding-will-bolster-canadian-coast-guard-and-canadian-hydrographic-service-in-the-arctic.html

Fisheries, Oceans and the Canadian Coast Gaurd. (2023, June 22). Canadian Coast Guard begins 2023 Arctic Season. Retrieved from Canada: https://www.canada.ca/en/canadian-coast-guard/news/2023/06/canadian-coast-guard-begins-2023-arctic-season.html

Forrester, W. D. (1983). Canadian Tidal Manual. Ottawa: Department of Fisheries and Oceans.

Foster, B., Hart, K., & Beduhn, T. (2017, March 6). What Can Variable Resolution Do For You? Retrieved from Teleydne CARIS HIPS/SIPS: https://www.teledynecaris.com/en/products/hips-and-sips/

Galway, R. S. (2000). Comparision of Target Detection Capablilities of the Reson Seabat 8101 and Reason Seabat 9001 Multibeam Sonars. Univsersity of New Brunswick, Department of Geodesy and Geomatics Engineering. Fredricton: University of New Brunswick. Retrieved November 5, 2022, from http://www.omg.unb.ca/omg/papers/MBSS_TermPaper.pdf

GEBCO. (2008). General Bahtymetric Chart of the Oceans (GEBCO): The GEBCO_08 Grid. Retrieved from General Bahtymetric Chart of the Oceans: https://www.gebco.net/data_and_products/gridded_bathymetry_data/documents/gebco_08.pdf

GEBCO. (2022). Mapping Progress. Retrieved from General Bathymetric Chart of the Oceans: https://seabed2030.org/mapping-progress

GEBCO. (2022). The GEBCO_2022 Grid. Retrieved from General Bathymetric Chart of the Oceans: https://www.gebco.net/data_and_products/gridded_bathymetry_data/gebco_2022/

GEBCO Complilation Group . (2021). GEBCO 2021 Grid. Retrieved from The Nippon Foundation - Gebco-Seabed 2030 Project: https://www.gebco.net/data_and_products/gridded_bathymetry_data/gebco_2021/

GEBCO, T. N. (2023). Seabed 2030 Our Mission. Retrieved from The Nippon Foundation - Seabed 2023: www.seabed2030.org/our-mission

Gille, S. T., Metzger, E. J., & Tokmakian, R. (2004). Seafloor topography and ocean circulation. OCEANOGRAPHY-WASHINGTON DC-OCEANOGRAPHY SOCIETY-, 17(1), 47-54.

Government of Canada. (2020, July 08). Ocean Protection Plan. Retrieved from Government of Canada: https://tc.canada.ca/en/initiatives/oceans-protection-plan

Great Lakes Observing System. (2021, January 1). Great Lakes Observing System - Lakebed 2030. Retrieved from Great Lakes Observing System: https://glos.org/priorities/lakebed-2030/

Guinan, J., McKeon, C., O'Keeffe, E., Monteys, X., Sacchetti, F., Coughlan, M., & Nic Aonghusa, C. (2021). INFOMAR data supports offshore energy development and marine spatial planning in the Irish offshore via the EMODnet Geology portal. Quarterly Journal of Engineering Geology and Hydrogeology, 54(1), qjegh2020-033.

Hu, M., Jin, T., Jiang, W., Chu, Y., Wen, H., & Li, J. (2022). Bathymetry Model in the Northwestern Pacific Ocean Predicted from Satellite Altimetric Vertical Gravity Gradient Anomalies and Ship-Board Depths. Marine Geodesy, 45(1), 24-46. doi: 10.1080/01490419.2021.1943576

Integrated Ocean & Coastal Mapping. (2023). Status of Seafloor Mapping Within U.S. Waters. Retrieved August 8, 2023, from Integrated Ocean & Coastal Mapping: https://iocm.noaa.gov/seabed-2030-status.html

International Hydrographic Organization. (2018, January). International Hydrographic Organization ENC Creation. Retrieved from Intarnational Hydrographic Organization: https://iho.int/iho_pubs/standard/S-57Ed3.1/S-57%20Appendix%20B.1%20Annex%20A%20UOC%20Edition%204.1.0_Jan18_EN.pdf

International Hydrographic Organization. (2020, September). S-44 Standards for Hydrographic Surveys ed. 6.0.0. Retrieved from International Hydrographic Organization: https://iho.int/uploads/user/pubs/standards/s-44/S-44_Edition_6.0.0_EN.pdf

International Hydrographic Organization. (2020, September). Standards and Specificaitons: S-67. Retrieved from International Hydrographic Organization: https://iho.int/uploads/user/pubs/standards/S-67/S-67%20Ed%201.0.0%20Mariners%20Guide%20to%20Accuracy%20of%20Depth%20Information%20in%20an%20ENC_EN.pdf

Kanari, M., Tibor, G., Hall, J. K., Ketter, T., Lang, G., & Schattner, U. (2020). Sediment transport mechanisms revealed by quantitative analyses of seafloor morphology: New evidence from multibeam bathymetry of the Israel exclusive economic zone. Marine and Petroleum Geology, 114, 104224.

Khazaei, Bahram, et al. "GLOBathy, the global lakes bathymetry dataset." Scientific Data 9.1 (2022): 36.

Kitchel, Z. J., Selden, R. L., Pinsky, M. L. (2022). The Role Of Continental Shelf Bathymetry In Shaping Marine Range Shifts In the Face Of Climate Change. Global Change Biology, 17(28), 5185-5199. https://doi.org/10.1111/gcb.16276

Lecours, V., Lucieer, V. L., Dolan, M. F., & Micallef, A. (2015). An ocean of possibilities: applications and challenges of marine geomorphometry.

Manson, G. K., Couture, N. J., & James, T. S. (2019). CanCoast 2.0: data and indices to describe the sensitivity of Canada's marine coasts to changing climate. Geological Survey of Canada. doi:https://doi.org/10.4095/314669

Mayer, L., Jakobsson, M., Allen, G., Dorschel, B., Falconer, R., Ferrini, V., . . . Weatherall, P. (2018, February 8). The Nippon Foundation - GEBCO Seabed 2030 Project: The Quest to See the World's Oceans Completely Mapped by 2030. Geosciences, 8(2). doi:10.3390/geosciences8020063

Nation, J. (2022). NOAA NCEI Bathymetry Team: Data Contribution, Sharing, Accessibility and Archive Overview. Lakebed 2030 Conference. Traverse City, Michigan: National Oceanic and Atmospheric Administration. Retrieved September 29, 2022

National Oceanic and Atmospheric Administration. (2022). Progress Report: Unmapped U.S. Waters. NOAA. Retrieved April 6, 2022, from https://iocm.noaa.gov/documents/mapping-progress-report2022.pdf

National Oceanic and Atmospheric Administration. (2023). Progress Report: Unmapped U.S. Waters. NOAA. Retrieved April 6, 2023, from https://iocm.noaa.gov/documents/mapping-progress-report2023.pdf

Natural Resources Canada. (2019, March 01). CanVec Series. Ottawa, Ontario, Canada. Retrieved from https://open.canada.ca/data/en/dataset/8ba2aa2a-7bb9-4448-b4d7-f164409fe056

Nippon Foundation and GEBCO. (2022). About the Seabed 2030 Project. Retrieved November 2, 2022, from The Nippon Foundation - GEBCO Seabed 2030 Project: https://seabed2030.org/about-us

Office for Coastal Management. (2023, July 24). Fast Fact / Great Lakes. Retrieved from Office for Coastal Management - NOAA: https://coast.noaa.gov/states/fast-facts/great-lakes.html

Rattray, A., Ierodiaconou, D., Laurenson, L., Burq, S., & Reston, M. (2009). Hydro-acoustic remote sensing of benthic biological communities on the shallow South East Australian continental shelf. Estuarine, Coastal and Shelf Science, 84(2), 237-245.

Rudolfsen, T. A., Watkinson, D. A., Charles, C., Kovachik, C., & Enders, E. C. (2021). Developing habitat associations for fishes in Lake Winnipeg by linking large scale bathymetric and substrate data with fish telemetry detections. Journal of Great Lakes Research, 47(3), 635-647.

Santillan, J. R., & Makinano-Santillan, M. (2016, July). Vertical accuracy assessment of 30-M resolution ALOS, ASTER, and SRTM global DEMS over the Northeastern Mindanao, PhilippinesS. The International Archives of the Photogrammetry, Remote Sensing and Spatial Information Sciences, 12-19.

Satake, K. (1988). Effects of bathymetry on tsunami propagation: Application of ray tracing to tsunamis. Pure and Applied Geophysics, 126, 27-36.

Sepúlveda, I., Tozer, B., Haase, J. S., Liu, P. L.-F., & Grigoriu, M. (2020, September 9). Modeling Uncertanties of Bahtymetry Predicted with Satellite Altimery Data and Application to Tsunami Hazard Assessment. Journal of Geophysical Research: Solid Earth, 25. doi:10.1029/2020JB019735

Statistics Canada. (2016, October 07). International Perspective. Retrieved from Statistics Canada: https://www150.statcan.gc.ca/n1/pub/11-402-x/2012000/chap/geo/geo01-eng.htm

Teledyne CARIS. (2023). CARIS Bathy DataBASE Suite. Retrieved from Teledyne CARIS: https://www.teledynecaris.com/en/products/bathy-database/

The Great Lakes Science Advisory Board's Science Priority Committee. (2018). Potential Ecological Impacts of Crude Oil Transport in the Great Lakes Basin. International Joint Commission. International Joint Commission.

Tozer, B., Sandwell, D. T., Smith, W. H., Olson, C., Beale, J. R., & Wessel, P. (2019, August 8). Global Bathymetry and Topography at 15 Arc Sec: SRTM15+. Earth and Space Science, 6. Retrieved from https://doi.org/10.1029/2019EA000658

Transportation Safety Board of Canada. (2021). Marine transportation safety investigation report M18C0225. Ottawa: Transportation Safety Board of Canada.

United Nations Convention on the Law of the Sea. (2022, February 11). United Nations Convention on the Law of the Sea of 10 December 1982. Retrieved April 26, 2022, from United Nations: https://www.un.org/Depts/los/convention_agreements/texts/unclos/unclos_e.pdf

Wang, F., Wan, X., & Annan, R. F. (2022). Accuracy requirement for altimetry observations for bathymetry inversion using gravity anomaly and gravity gradients. Arabian Journal of Geosciences, 15(627). doi:https://doi.org/10.1007/s12517-022-09901-x

Weatherall, P., Marks, K. M., Jakobsson, M., Schmitt, T., Tani, S., Arndt, E., . . . Wigley, R. (2015, June 29). A new digital bathymetric model of the world's oceans. Earth and Space Science. doi:https://doi.org/10.1002/2015EA000107

Westington, M., Varner, J., Johnson, P., Sutherland, M., Armstrong, A., & Jencks, J. (2018). Assessing Sounding Density for a Seabed 2030 Initiative. 2018 Joint Canadian Hydrographic and National Surveyors' Conference. Victoria, British Columbia. Retrieved from https://www.eiseverywhere.com/ehome/chc-nsc2018/711593/

Wölfl, A.-C., Jencks, J., Johnston, G., Varner, J., & Devey, C. (2017). Identifying deep-sea target areas for a pilot Atlantic seabed mapping project using GIS techniques. Journal of Ocean Technology, 12(4), 28-42.

Wölfl, A.-C., Snaith, H., Amirebrahimi, S., Devey, C. W., Dorschel, B., Ferrini, V., . . . Wigley, R. (2019, June). Seafloor Mapping - The Challenge of a Truly Global Ocean Bathymetry. Frontiers in Marine Science, 6(283). doi:10.3389/fmars.2019.00283

Xie, S., Hafner, J., Tanimoto, Y., Liu, W. T., Tokinaga, H., and Xu, H. (2002). Bathymetric effect on the winter sea surface temperature and climate of the Yellow and East China Seas, Geophys. Res. Lett., 29(24), 2228, doi:10.1029/2002GL015884.

Xie, X., Liu, Q., Zhao, Z., Shang, X., Cai, S., Wang, D., & Chen, D. (2018). Deep sea currents driven by breaking internal tides on the continental slope. Geophysical Research Letters, 45(12), 6160-6166.

Yesson, C., Letessier, T. B., Nimmo-Smith, A., Hosegood, P., Brierley, A. S., Harouin, M., & Proud, R. (2020). Improved bathymetry leads to 4000 new seamount predictions in the global ocean. UCL Open: Environment Preprint.

Zhong, Y., Notaro, M., & Vavrus, S. J. (2019). Spatially variable warming of the Laurentian Great Lakes: an interaction of bathymetry and climate. Climate Dynamics, 5833-5848.

CHAPTER 3

3 Comparison of Barometric Pressure Enhanced Predicted Tides to Ellipsoid Referenced Hydrographic Surveys

3.1 Introduction

There has been a significant reduction in Arctic sea ice due to climate change (e.g., Moore & McNeil, 2018; Plank et al., 2019). Over the past 33 years (1985-2018) sea ice loss has increased and as a result extreme wave heights have increased in the Arctic. (IPCC, 2019). In addition to the detrimental erosion effects on coastal regions, extreme wave heights pose a threat to the infrastructure of coastal communities (Schädel, 2022). Coastal community infrastructure is vital for Arctic communities as they rely heavily on sea-based transportation to support the local economy. The reduction of sea ice increases the potential for polar transiting maritime vessels (Pizzolato et al., 2016). Projections indicate that a global warming change of as little as 1˚C will create 100% probability of marine navigation to for part of the year in some Arctic areas, where an increase of 4˚C will see an increase up to 300 days per year in the Beaufort Sea (Mudryk et al., 2021). According to the Intergovernmental Panel on Climate Change's Special Report on the Ocean and Cryosphere, summertime Arctic ship-based transportation has increased over the past two decades, which has implications for global trade that use traditional shipping corridors in the Arctic. Arctic transiting vessels have an increased exposure to navigational hazards due to poor weather conditions, poor communications, and poor navigational charts (Tulaktarvik Inc. 2014). Developing navigational charts and surveying Canada's waters is the responsibility of the Canadian Hydrographic Service (CHS) (CHS 2017). The motto of CHS is '*Nautical charts protect lives, property and the marine environment*' (CHS 2019). To ensure safety, nautical charts rely on the accuracy and precision of hydrographic surveys, in particular bathymetry. Setting the foundation for hydrographic survey accuracies, the International Hydrographic Organization's (IHO) Standards for Hydrographic Surveys (S-44) dictates the minimum requirements necessary to derive high quality bathymetry products. The CHS modifies those requirements to ensure Canada's standards for hydrographic surveys are more stringent than IHO's standards.

In order to achieve the best possible vertical accuracies of hydrographic surveys, meteorological and oceanographic variables that influence sea level heights should be included in predicted tide vertical reduction methods. Meteorological variables such as barometric pressure influence sea level heights (Wunsch & Stammer, 1997; LINZ, 2015; Smith, 2016). Tidal prediction algorithms use a standard barometric pressure of 1013.25 hectopascals (hPa) (Wunsch & Stammer, 1997; LINZ, 2015); however, it has been well documented that ±1 hPa can influence water level heights by ± 1 cm (Forrester 1983; Wolski et al., 2014; Gregory et al., 2019). This effect is known as the inverse barometric pressure effect (IBE). The direct relationship of an increase (decrease) of 1 hPa to the decrease (increase) of 1 cm of water level is only true in the absence of other forces (Forrester, 1983). In fair weather conditions, IBE is difficult to separate from other influential factor such as the rise of fall in the surface height of the waterbody due to wind action, referred to as wind set-up.

With the advances of satellite radar altimetry technology, studies on the IBE can be conducted on a global scale. In a study by Vandam and Wahr (1993) a comparison between Geosat satellite radar altimetry derived sea surface heights (SSH) and a mathematical barometric pressure gradient model resulted in 60-70% deviation from the IBE theoretical response. Using the TOPEX/Poseidon satellite, the deviation from the IBE theoretical response was 110%, equating to 1.11 cm/hPa (Fu & Pihos 1994). This led the authors to conclude that the disagreement was the result of other environmental variables and suggested wind-driven sea surface variability as the source. It has been noticed that the influence of wind-driven sea surface fluctuation is relatively small in comparison to IBE (Hamon, 1966; Ponte, 1994). Studies compared the atmospheric pressure forcing and wind set-up and concluded that there is an anti-correlation between the two variables in that as one increased the other decreased and vice versa. (Vandam & Wahr, 1993; Ponte, 1994).

IBE and wind set-up are considered meteorological effects, which are non-periodic phenomenon and thus can be separated from tidal predictions (Miller, 1958). A simple relationship between wind stress fluctuation and tidal energetics is difficult to determine (Kurapov et al., 2010) because the slope of the water surface is dependent on the topography of the study area (LINZ, 2015), the speed and duration of wind forcing, and fetch which is the length of omnidirectional winds across open water. Ocean topography can be accounted for by high resolution bathymetry, and wind speed and the duration of wind forcing is easily obtainable through reanalysis models and/or

downloaded from Environment and Climate Change Canada (ECCC) historical data collected from airports; on the other hand, fetch is difficult to determine because it is not data that are directly observed by instruments.

Persistent winds can lower or raise water level heights over several days, but shorter duration effects over hours can be noted as well (Miller, 1958). The water surface will raise in the direction of wind stress and lower in the opposite direction (LINZ, 2015). Strong offshore winds can exaggerate low-tide exposure along shorelines; conversely, strong onshore winds can virtually eliminate low-tide (NOAA, 2017). Sea surface variations caused by wind set-up are a function of wind speed and direction, fetch, atmospheric pressure and bathymetry (USACE, 1984).

Fetch is a variable that can be used for a direct calculation of the change in sea level height based on wind speed, length of fetch and average depth of a cross section of bathymetry (Forrester, 1983) and plays an important role in wind driven sea surface heights, thus forcing a deviation from predicted tide models. In several studies aimed at modelling wave predictions and storm surges, fetch was calculated and used as an input variable (Fagherazzi & Wiberg, 2009; Rusu & Soares, 2015). These studies used the Simulating WAves Nearshore (SWAN) model (Booij et al., 1997) to determine the direction and height of waves with input data from the National Climate Environmental Prediction's (NCEP) Climate Forecast System Reanalysis version 2 (CFSRv2) (Saha, et al., 2014) model for inputs of surface wind direction and speed, as well as sea surface height (SSH). Using the SWAN models and CFSRv2 models, fetch was calculated as an intermediate step.

SSH variability is separated into two fundamental components. The first, barotropic, which is changes in the mass of a water column, namely due to gravitational forces, and the second, baroclinic, stems from steric changes in the water column (Baker-Yeboah et al., 2009). Nagano & Wakita (2019) used the Rossby wave model forced by wind stress to determine variations in SSH on a decadal scale and suggest that the SSH is primarily caused by barotropic Rossby wave response to an Aleutian Low in the North Pacific northwest of Japan. These decadal changes are on the scale of centimeters in the variation of SSH (Nagano & Wakita, 2019).

Fluctuation in SSH, forced by wind stress, will not affect hydrographic ellipsoidal referenced surveyed depth measurements; however, this cannot be said for the predicted tide methodology to vertically reduce bathymetry to Chart Datum. Chart Datum (CD) is the vertical datum in which all

soundings are referenced and is defined as ‘a plane so low that water but seldom falls below it’ (Forrester, 1983). Canada has chosen Lower Low Water Large Tide (LLWLT) to define where CD is at all tidal stations. LLWLT is the average lowest low waters, 1 from each 19 years of (CHS, 2022). Large fluctuations in SSH stemming from wind stress and storm surges can cause diversions from predicted tides in the magnitude of several meters; however, hydrographic surveys will not conduct operations in these types of conditions. Therefore, the influence of wind set-up is expected to be minimal. The largest meteorological variable to affect SSH will be atmospheric pressure forcing. As mentioned previously, predicted tides do not consider variations in these meteorological variables and they do not consider water column density either.

Water column density influence on water level heights is regionally dependent. Steric heating was shown to account for 30% of SSH variability between 30°S and 30°N and nearly 70% in equatorial regions between 10°N and 10°S (Vivier et al., 1999). In polar regions, where water temperature is more consistent, the influence of water column density is shown to be less; however, the influx of freshwater from the melting of polar ice sheet and glaciers may offset and possibly exaggerate the water column density effect. Stratified water column impacts tidal heights shown by the tidal constituent M2, the semidiurnal lunar constituent (Postlethwaite et al., 2011). Investigation into the interaction between ocean tides and sea ice, found that the salt budget model was regionally dependent when tide was included in the model. It is also noted that discrepancies in the model may be a result of anomalous atmospheric forcing (Postlethwaite et al., 2011). In another study by Chuang and Wang (1981), it was shown that density fronts have strong effects on the generation and propagation of internal tides. It is suggested in this study that tides, at continental margins, are affected by surface tide and topographic features such as steep slopes. These slopes facilitate the transport of dense water, thus affecting the water level height above. For seaward-inclined density fronts, the tidal frequency increases towards the continental shelf (Chuang & Wang, 1981). It is hypothesized that since water column density is regionally and seasonally unique due to variables such as seafloor topography, sea ice melting, and freshwater influx, a comparison between sea surface height corrected for water column density will deviate from predicted tides.

In studies conducted by hydrographic offices around the world such as CHS, United Kingdom Hydrographic Office, and US naval Oceanographic Office, and summarized in the Federation of International Surveyors (FIG) Publication No. 62, Global Navigation Satellite System (GNSS) defined tides were compared to observed tides, resulting in a direct comparison between vertical

reductions techniques involved with Ellipsoidal Referenced Surveys and traditional reduction methods. A recommendation was made by Dodd and Mills (2014) to ensure validation checks remain common practice. The authors recommended that validation checks include the installation of tide gauges at the survey sites in that they serve two purposes, i) to validate the GNSS observations, the inherently recorded tidal signature, and ii) validate the hydrographic vertical separation models being used (Dodd & Mills, 2014). The downside of that recommendation is, in-situ tide gauges increase the cost and effort to conduct hydrographic surveys. Validating observed tides against GNSS tides adds confidence to the finalized bathymetry; however, meteorological-enhanced predicted tides can offer a less expensive alternative as it eliminates the time required to deploy, retrieve and calibrate in-situ tide gauges. After examining and reviewing literature, not a single case comparing meteorologically enhanced predicted tides and Ellipsoidal Referenced Surveys could be found. We hypothesize that the reason for this lack of comparisons is twofold. First is because Ellipsoidal Referenced Surveys techniques are relatively new (2009). Second is that hydrographic offices have followed the recommendations of the FIG publication No. 62 and have used observed tides for validation. The hydrographic survey case studies have been conducted in areas where permeant tide gauges exist, making comparisons between observed tides and GNSS tides easier.

This paper presents the first comparisons between Ellipsoidal Referenced Surveys and meteorologically enhanced predicated tides for the Canadian Arctic. This was done through investigating and isolating the barometric pressure variable so that the influence of barometric pressure on predicted tide could be examined..

3.2 Materials and Methods

3.2.1 Study Areas

As a result of the significant decrease in summer first-year ice and subsequent multi-year ice trends in the Canadian Arctic, access to shipping corridors is expanding (Mudryk et al., 2021). Trends show that in recent years sea ice has been retreating towards earlier open water (-7.7 days per decade) and later final freeze (10.6 d per decade) (Dauginis & Brown, 2021) as well as the lengthening shipping season from June to October (Pizzolato et al., 2014). There is an increasing demand on charting the Canadian Arctic to support the increase in marine traffic. The geographic focus of this research is the Canadian Arctic due to the increase in polar transiting marine traffic

and the low zenith GNSS signals that affect highly accurate ERS surveys. Hydrographic surveys were conducted by the Canadian Hydrographic Service between 2016-2019, expanding data collection in four distinct tidal regions (**Figure 16**). The tidal zones are defined by the Canadian Hydrographic Service: each zone holds a specific reference port whereby the tidal regime of secondary ports in that zone can be calculated (time and height differences) relative to the reference port (Department of Fisheries and Oceans 2023). An increase in all data acquisition occurred between the months of August and October when ice conditions were favorable.

For this study, 12 sites were selected ranging from 3.7 to 841.6 km^2 with a latitudinal range from 58.98˚N to 74.56˚N (**Figure 16, Table 8**). The selected sites were chosen as they were successfully processed by the CHS using ellipsoidal referenced survey (ERS) techniques.

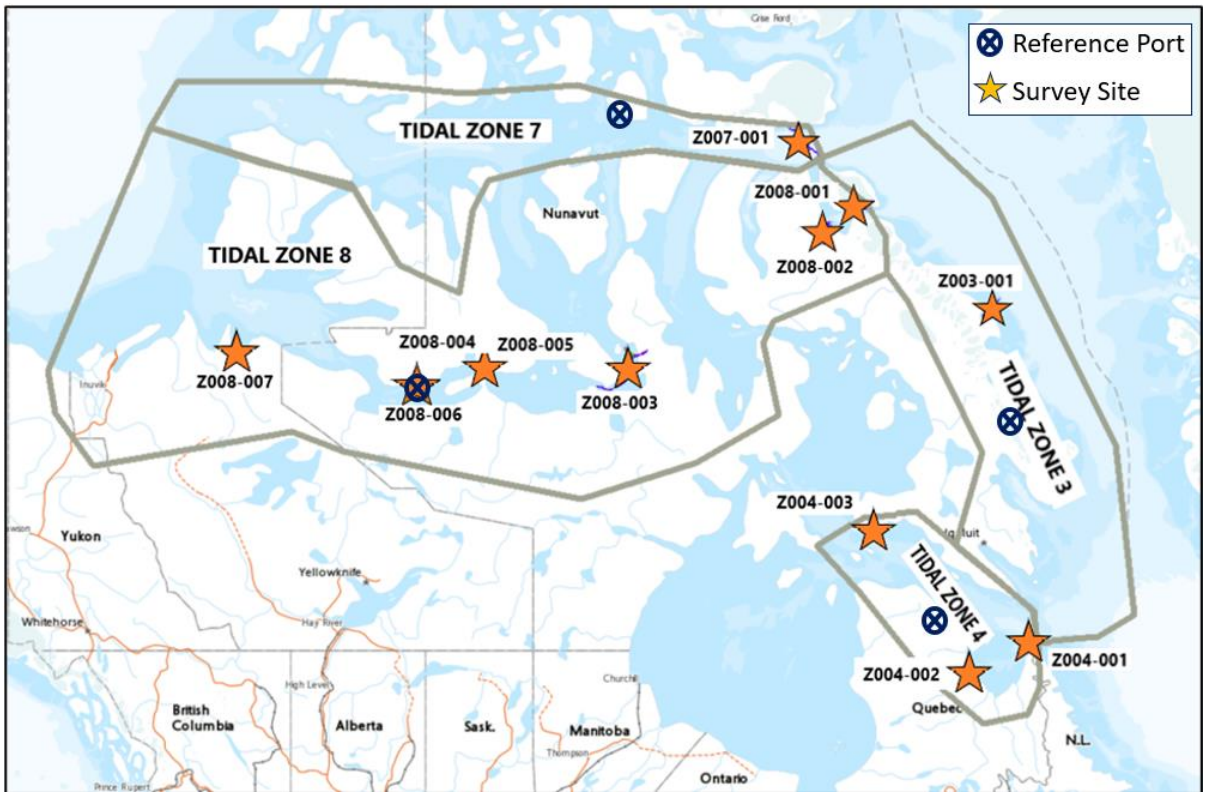

Figure 16. Survey site locations across the Canadian Arctic with the associated tidal zone. The primary tidal station for each zone is shown by the blue circled X.

Table 8. Study site in the Canadian Arctic and the associated spatial extents.

Site ID Number	Site Name	Northeast Extent	Southwest Extent
Z003-001	Clyde River	70.53° N, 67.94° W	70.32° N, 68.61° W

Z004-001	Forbes Sound	60.38° N, 64.81° W	60.37° N, 64.94° W
Z004-002	Approaches to Leaf Bay	59.12° N, 68.70° W	58.98° N, 68.85° W
Z004-003	Cape Dorset	64.28° N, 76.32° W	64.23° N, 76.40° W
Z007-001	Lancaster Sound	74.56° N, 80.63° W	73.98° N, 82.99° W
Z008-001	Pond Inlet	72.89° N, 77.31° W	72.72° N, 79.05° W
Z008-002	Milne Inlet	72.58° N, 80.03° W	72.07° N, 80.81° W
Z008-003	St. Roch and Rasmussen Basin	69.58° N, 93.56° W	68.38° N, 97.29° W
Z008-004	Cambridge Bay West	68.99° N, 105.37° W	68.94° N, 105.80° W
Z008-005	Cambridge Bay East	69.05° N, 104.99° W	68.99° N, 109.30° W
Z008-006	Edinburgh Channel	68.49° N, 110.83° W	68.45° N, 111.11° W
Z008-007	Paulatuk	69.43° N, 124.13° W	69.36° N, 124.23° W

3.2.2 Data Sources

3.2.2.1 Hydrographic Survey Data

The 12 survey sites identified in this study were acquired by the CHS to target high priority navigational corridors and were chosen for this study as they were all successfully processed using ERS techniques. Although a variety of platforms were used for acquisition, ranging from 100 m+ Class 4 Icebreakers to 8.5 m hydrographic survey launches, each were equipped with the hardware necessary to meet International Hydrographic Organizations (IHO) S-44 standards. The IHO S-44 standards set the expectations for the horizontal and vertical accuracies within defined depth ranges. All processing followed the CUBE (Combined Uncertainty and Bathymetric Estimator) algorithm (**Figure 17**). The CUBE algorithm has been incorporated into all major commercial hydrographic processing software as it is notably faster for processing large datasets and is statistically robust (Calder & Wells 2007)

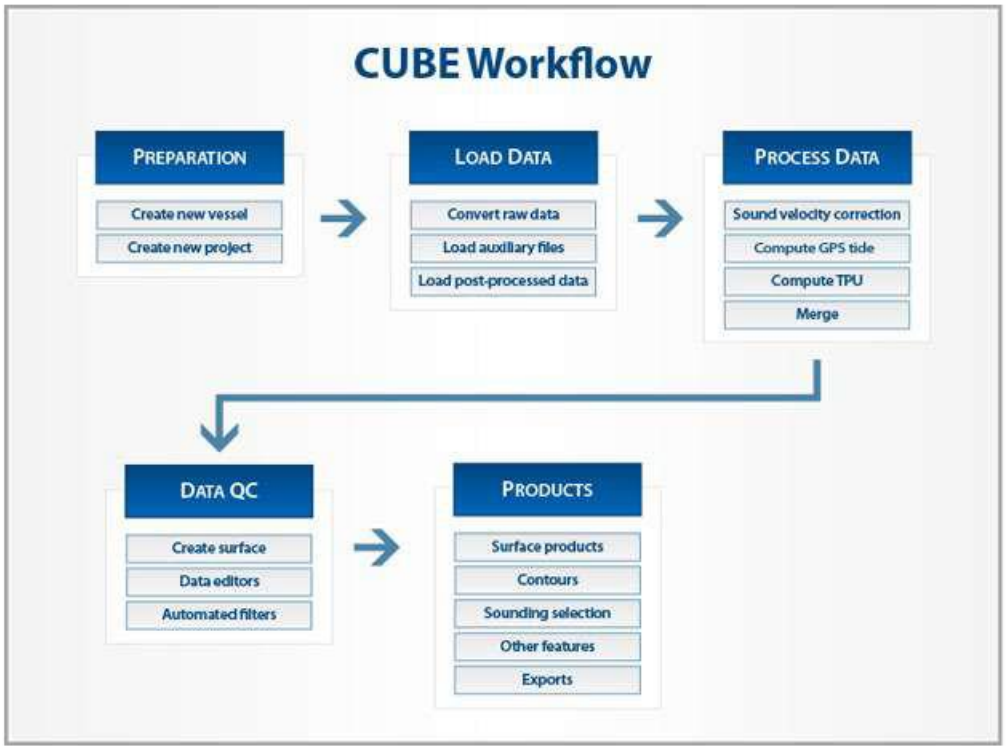

Figure 17. Canadian Hydrographic Service CUBE processing workflow.

3.2.2.2 Predicted Tide Data

Direct observation tidal stations in the Canadian Arctic are sparse. In total, there are five permanent tidal stations currently in operation across the vast Canadian Arctic (CHS 2023). The sparseness of tidal observations has been offset by temporary or seasonal tidal stations to densify the tidal network. There have been approximately 380 temporary tidal stations established in the Canadian Arctic, with one dating as far back as 1848 (CHS 2023). To be considered temporary tidal stations, permanent benchmarks are established at each site so that direct observations can be tied to a known vertical datum, however, permanent instrumentation is not installed and relies on temporary observations. The quality of the tidal predictions has a direct correlation to the length of the observations record (Ducarme 2009). Noted in **Table 9** are the length of observations to generate the harmonic analysis tidal constituents and predicted tide files as well as the large tide range to provide context into the amplitude difference between the stations.

Predicting tidal signatures (frequency and phase) has been well established by using the Harmonic Analysis mathematical model (Doodson 1921; Cartwright & Edden 1973; Godin 1973; Foreman & Henry 1989). Harmonic Analysis involves breaking down the tidal observations into sinusoidal

functions called tidal constituents by taking advantage of a least-squares regression approach. Tidal predictions for deep water areas can be adequality resolved by using 60 tidal constituents, whereas shallow water requires 114 constituents to resolve and typically require 365 days of observation to account for major celestial movements (Hibbert et al., 2015).

Predicted tides were acquired from the Canadian Hydrographic Service's Tides, Currents, and Water-level stations (CHS, 2023). Hidecast predictions were extracted to cover the temporal frame for each survey site. In most cases, a single secondary tidal station was used to generate the predicted tide; however, for the two larger sites, Z008-002 and Z008-003 (**Figure 18**), multiple stations were used and a weighted mean average between the stations was applied using the Teledyne CARIS HIPS/SIPS software package. (**Figure 17**). Predicted tides were exported at a high frequency of 3-minute intervals to assist in the hydrographic processing.

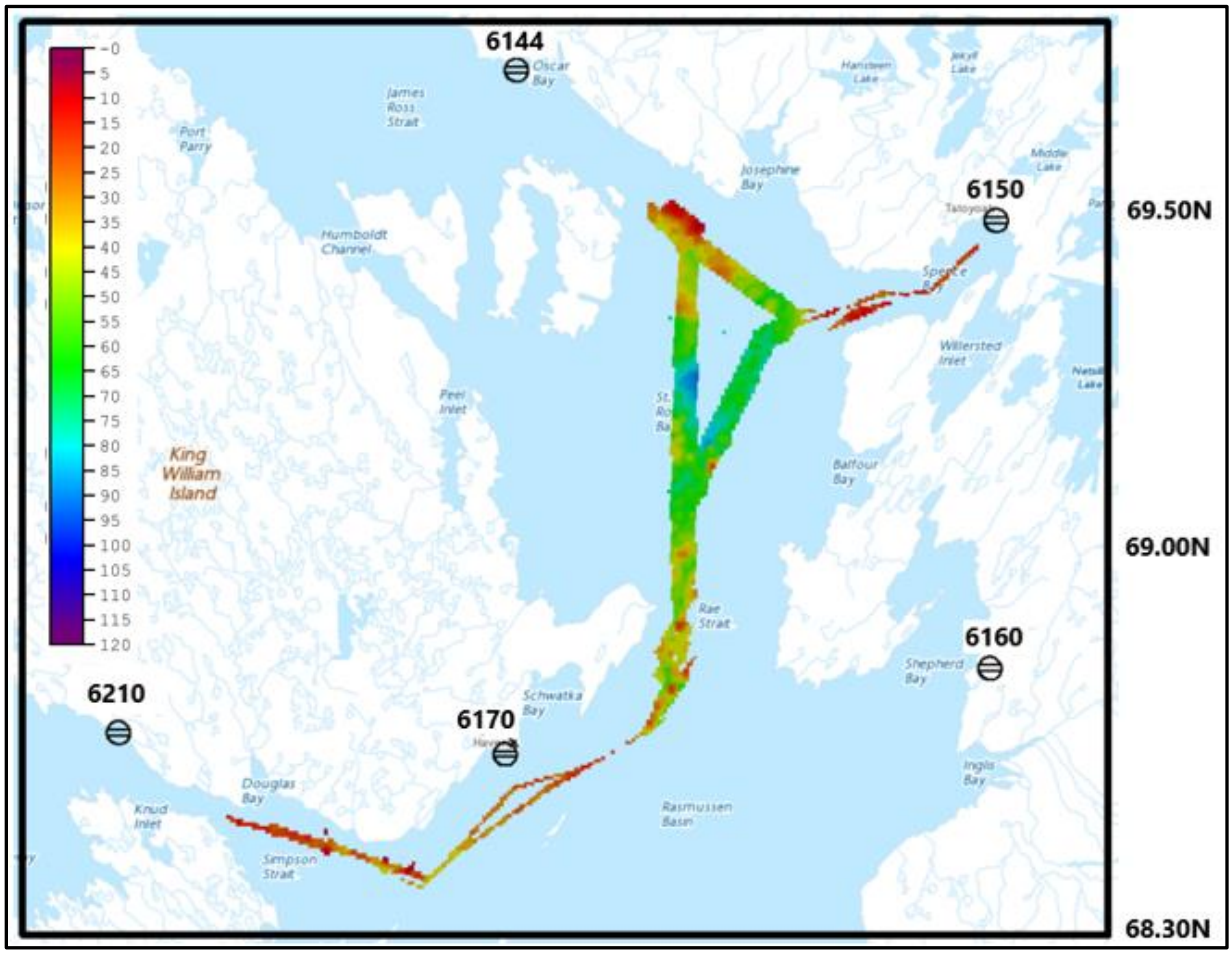

Figure 18. Site Z008-003 St. Roch and Rasmussen Basin. This figure shows the extent of the hydrographic survey, colour band indicating depth, as well as the location of all the tidal

prediction station used for the zone definition file. The zone definition file is an average weighted mean of the predicted tide time-series based on distance between stations.

Table 9. Tidal stations used in this study. The length of observations (in days) to generate the tidal constituents as well as the large tide range to indicate amplitude of the tide at the stations.

Site ID Number	Tide Station Number	Tide Station Name	Location	Length of Obs. (days)	Larger Large Tide (m)	Tidal Predictions Date Range
Z003-001	3940	Clyde River	70.46° N, 68.59° W	374	1.533	Aug 19-22, 2019
Z004-001	4265	Port Burwell	60.38° N, 64.81° W	29	6.758	Oct 3, 2018
Z004-002	4325	Hopes Advance Bay	59.35° N, 69.63 ° W	29	12.521	Oct 7-8, 2019
Z004-003	4245	Cape Dorset	64.23° N, 76.50° W	49	8.337	Oct 11, 2018
Z007-001	5430	Dundas Harbour	74.52° N, 82.42° W	29	2.766	Sept 3, 2019
Z008-001	5800	Pond Inlet	72.72° N, 77.98° W	277	2.342	Aug 31 – Sept 1, 2019
Z008-002	5790	Koluktoo Bay	72.10° N, 80.78° W	29	2.366	Sept 22 – Oct 1, 2016
	5792	Low Is.	72.24° N, 80.63° W	13	2.335	
	5795	Pisktarfik Is.	72.58° N, 80.35° W	15	2.464	
Z008-003	6210	Gladman Point	68.66° N, 97.74° W	362	0.551	Aug 7 – Sept 19, 2017
	6170	Gjoa Haven	68.63° N, 95.88° W	328	0.648	
	6160	Shepherd Bay	68.77° N, 93.57° W	2	0.301	
	6150	Taloyoak	69.53° N, 93.53° W	339	0.517	
	6144	Oscar Bay	69.78° N, 95.83° W	26	1.627	
Z008-004	6240	Cambridge Bay	69.12° N, 115.08° W	365	0.820	Aug 27 – Sept 10, 2018
Z008-005	6240	Cambridge Bay	69.12° N, 115.08° W	365	0.820	Aug 27 – Sept 10, 2018
Z008-006	6280	Johansen Bay	68.59° N, 111.35° W	371	0.465	Aug 7 – Sept 19, 2017
Z008-007	6350	Paulatuk	69.35° N, 124.07° W	29	0.619	Aug 19 – 23, 2018

3.2.2.3 Hydrographic Vertical Separation Surface

In 2016, the Canadian Hydrographic Service finalized a hydrographic vertical separation surface (HyVSEP) linking the Global Reference System of 1980 (GRS80) ellipsoid in the North American Datum of 1983 - Canadian Spatial Reference System (NAD83(CSRS)) reference frame to chart datum (Robin et al., 2016). In Canada, the vertical reference for hydrographic surveys and nautical charts is Chart Datum, which is recognized as Lower Low Water Large Tide (LLWLT) (Forrester, 1983). LLWLT is the average lowest low waters, 1 from each of the 19 years of predictions (CHS, 2023). Due to emerging technologies in marine navigation and the increase in the usage and adoption of Electronic Navigational Charts, the IHO adopted World Geodetic System 1984 (WGS84) for horizontal datum as the standard to uphold continuity on a global scale (IHO, 2018).

Although Canada adopted NAD83(CSRS) for all geospatial data and products (Natural Resources Canada, 2021), Electronic Navigational Charts remained referenced to WGS84 to ensure continuity between adjacent ENCs regardless of the nation producing them, therefore, Canada kept WGS84 as the horizontal datum for hydrographic data. WGS84 is closely aligned with the International Terrestrial Reference Frame (ITRF) with a 7-paramter transformation designed to be zero in all components and as a result, most hydrographic data collection uses the ITRF (Office of Geomatics, 2023). NAD83(CSRS)v6, epoch 2010 is considered equivalent to ITRF of 2008 (ITRF08) (Natural Resources Canada, 2022), and therefore the official HyVSEP that covers the extent of the Canadian Arctic and the one used for the vertical reduction of the hydrographic surveys in this study is the CANNORTH2016v1HyVSEP_ITRF08_CD (**Figure 19**).

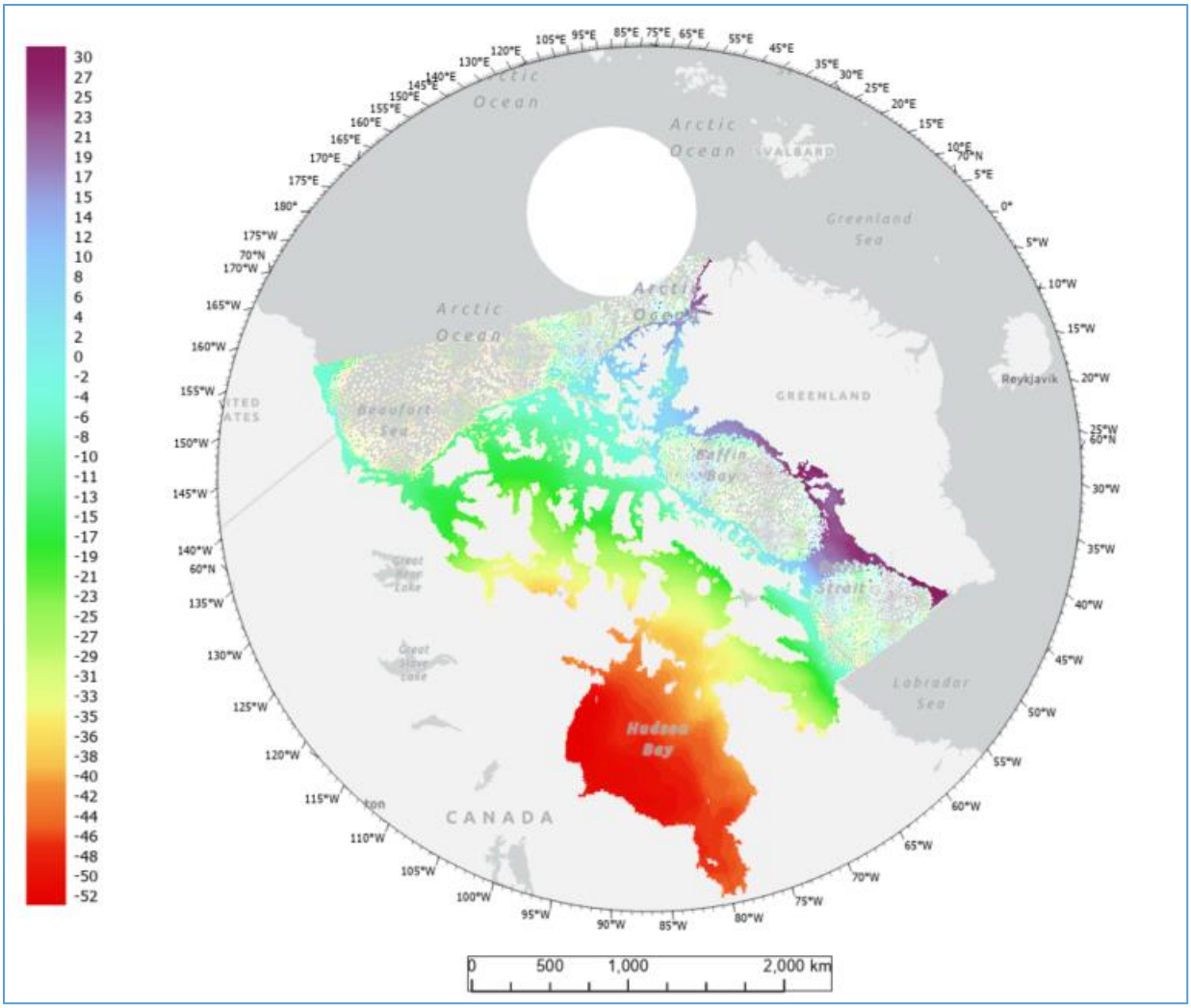

Figure 19. CANNORTHv1HyVSEP_ITRF08_CD. The colour scale depicts the separation between the International Terrestrial Reference Frame, epoch 2008 ellipsoid and chart datum in meters.

The separation between ITRF08 ellipsoid and CD are well known at the tidal stations due to strong efforts made to recover and occupy as many reference benchmarks as possible over the course of decades beginning in the early 1990's (Robin et al., 2016). Satellite altimetry and dynamic ocean models were used offshore. A 2D Laplacian algorithm was used to interpolate and transfer information across the grid, taking 2D potential flow or heat conduction as an interpolating factor (Robin et al., 2016). Since the HyVSEP model used in our study is closely coupled to tidal station benchmarks, uncertainty at those stations are ±1-2 cm. Offshore, the uncertainty increase to is ±10 cm. All of the tidal stations used for tidal predictions in this study were also used in the

development of the HyVSEP; therefore, we can assume the contributing amount of uncertainty in the vertical component of the ERS reduction solution, stemming from the HyVSEP model will adhere to the uncertainty estimates described by Robin et al. (2016).

3.2.2.4 ERA5 Barometric Pressure Data

Developed by the European Center for Medium-Range Weather Forecasts (ECMWF), the ECMWF Reanalysis version 5 (ERA5) is a high resolution atmospheric reanalysis global climatic dataset, covering a period from 1940 to present day (minus 5) and a spatial resolution of 0.25˚ x 0.25 ˚ (Hersbach et al., 2018). Data from the ERA-Interim dataset (precursor to ERA5) estimated the uncertainty in the ECMWF surface pressure to be under 3 hPa^2 over the majority of the oceans, with typical uncertainty being under 1 hPa^2 (Ponte & Joël, 2003). ERA-Interim mean surface pressure data was based on 6-hour temporal frame. In contrast, ERA5 mean sea level data is based on 1-hour temporal frame and can ingest data from modern satellite that use hyperspectral data. ERA5 is an improvement on ERA-Interim dataset (Hersbach et al., 2019). For this study, hourly mean sea level pressure data were downloaded from freely available ERA5 dataset . The mean sea level is calculated based on data assimilation from a combination of observed surface pressure measurements from weather stations, ships, buoys and satellite data (Hersbach et al., 2018). ERA5 mean sea level pressure does not directly account for gravitational effects at specific locations but does calculate the force per unit area of the atmosphere at the surface of the Earth, adjusted to the height of mean sea level (Hersbach et al., 2018).

A single cell as close to the center of each individual survey extent was chosen (**Table 10**), except for sites Z008-002 and Z008-003. For these two sites, a cell covering the predicted tidal station location was chosen so that the zone definition file could be used to allow for a more robust comparison. The ERA5 mean sea level pressure data was extracted at a 1-hour frequency covering the temporal extents that the hydrographic survey conducted operations.

Barometric pressure obtained through the ERA5 reanalysis is summarized in **Table 10**. The overall average barometric pressure between all sites was 101.145 kPa, slightly below the standard 101.325 kPa used for the predicted tide generation.

Table 10. ERA5 mean sea-level pressure data cell location, associated tidal station number and the max, min, mean and range of the barometric pressure over the course of hydrographic survey operations.

Site ID Number	Tide Station Number	Duration (days)	Location	Min kPA	Max kPA	Mean kPA	Range kPa
Z003-001	3940	4	70.50° N, 68.00° W	101.370	101.817	101.626	0.447
Z004-001	4265	1	60.50° N, 65.00° W	101.509	101.959	101.654	0.450
Z004-002	4325	2	59.00° N, 68.75 ° W	98.911	101.121	99.606	2.210
Z004-003	4245	1	64.25° N, 76.50° W	101.590	101.929	101.830	0.339
Z007-001	5430	1	74.25° N, 82.00° W	100.740	101.119	100.973	0.379
Z008-001	5800	2	72.75° N, 77.98° W	100.036	100.392	100.227	0.356
Z008-002	5790	10	72.10° N, 78.25° W	100.379	102.174	101.474	1.795
	5792		72.00° N, 80.75° W	100.413	102.171	101.469	1.757
	5795		72.50° N, 80.50° W	100.409	102.152	101.445	1.743
Z008-003	6210	44	68.75° N, 97.75° W	98.704	102.343	101.112	3.639
	6170		68.50° N, 95.75° W	98.620	102.290	101.111	3.671
	6160		68.75° N, 93.75° W	98.719	102.320	101.112	3.601
	6150		69.50° N, 93.50° W	98.977	102.428	101.112	3.452
	6144		69.75° N, 95.75° W	99.055	102.452	101.125	3.397
Z008-004	6240	15	69.12° N, 115.08° W	99.858	102.205	100.831	2.347
Z008-005	6240		69.12° N, 115.08° W	99.858	102.205	100.831	2.347
Z008-006	6280	44	68.59° N, 111.35° W	99.365	102.517	101.095	3.152
Z008-007	6350	5	69.35° N, 124.07° W	101.198	102.217	101.656	1.019

3.3 Methodology

Predicted tides were generated using the CHS's internal Tides, Currents, Water Level application that reconstructs tidal constituents based on harmonic analysis into a time series. Three-minute interval frequency was chosen as this is typical for time-series data in hydrographic surveying. The ERA5 mean sea level pressure data was processed using MATLAB. A linear interpolation spline method was used to densify the 1-hour frequency barometric pressure data to align with the 3-minute predicted tide data. Time shifting the time-series to account for time zones was necessary to ensure temporal-spatial alignment prior to further processing.

Further processing was required to directly apply gravitational influence at each cell of interest by applying the World Geodetic System 84 Ellipsoid Gravity Formula (**Equation 1**). This was chosen to ensure a similar reference frame was used throughout the study. For this study it is assumed that WGS 84 and ITRF08 result in negligible spatial differences (Office of Geomatics 2023).

$$g\{\emptyset\} = G_e \left[\frac{1+k\sin^2\emptyset}{\sqrt{1-e^2\sin^2\emptyset}}\right] \quad (1)$$

where:

$\emptyset$ is the latitude in degrees;

$e^2 = 1 - (b/a)^2$;

a is the equatorial semi-axis which is 6378137.0 m;

b is the polar semi-axis which is 6356752.314245 m;

G_e is the defined gravity at the equator which is 9.7803253359 $m \cdot s^{-2}$;

G_p is the defined gravity at the poles which is 9.8321849378 $m \cdot s^{-2}$;

$$k = \frac{bG_p - aG_e}{G_e}$$

Free air correction is the anomaly when comparing observed gravity to theoretical gravity at a given location and then adjusted for height above or below mean sea level (**Equation 2);** however, due to dynamic heights of the vessel's reference point in relation to mean sea level at each spatial and temporal frame, it was assumed to be equivalent to mean sea level, i.e. a zero height adjustment was applied.

$$FAC = -3.086 \times 10^{-6} * h \quad (2)$$

Where FAC is the Free Air Correction and *h* is height above or below mean sea level in meters. Gravity influence at each cell was the summation of gravity at the latitude of interest plus the FAC (**Equation 3**).

$$gr = g + FAC \quad (3)$$

Where gr is the finalized gravity influence at the latitude of interest; g is the WGS84 gravity calculations (**Equation 1**) and FAC is the Free Air Correction (**Equation 2**)

The inverse barometric pressure effect (IBE) was calculated (**Equation 4**) (Wunsch & Stammer 1997) whereby the gravity influence on the mean sea level pressure record was accounted for. Two additional variables required for this calculation are global standard atmospheric pressure at sea-level, which is 101325 Pa (Roquet et al., 2015), and the average surface sea water density for polar regions, which is 1026.6 kg/m^3 (Roquet et al., 2015).

$$\mathrm{IBE} = -\left(\frac{\Delta P_{atm}}{\rho_{water} * gr}\right) \quad (4)$$

Where ΔP_{atm} is the difference between the mean sea level pressure in pascals from ERA5 data and the global standard atmospheric pressure at sea-level in pascals; pa is the global standard atmospheric pressure at sea-level of 101325 pascals; ρ_{water} is sea water density in kg/m^3; and gr is the influence of gravity at the latitude (in decimal degrees) of interest (**Equation (3)**).

Applying the IBE to the predicted tidal record was then done for single point stations. The two time-series (Predicted Tide (PT) and Barometric Pressure Enhanced Predicted Tide (BT)) were then compared and used to calculate the residuals for each record as a visual check on the data quality (**Figure 20**).

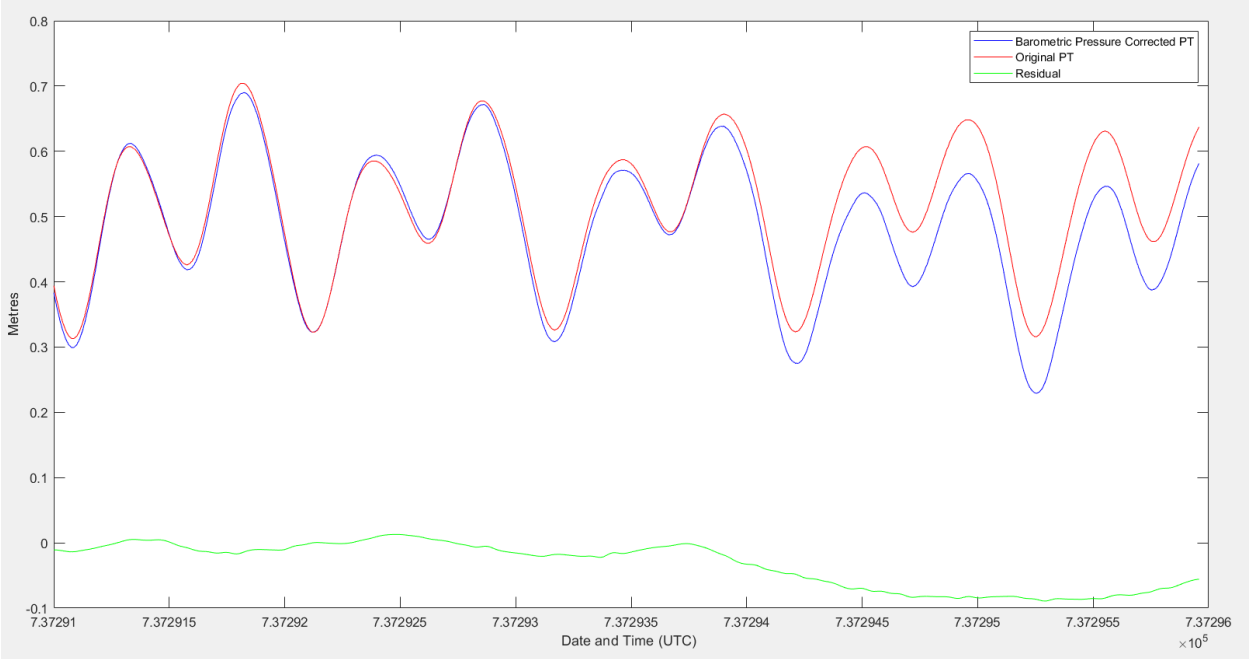

Figure 20. Time-series of Z008-007 (Paulatuk) showing the predicted tide (red) to the barometric pressure corrected predicted tide (blue) along with the residual (green). This record indicates good agreement in the first half of the record (101.430 kPa) and a gradual separation occurring during the second half as barometric pressure began to rise (101.880 kPa).

For sites Z008-002 and Z008-003, a further step was conducted to apply the zone definition file to the data, blending the barometric pressure enhanced predicted tidal records from each station by weighted mean averaging.

Final processing was completed in Teledyne CARIS HIPS/SIPS using the CUBE process by replacing the tidal solution with one of 3 possibilities: ERS (GPS), predicted tide - no barometric pressure correction (PT), or barometric pressure enhanced predicted tides (BT). The resulting outputs were then compared on three levels of analyses.

The first analysis was investigating the difference in the timeseries of PT vs BT to highlight survey sites that may have been greatly affected by the atmospheric conditions at the time of acquisition. The second analysis was to identify individual survey lines where known degradation in GNSS signal occurred. Each survey line was interrogated for GNSS drop out or degradation as well as an increase in uncertainty associated with the uncertainty band of the dataset. The third analysis was done on each site as a whole to investigate if applying the BT reduction made a significant impact on the extents of the bathymetry. Each level of analysis followed the same processing steps (CUBE algorithm) and each compare all three outputs to each other (GPS vs PT, GPS vs BT, PT vs BT).

3.4 Results and Discussion

3.4.1 Predicted Tides versus Barometric Pressure Enhanced Predicted Tides Time-series Comparison

Comparison between the time-series of the PT and the BT solutions show relatively small variation in their means, with the exception of two sites, Z004-002 and Z008-001 (0.174 m and 0.109 m respectively) (**Table 11**). The barometric pressure at these two sites was below the standard barometric pressure of 101.325 kPa over the entire course of the data acquisition period, with a maximum of 101.121 kPa and 100.227 kPa respectively (**Table 10**). At both locations the standard deviation between the two vertical reduction solutions, PT and BT, was relatively low as well, at 0.057 m and 0.012 m; however only Z008-001 BT solution had a significant ($p < 0.01$) influence on the Large Tide Range (LTR) (**Table 11**). This was due to the smaller amplitude of the tides at Z008-001 (2.342 m LTR) compared to the large amplitude of the tide at Z004-002 (12.521 m LTR) (**Table 9**).

Sites Z008-002 and Z008-003 are both geographically large sites (302.8 and 841.6 km^2, respectively). These two sites required Zone Definition Files (ZDF) to produce a weighted mean average between the tidal stations in the area. Each of the tidal stations at these sites resulted in slight changes in the minimum and maximum difference between the PT and the BT solutions; however, the mean difference remained constant regardless of the tidal station, -0.006 m for Z008-002 and +0.023 m for Z008-003. Standard deviation between PT and BT for each tidal station at the two sites was consistent as well, being 0.047 m +/- 0.001 m and 0.061 m +/- 0.001 m respectively. Using a single factor ANOVA F-Test, site Z008-002 did not show significant change by applying ERA5 mean sea level pressure to PT ($p > 0.4$); additionally, the mean difference between the PT and the BT solutions had minimal influence on the LTR at ~ 0.25%, with a maximum influence relative to LTR at 4.015% for tidal station 5790. Conversely, site Z008-003 did show a significant change by applying ERA5 mean sea level pressure to PT ($p < 0.000$). At Z008-003, maximum mean influence was 7.641% of the LTR at station 6160; however, the maximum difference between the PT and the BT solution at station 6160 was 0.259 meters, which equates to 86.047% of the LTR, a substantial amount of the tidal range.

Table 11. Difference in the time series of the predicted tidal records before and after applying ERA5 mean sea level pressure corrections. The results compared to the Larger Large Tide derives the influence, as a percentage of the height of the Larger Large Tide for each station is calculated.

General Info.		Differences between PT and BT					Comparison to LTR	
Site ID Number	Tide Station Number	Min	Max	Mean	Std Dev.	Anova F-Test p value	Mean % of LTR	Max % of LTR
Z003-001	3940	-0.050	-0.004	-0.030	0.011	< 0.000	1.957%	3.262%
Z004-001	4265	-0.061	0.433	-0.015	0.116	0.775	0.222%	6.407%
Z004-002	4325	0.021	0.242	0.174	0.057	0.603	1.390%	1.881%
Z004-003	4245	-0.057	-0.027	-0.049	0.007	0.784	5.901%	6.837%
Z007-001	5430	0.020	0.058	0.035	0.013	0.494	1.265%	2.097%
Z008-001	5800	0.092	0.128	0.109	0.012	0.000	4.654%	5.465%
Z008-002	5790	-0.085	0.095	-0.006	0.048	0.512	0.254%	4.015%
	5792	-0.084	0.091	-0.006	0.047	0.486	0.257%	3.897%
	5795	-0.082	0.091	-0.006	0.046	0.569	0.244%	3.693%
Z008-003	6144	-0.113	0.228	0.022	0.060	< 0.000	0.307%	14.013%
	6150	-0.110	0.235	0.023	0.061	< 0.000	4.449%	45.455%
	6160	-0.099	0.259	0.023	0.062	< 0.000	7.641%	86.047%
	6170	-0.096	0.269	0.023	0.062	< 0.000	3.549%	52.512%
	6210	-0.101	0.260	0.023	0.061	< 0.000	4.174%	47.187%
Z008-004	6240	-0.088	0.146	-0.047	0.062	< 0.000	5.732%	17.805%

Z008-005	6240	-0.088	0.146	-0.047	0.062	< 0.000	5.732%	17.805%
Z008-006	6280	-0.030	0.131	0.037	0.045	< 0.000	7.957%	28.172%
Z008-007	6350	0.013	0.085	0.021	0.028	< 0.000	3.392%	13.732%

Applying ERA5 mean sea level pressure to PT, sites Z003-001, Z008-001, Z008-003-007 indicated significant variance between the PT and the BT solutions ($p < 0.000$). This can be attributed to the small tide range of these sites (**Table 9**). When a change in barometric pressure applies a force on the waterbody, compressing or expanding the water column, the relative influence is greater on tidal areas where the amplitude of the tide is not as large. In large tide regions, such as tidal zone 4 (Z004-001/002/003), the influence of the barometric pressure on the water column has a much smaller impact compared to the > 6 meter tide range found there.

3.4.2 Predicted Tide versus Barometric Pressure Enhanced Predicted Tide Hydrographic Survey Line Influence

The heave of a vessel, the high frequency vertical movement, is measured at the vessel's reference point (RP) in relation to the water surface (**Figure 21a**). The heave is logged by onboard computers from the vessel inertial motion unit. The heave can also be derived from the height of the Global Positioning System (GPS) antennas, typically dual antennas which aid in determining overall vessel movement in a 3D cartesian coordinate system, setting up favorable conditions for redundancy. The two signatures, heave and GPS height, are identical but relative to differing RPs. Heave is relative to the vessel RP, the point in which all acquisition hardware component spatial offsets are measured, which is either the theoretical center of gravity of the vessel, the point of origin (0,0) in the Cartesian coordinate system of the inertial motion unit (typically marked by the manufacturer on the inertial motion unit's outer casing) or at the transmit face of the echosounder transducer.

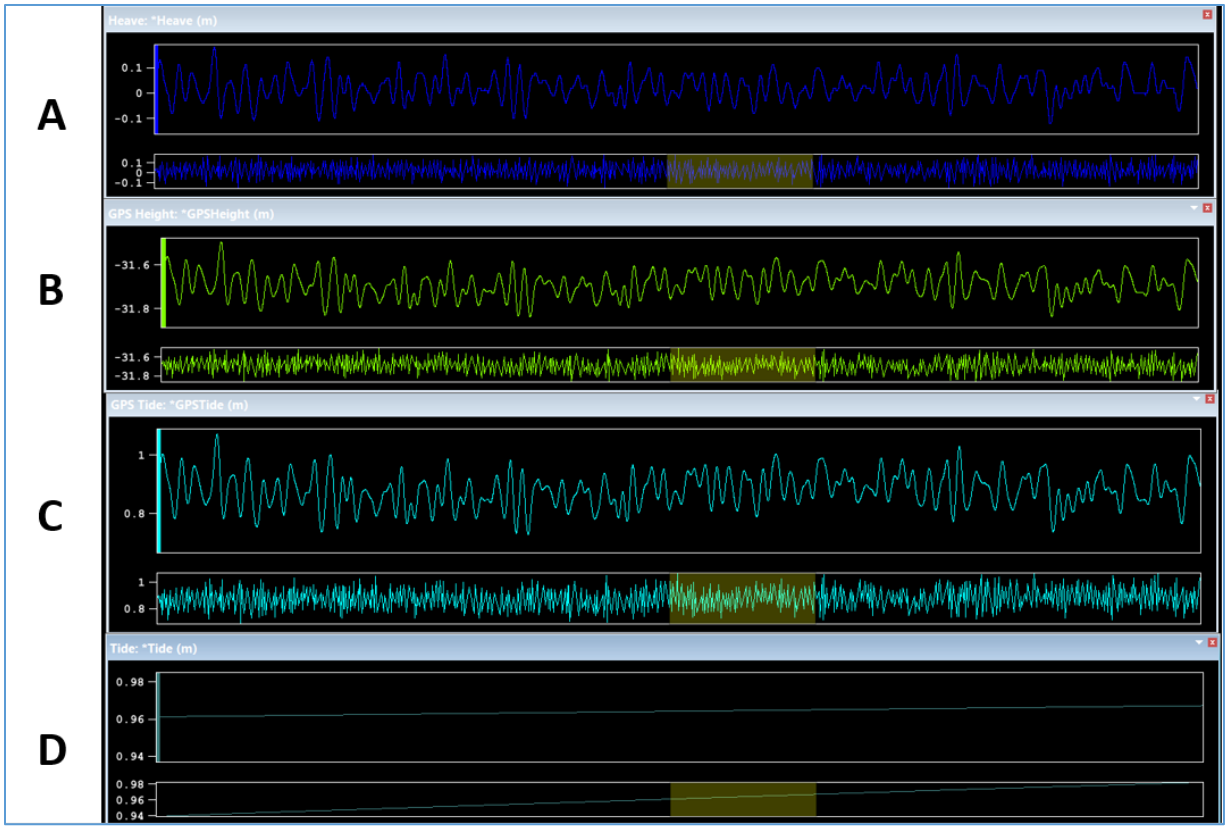

Figure 21. Single line investigation from post processed data. Two figures per section, where the bottom figure is the variable signature over the time series of a specific survey line and the top figure is the examined timescale defined by the highlighted yellow box in the bottom box. (A) Heave signature of the vessel, (B) The GPS Tide height referenced to the ellipsoid, (C) GPS Tide solution - post processing using CANNORTH2016v1HyVSEP_ITRF_CD model corrects the GPS Tide height in relation to CD(note the heave signature is still embedded, when viewing the individual line but it is overwritten with either delayed heave or real-time heave during the georeferenced bathymetry processing step in CARIS HIPS), and (D) the predicted tide signature over the course of the line, referenced to CD. This is a smoothed line as it has been interpolated between 3-minute intervals.

The GPS height is referenced to the ellipsoid (**Figure 21b**). By applying the HyVSEP model to the recorded GPS heights, a GPS tidal signature can be derived (**Figure 21c**). The GPS tide signature is referenced to the vertical datum defined by the HyVSEP model, which in this study is Chart Datum. The GPS tidal solution's graphical depiction continues to retain the heave motion in the signature; however, during the georeferencing process in CARIS HIPS software, the GPS tide

is resolved by removing the heave signature. The finalized GPS tidal signature is a smoothed line of best fit that mimics theoretical observed tides (**Figure 21d**).

The change in the effect of applying ERA5 mean sea level pressure to an individual survey line (Line ID 2018TR2531845) is shown in **Figure 22** as an example. At site Z008-004, on September 10, 2018 at 19:00 UTC, the mean sea level pressure was 100.015 kPa, 1.310 kPa below the global standard of 101.325 kPa. Considering the gravitational effect at a latitude of 69 ˚N results in the expansion of the water column by 0.1306 m. This can be integrated into the tidal signature by vertically shifting the tidal signature's amplitude at that specific time. When ERA5 mean sea level pressure is applied in this scenario, the PT shifts in the positive (vertically upward) direction, indicating an expansion in the water column, and showing a better fit with the GPS Tidal reducing solution (**Figure 22**). The opposite vertical shift and water column compression would be true during times of high pressure (**Figure 23**). As ellipsoid referenced surveys remove vertical vessel motion, including the vertical movement from the compression and expansion of the water column due to atmospheric pressure, and directly connects the GNSS height to the ellipsoid at any given location, ERS is considered to be "the truth". Predicted tides from harmonic analysis do not account for in-situ environmental variables, such as barometric pressure. Applying in-situ barometric pressure observations to the predicted tide at the site would theoretically provide a solution that better aligns with ERS solution. Since observed barometric pressure was not acquired during hydrographic survey operations, ERA5 mean sea level pressure was extracted and applied to the predicted tide time-series, showing a closely fit solution compared to the GPS tide results.

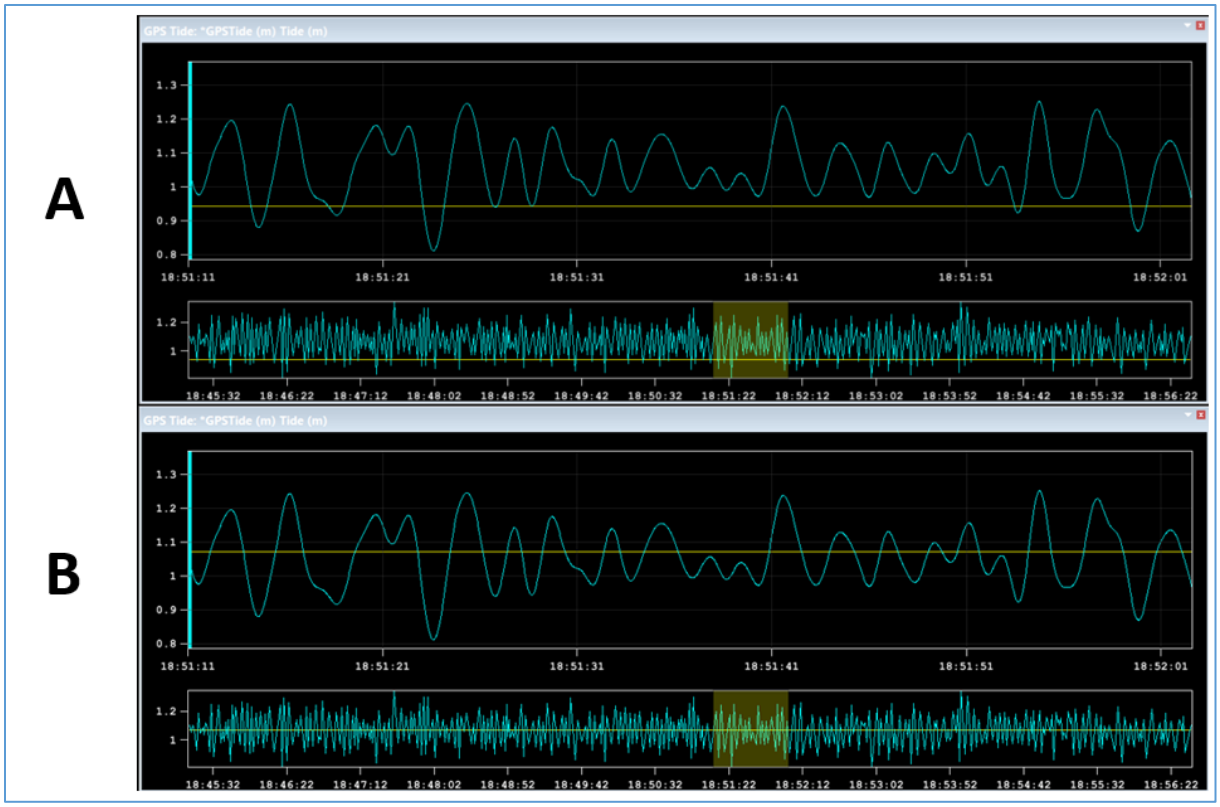

Figure 22. Site Z008-004 (Cambridge Bay West) - Line ID 2018TR2531845 (A) Fluctuating line (blue) is the GPS Tide solution with Heave embedded and the smooth line (yellow) is predicted tide from station 6240 (the highlighted yellow box is the examined timescale, shown in the top graph), (B) is the GPS Tide solution (blue) compared to the barometric pressure enhanced predicted tide (yellow). This shows good alignment between GPS Tide solution and barometric pressure enhanced predicted tide, shown by the 0.131 m vertical shift in the predicted tide.

Site Z004-002 (Hopes Advance Bay) resulted in a negative vertical shift in the water column. ERA5 mean sea level pressure on September 16, 2019 at 12:00 UTC was 1022.169 kPa, when coupled with gravitation effects at 59˚N latitude (**Table 11**), the result was a -0.092 m shift in the downward direction. This too, slightly better aligned with the GPS tidal reduction solution; however, there is a large vertical offset noted between the GPS solution and the PT/BT solutions of approximately 1.005 m (**Figure 23**).

The data was acquired by the Canadian Survey Launch Petrel which is measured at 6.4 m length between the forward and aft perpendiculars. The forward perpendicular is a vertical line through

the forward extremity of the design waterline (the waterline in which the vessel was designed to float upon). The aft perpendicular is the vertical line at the stern of the vessel. Prior to data acquisition, a spatial alignment survey of the vessel was conducted using 3D laser scanner to accurately measure the spatial and rotational offsets between the of all physical vertical components. The final report indicates that there is a 0.002 m uncertainty in the accuracies of the spatial alignment survey. While investigating the source of the 1.005 m offset, the values entered into the onboard acquisition computers were confirmed to match the vessel alignment survey reports, indicating the offset is stemming from external source(s) such as wind setup, barometric pressure, and water column density. Uncertainty in the final GPS tide reduced surface was stated to be 0.233 m with a standard deviation of 0.082 m. Tidal record predictions were generated from only 29 days of observations (**Table 10**) and the LTR at site Z004-002 is 12.521 m (**Table 10**). We theorize that the short tidal observation period in an extremely large tidal region is contributing to the discrepancy between the GPS tide solution and the PT/BT tide solution; regardless, since we are holding the GPS tide solution to be true, applying the BT solution provides a slightly better result than the PT solution.

In events when observed tides are not possible or too costly to acquire, traditional vertical reduction methods such as predicted tides are used by hydrographers to shift the soundings to chart datum. Since the advancement in satellite technology has enabled hydrographic surveys to be measured to the ellipsoid and the use of separation models to shift to chart datum, predicted tides are becoming increasing redundant; however, predicted tides allow for backup in the event satellite degradation or dropout occur. Additionally, predicted tides allow for a quick quality assurance or quality control of the data as comparison between the two solutions should align within the uncertainties of both solutions. Applying barometric pressure to the predicted tide should further align to the ellipsoid referenced survey, reducing the uncertainty even further.

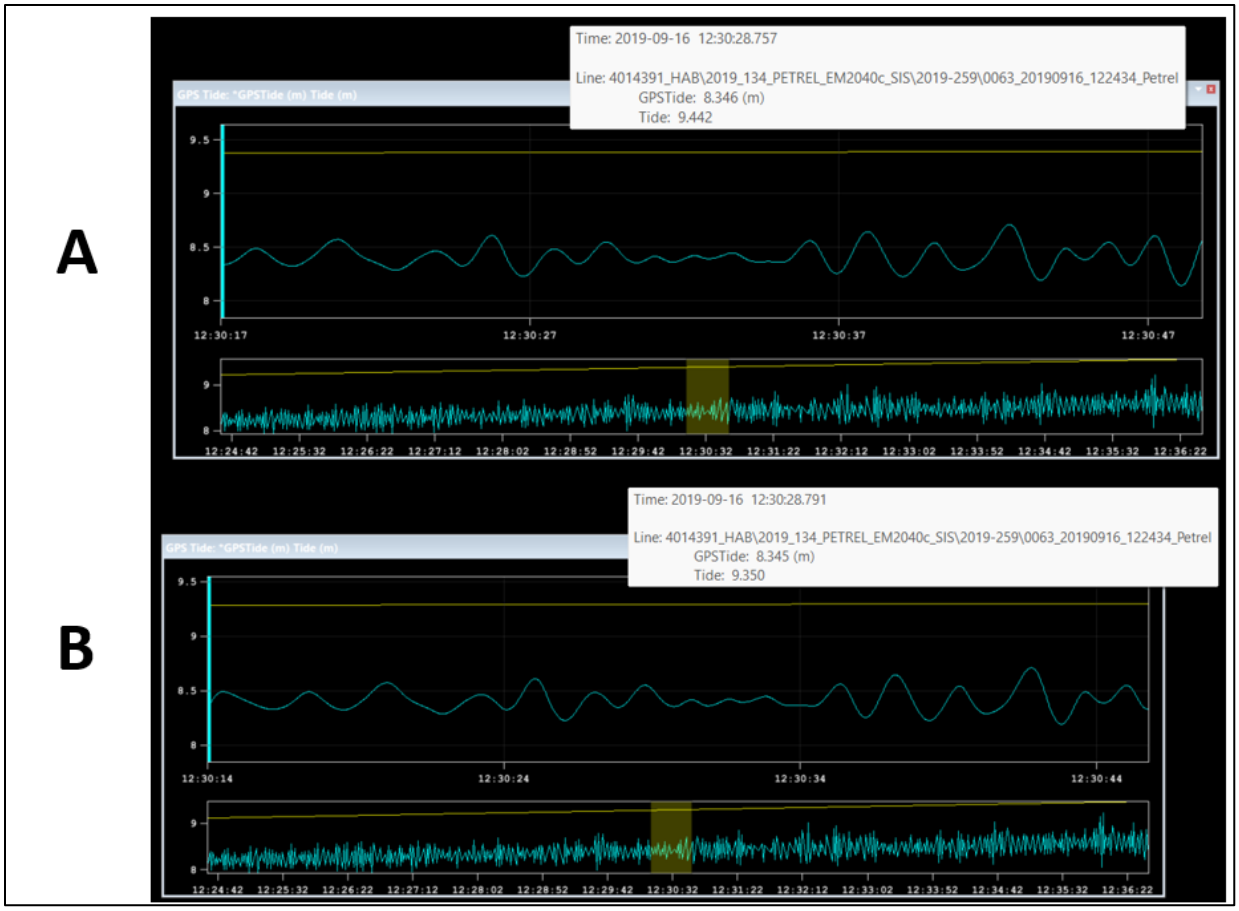

Figure 23. Site Z004-002 (Hopes Advance Bay) Line ID 0063_20190916_122434_Petrel. (A) GPS Tide (blue) overplotted with PT solution from station 4325. Note GPS tide at tool tip is 8.346 m and Predicted Tide is at 9.442 m. (B) GPS Tide (blue) overplotted with BT solution from station 4325. Note GPS tide at tool tip is 8.345m (slight difference in the time tag between A and B) and BT is at 9.350 m, showing a vertical shift in the predicted tide by -0.092 m.

A vertical offset between the GPS tide solution and the PT/BT solution is common throughout all survey lines, regardless of site; however, the variability in the offsets differ. GPS tide solution for site Z003-001 Clyde River (Line ID 4013_20190822_060735_LSSL) averages approximately 1.9 m above CD, and there is an inherent ~ 1 m offset between the PT and GPS tidal solutions (Figure 9). Predicted tide during the course of survey line ranged from 0.882 m to 0.912 m. ERA5 mean sea level pressure was 101.503 kPa over the same temporal span, differing from the standard 101.325 kPa by 0.178 kPa. The increase in pressure above the standard compresses the water column. Applying the ERA5 mean sea level pressure, barometric pressure enhanced predicted

tides was 0.864 m to 0.894 m. The compression of the water column due to atmospheric forcing further separates the GPS tide solution from the predicted tide solution. It was also noted that the LTR for site Z003-001 – Clyde River is 1.533 meters based on predictions from station 3940 (**Table 10**). The GPS tide solution averages 1.950 meters (Figure 9a). A GPS tidal height well above the LTR (+0.417 m) is an indicator there are possible errors introduced into the data.

The vessel used at this site was the Canadian Coast Guard Ship Louis S. St. Laurent, an Arctic Class 4 Icebreaker. Spatial alignment survey was conducted on the vessel prior to data acquisition and the spatial and rotational offsets of the vertical components were verified to be entered into onboard systems appropriately. It is difficult to identify the source of error; however, since a spatial survey was conducted, we can eliminate physical and rotational offset errors onboard the vessel, therefore the uncertainty is stemming from external influences. Main contributors of the error can reside in either the HyVSEP model for this particular area, poor quality tidal observations used to generate tidal predictions, degradation in the GNSS signal, or dynamic in-situ environmental and/or oceanographic variable (wind setup, barometric pressure, water column density).

Since the HyVSEP model is tied to the vertical datum benchmarks at station 3940, uncertainty in the HyVSEP model at those benchmarks is less than uncertainty further offshore. The uncertainty of CANNORTH2016v1HyVSEP_ITRF08_CD is 1-2 cm at benchmark stations and ±10 cm offshore (Robin, et al., 2016); however, the location of site Z003-001 Clyde River is relatively close to the tidal station (average 18 kms) (**Figure 24**), so the uncertainty is in the centimeter range..

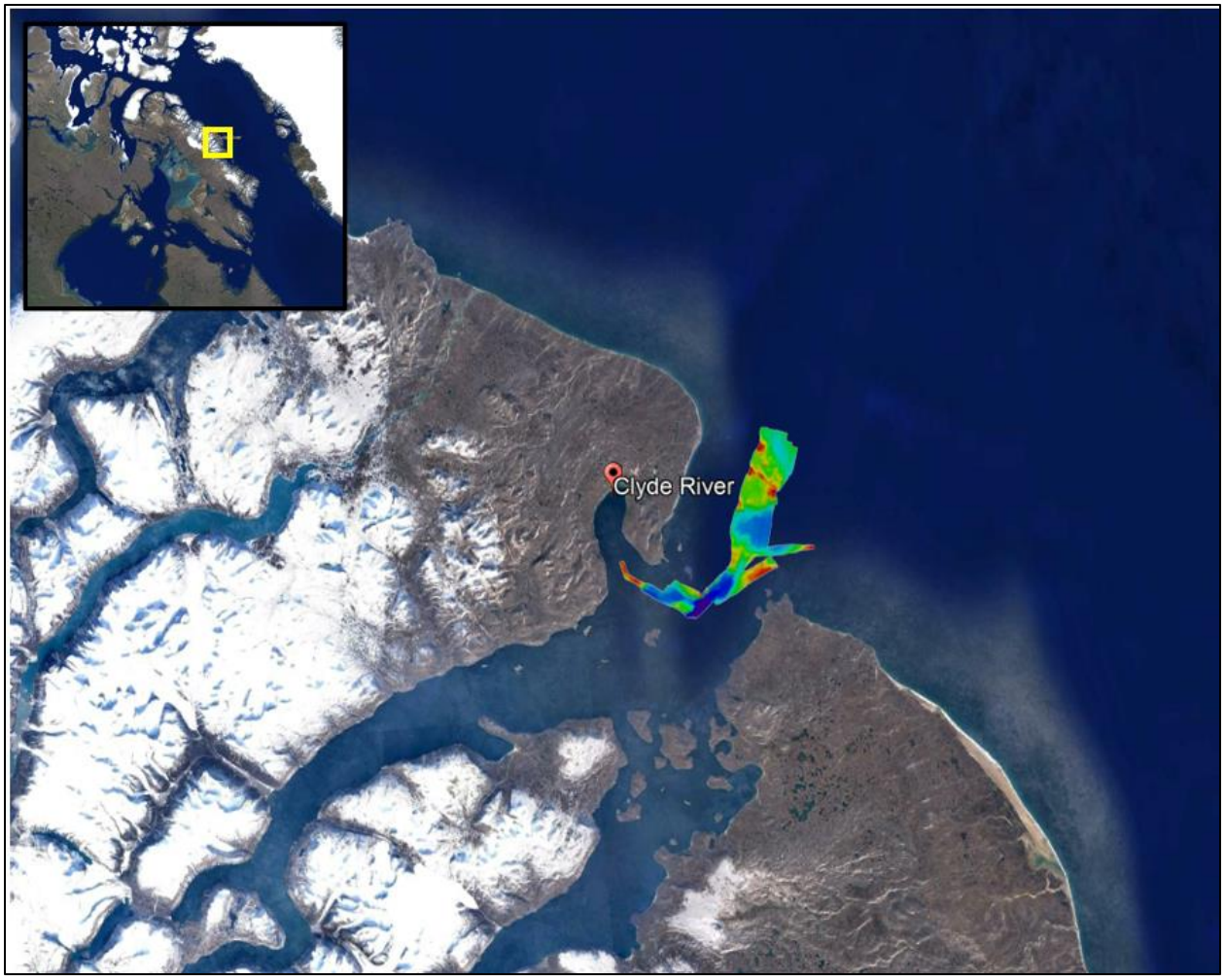

Figure 24. Site Z003-001 (Clyde River) is located on the northeast coast of Baffin Island, Canada. The survey site averages 18km from Clyde River tidal station 3940.

A contributing factor into the uncertainty in the tidal predictions that use harmonic analysis is the equipment used to observed tides and the length of the observation period. Observation periods shorter than 6 months can reach uncertainty of 7.10^{-4} percentage of the tide range (Ducarme, 2009); however, tidal observation at station 3940 – Clyde River were acquired in 2018 with 374 days of observation. This was a year before the hydrographic survey acquisition. The tidal observations used modern techniques and equipment, decreasing uncertainty even further. Records over 365 days will be able to resolve 37 major harmonic constituents from gravitational forces of the sun and moon. Residual between predicted tide and observed tide was 0.085 m which accounts for unsolvable signals in tidal signature and can be attributed to uncertainty stemming from external sources outside of gravitational effects, i.e. atmospheric or oceanographic variables.

Degradation of the GNSS signal will have an effect on the final GPS tide solution; however investigation in to the stability of the GNSS record showed a very slight sign of instability. Occurring in the first third of the line (timestamps 06:10:20 – 06:19:11), the GNSS height was constantly above the heave signal when overplotted on the same vertical scale (**Figure 25b**). The GNSS signal stabilized for the remainder of the line. The instability of the GNSS signal increases uncertainty by an average of 0.2 m for this line. This will account for some of the uncertainty in the line; however, additional external factors contributing to the large vertical offset between the GPS tide solution and PT/BT solution must be influencing the outcome.

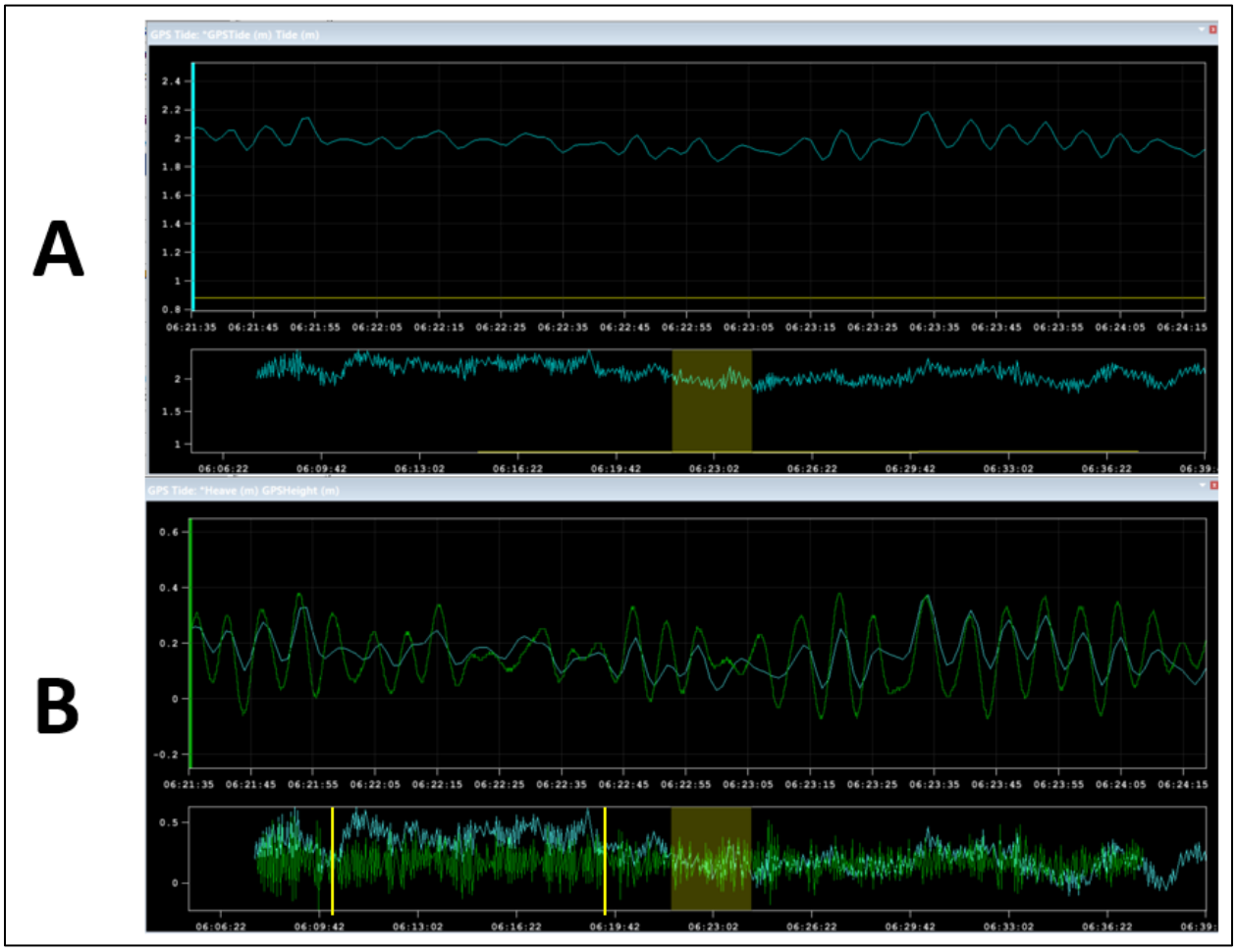

Figure 25. Site Z003-001 (Clyde River) Line ID 4013_20190822_060735_LSSL. This figure depicts a large vertical offset between the GPS Tide solution and the BT solution of approximately 1 meter. The GPS solution is above the predicted Larger Large Tide range of 1.533 meters (station 3940) by ~0.4 meters.

Site Z007-001 (Line ID 4801_20190902_172106_LSSL) showed a highly unstable GPS tidal solution (**Figure 26**), presumably due to the high latitude of the survey site (74˚N) and the low horizonal satellite constellation. When satellites are low on the horizon, the propagation of the radio frequency of the GPS signal is disrupted due to the free electrons in the ionosphere. The ionosphere is one of the largest sources of range error for high accuracy GPS (MacGougan, Lachapelle, & Nayak, 2001). Since the satellite constellations center over the lower North American continent, where the vast majority of GPS signal users are located, the signal passes through much more ionosphere at a low zenith compared to those further south where the constellation is closer to nadir. Quality control of this line comparing the heave signature to the GPS tide signature shows similar trends at the onset of the survey line (**Figure 26a**), with the GPS tide solution being vertically offset from the BT solution by ~ 1m. The GPS signal over the course of 12 minutes drifted, dropped, spiked, and declined, before recovering (**Figure 26b**); however, when the GPS signal finally stabilized, it settled below the BT tide solution at an average of 0.4m (**Figure 26c**). The heave signal did not fluctuate over same temporal period, indicating that issue was not in the motion of the vessel but in the GPS receiving signal. In situations similar to this, GPS tide reduction should not be used in the final solution and should be replaced by traditional tide reduction methods (i.e., observed or predicted tides). If observed tides are not available then BT tide is the next best option, reducing the uncertainty from the PT solution by the standard deviation between the two solutions (PT and BT).

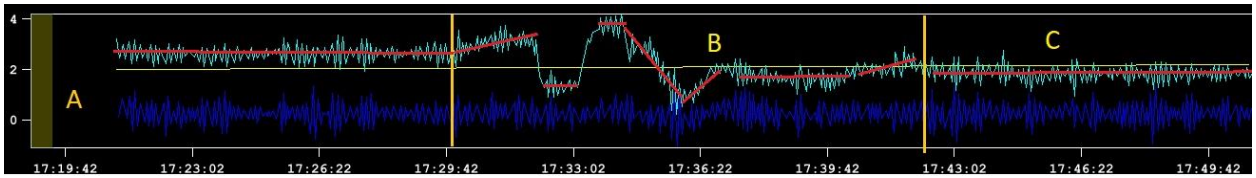

Figure 26. Site Z007-001 (Lancaster Sound) (Line ID 4801_20190902_172106_LSSL) shows highly unstable GPS signal (light blue) in comparison to the vessel heave (dark blue). A) Stable GPS signal but above the BT solution (green horizontal line). B) Highly unstable GPS signal on line. C) Stabilized GPS signal but below the tide BT solution.

3.4.3 Full Surface Comparisons

The final analysis compared the differences between the three solutions spatially for each survey site. Gridded surfaces at site specific resolution were compared, analyzing the absolute mean difference and standard deviation of each paired solution. Of the 12 sites investigated, 7 had a movement in the positive direction better aligning with GPS Tidal reduction solution and 5 had the opposite effect, moving slightly further from the GPS Tidal reduction solution. However, for all 5 that the mean moved further from the GPS comparative surface, the standard deviation decreased. This indicates that although there was an increase in the central tendency of the BT solution, compared to the PT solution, the variability within the BT solution decreased, implying there is slightly less uncertainty in the BT solution. (**Table 12**).

Table 12. Full surface comparisons and the resulting effect of applying ERA5 mean sea level pressure as the vertical reduction technique.

	PT - BT		GPS - PT		GPS - BT		Effect of applying BT
Site ID Number	Mean (abs) (m)	Std Dev.	Mean (abs) (m)	Std Dev.	Mean (abs) (m)	Std Dev.	
Z003-001	0.055	0.141	1.114	0.686	1.169	0.670	Negative
Z004-001	0.021	0.031	0.172	0.220	0.192	0.221	Negative
Z004-002	0.020	0.061	0.460	0.294	0.439	0.306	Positive
Z004-003	0.044	0.060	0.858	0.227	0.813	0.230	Positive
Z007-001	0.055	0.052	0.178	1.165	0.123	1.165	Positive
Z008-001	0.099	0.065	0.872	1.192	0.773	1.193	Positive
Z008-002	0.004	0.059	0.160	0.113	0.165	0.088	Negative
Z008-003	0.000	0.114	0.002	0.142	0.000	0.108	Positive
Z008-004	0.129	0.002	0.097	0.076	0.032	0.076	Positive
Z008-005	0.011	0.067	0.069	0.089	0.080	0.083	Negative
Z008-006	0.009	0.016	1.710	0.542	1.686	0.557	Positive
Z008-007	0.054	0.081	0.360	0.157	0.415	0.143	Negative
AVG	0.042		0.504		0.491		Positive

Site Z008-004 showed the largest mean difference between the PT and BT surfaces at a mean of 0.129 m and a very low standard deviation of only 0.002 m. The difference was reflected when compared to the GPS tide reduced surface, moving the tidal solution to 0.097 m if using the PT solution and further improving the agreement between GPS and BT to 0.032m. Standard Deviation between the means remained identical, highlighting the overall improvement as demonstrated by the superior coupled GPS-BT solution.

The lowest absolute mean difference between the PT and the BT solutions was site Z008-003. This was a result of the barometric pressure cell selected in the analysis at the location the tidal station and then weighted mean averaging over the entirety of the survey site. Standard deviation between the two solutions was 0.114 meters; however, due to the large survey site (841.62 km^2) coupled with the multiple stations tidal stations used, and the small tide range of the area (< 2m in amplitude), the impact was negligible. The Inverse Barometer Effect had a significant impact on the tide range in this region ($p < 0.01$), but this was due to the relatively small LTR. Similarly, the GPS/PT and the GPS/BT comparisons resulted in similar CUBE solutions.

Site Z008-005, Cambridge Bay East, showed that applying barometric pressure to predicted tides from tidal station 6240 (Cambridge Bay) produced slightly poorer results in the compassion to the GPS tide solution. Alternatively, Site Z008-004, Cambridge Bay West, showed the opposite effect, slightly better alignment to the GPS solution. Both of these sites used the same tidal station and the same ERA5 mean sea level pressure data. The cell was centered between the two sites. Cambridge Bay East is geographically in closer proximity to the tide station (**Figure 27**). One would expect Z008-005, being closer to the tidal station would result in a more accurate comparison; however, this was not true.

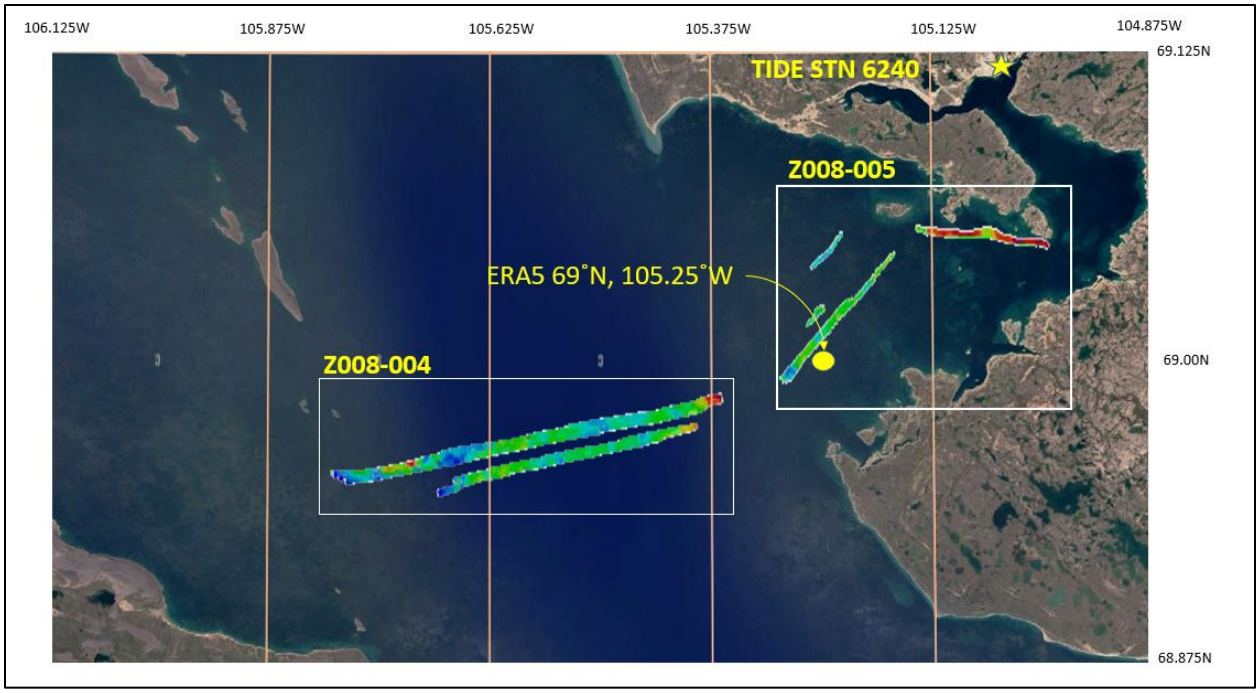

Figure 27. Site locations of Z008-004 (Cambridge Bay West) and Z008-005 (Cambridge Bay East) with a visual display of the ERA5 0.25˚ x 0.25˚ grid (Orange Grid). Final results in the comparison between GPS tidal solutions and the BT solution showed conflicting agreement at both sites.

Z008-004 is open ocean with no shelter from nearby landmasses. Conversely, a large portion of Z008-005 is near shore in shallower waters. Sheltered by landmasses to the north, east and south, other environmental conditions should be considered at this site. Wind setup will have a larger effect on this area compared to the open ocean of Z008-004. Additionally, there may be other influences that affect the height of the water column in the sheltered bay such as sea water density.

The results of the comparisons between the gridded surfaces for all three solutions suggests that at the majority of the sites, improvements can be made to the final solution by applying barometric pressure to the predicted tide record to get better align to theoretical observed tides; however, these results also suggest that it is site specific. This is consistent with the results found in previous studies (Dodd & Mills 2014).

3.5 Conclusion

In this study, we investigated the difference between predicted tides and the enhancement of predicted tides by incorporating mean sea level pressure (barometric pressure) from the ERA5 dataset. Our results demonstrated that including barometric pressure in the prediction models improved the agreement to ERS vertical reduction technique solutions in 7 of the 12 test sites. This suggests that applying external environmental variables can be a valuable variable to consider during hydrographic surveying when GPS signal degrades or drops out in high latitude regions.

Isolating the effects of barometric pressure from other environmental variables proved to be site specific. The influence of barometric pressure on the height of water relative to chart datum was found to be significant ($p < 0.01$) in regions with relatively small tidal signatures (< 2 m). In large tidal regions, the impact would not make a significant impact ($p > 0.4$) The influence of the barometric pressure corrections at the decimeter level would not have significant impact in deep waters; however, where under keel clearance is critical such as ports or shallow navigational channels, coupled with small tidal areas, the decimeter level impact becomes increasingly critical.

Theoretical observed tides at the survey locations are ideal for comparison to ERS surveys. Concern should be considered when using predicted tides alone, as harmonic analysis of the sinusoidal signature does not account for in-situ environment or oceanographic conditions. Additionally, the length of tidal predictions observation period have an influence on the overall quality of the derived tidal predictions, and are only valid at the station where they were surveyed. The quality of the tidal predictions degrade at further distance from the location of observation, increasing the uncertainty.

Assessing the impact of incorporating barometric pressure on predicted tides, we used validated ERS reduced hydrographic products to compare and contrast the differences between predicted tides and barometric pressure enhanced predicted tides. By comparing the accuracy of tide predictions with and without barometric pressure, we were able to determine the extent to which this variable influenced the final solutions.

Our findings revealed that including barometric pressure in the tidal prediction models resulted in improved accuracy at 58% of the test sites. This indicates that barometric pressure can provide valuable information that adds to existing tidal predictions. The inclusion of this variable allows

for a more comprehensive understanding of the factors that influence tides and provides more precise predictions. It is important to note that the effectiveness of incorporating barometric pressure varied across the test sites. While seven sites demonstrated improved accuracy, the remaining five sites failed to show any significant improvement. This suggests that the influence of barometric pressure on tidal behavior may be site-specific and local factors need to be considered. Therefore, using specific characteristics for each location would be beneficial when developing tide prediction models that incorporate barometric pressure.

It is important to recognize the limitations of our study. First, the analysis held ERS reduced surveys as the baseline of comparison, and the performance of the prediction models may vary in real-time scenarios. Second, our study focused on a limited number of test sites with a wide range of conditions including varying depths, varying proximity to landmasses, sheltered vs non-sheltered sites among others. Third, our study used a single ERA5 data point contributor with a centroid node close to the center of the survey site at all but two of the sites. At those two sites, weighted mean averaging was used where the ERA5 data was extracted at the node with the closest proximity to the tidal stations. Further studies should incorporate gridded time-series ERA5 data covering the entire extent of the survey site, not just a single node.

Other variables such as sea water density and wind setup should be investigated to further improve the accuracy of tide predictions. These factors can significantly impact tidal behavior and may provide additional insights for predictive models. Future research should aim to incorporate these variables and assess their influence on tide predictions. Exploring the combined effects of multiple variables could potentially lead to more accurate and reliable tide predictions. We recommend that future research is conducted to investigate the influence of wind set and sea water density on the overall height of the water column in comparison to predicted tides. ERS should continue to record real-time heave to assist in quality control the GPS height signal as this will have direct implications for the GPS tide solution and identify where drop out or signal degradation occurs, ultimately identifying survey lines that should be replaced by traditional tidal reduction methods. If observed tides is not available then BT tide is the next best option, reducing the uncertainty from the PT solution by the standard deviation between the two solutions (PT and BT).

Additional research should be conducted to investigate the differences seen between near shore, restricted waterways compared to open ocean sites. Special attention should be given to areas

where under keel clearance is critical, as barometric pressure can significantly change the predicted tide height in low tidal areas, increasing the risk of a marine navigational incident. Furthermore, it is recommended to investigate how observed tides compare to barometric pressure enhanced predicted tides by acquiring in-situ tidal observations in the survey site coupled with barometric pressure observations aboard the acquisition vessel. This will provide a method to validate the ERA5 mean sea level pressure dataset for offshore regions, but also reduce the overall vertical uncertainty of hydrographic surveys, ultimately contributing towards safer marine navigation.

3.6 References

Baker-Yeboah, S., Watts, D. R., & Byrne, D. A. (2009, December). Measurements of Sea Surface Height Variability in the Eastern South Atlantic from Pressure Sensor–Equipped Inverted Echo Sounders: Baroclinic and Barotropic Components. *Journal of Atmospheric and Oceanic Technology*, *26*(12), 2593-2609. doi:10.1175/2009JTECHO659.1

Booij, N., Holtuijsen, L. H., & Ris, R. C. (1997). The "Swan" Wave Model for Shallow Water. *Coastal Engineering 1996-1997.*

Calder, B. R., & Wells, D. E. (2007). *CUBE User's Manual.* Center for Coastal and Ocean Mapping. Retrieved from https://scholars.unh.edu/ccom/1217

Canadian Hdyrographic Service. (2021, March 10). *Standards for Hydrographic Surveys*. Retrieved from Fisheries and Oceans Canada: Canadian Hydrographic Service: https://www.charts.gc.ca/data-gestion/standards-normes/pre-eng.html

Canadian Hydrographic Service. (2017, December 08). *About the Canadian Hydrographic Service*. Retrieved from Department of Fisheries and Oceans Canada: https://www.dfo-mpo.gc.ca/career-carriere/science/chs-shc/index-eng.html

Canadian Hydrographic Service. (2019, November 21). *Why hydrography matters*. Retrieved from Fisheries and Oceans Canada: http://charts.gc.ca/help-aide/about-apropos/index-eng.html

Canadian Hydrographic Service. (2023, June 19). *Tidal and water level stations*. Retrieved from Tides, Currents, and Water Levels: https://www.tides.gc.ca/en/stations

Canandian Hydrographic Service. (2022, January 27). *Definitions for content on tides and currents*. Retrieved from Tides, Currents, and Water Levels: https://tides.gc.ca/en/definitions-content-tides-and-currents

Cartwright, D. E., & Edden, A. C. (1973, September 1). Corrected Tables of Tidal Harmonics. *Geophysical Journal International, 33*(3), 253-264. doi:10.1111/j.1365-246X.1973.tb03420.x

Chuang, W.-S., & Wang, D.-P. (1981, October). Effects of Density Front on the Generation and Propagation of Internal Tides. *American Meteorological Society, II*, 1357-1374.

Chuang, W.-S., & Wang, D.-P. (1981, October). Effects of Density Front on the Generation and Propagation of Internal Tides. *American Meteorological Society, II*, 1357-1374. doi:10.1175/1520-0485(1981)011<1357:EODFOT>2.0.CO;2

Costello, Mark. (2019, March 1). *The ocean floor is less well mapped than the surface of other planets'.* Retrieved from the University of Auckland New Zealand: https://www.oceansofbiodiversity.auckland.ac.nz/2019/03/23/the-ocean-floor-is-less-well-mapped-than-the-surface-of-other-planets/

Dauginis, A. A., & Brown, L. C. (2021). Recent changes in pan-Arctic sea ice, lake ice, and snow-on/off timing. *The Cryosphere, 15*, 4781-4805. doi:10.5194/tc-15-4781-2021

Department of Fisheries and Oceans. (2023, March 28). *Canadian Tide and Current Tables.* Retrieved from Fisheries and Oceans Canada - Canadian Hydrographic Service: https://charts.gc.ca/publications/tables-eng.html

Dodd, D., & Mills, J. (2014, May). *FIG Publication No. 62 - Ellipsoidally Referenced Surveying for Hydrography*. Retrieved from International Federation of Surveyors (FIG): https://www.fig.net/resources/publications/figpub/pub62/Figpub62.pdf

Doodson, T. (1921, December 1). The harmonic development of the tide-generating potential. *Proceedings of the Royal Society A - Mathematical, Physical and Engineering Sciences, 100*(704). doi:10.1098/rspa.1921.0088

Ducarme, B. (2009, December 15). Limitations of High Percision Tidal Prediction. *Marees Terrestres Bulletin D'Informations*, pp. 11663-11678.

Fagherazzi, S., & Wiberg, P. L. (2009, September). Importance of wind conditions, fetch, and water levels on wave-generated shear stresses in shallow intertidal basins. *Journal of Geophysical Research: Earth Science, 114*(F3). doi:10.1029/2008JF001139

Foreman, M. G., & Henry, R. F. (1989). The harmonic analysis of tidal model time series. *Advances in Water Resources, 12*(3), 109-120. doi:10.1016/0309-1708(89)90017-1

Forrester, W. D. (1983). *Canadian Tidal Manual.* Ottawa: Department of Fisheries and Oceans.

Fu, L. L., & Pihos, G. (1994). Determining the response of sea level to atmposheric pressure forcing using TOPEX/POSEIDON data. *Journal of Geophysical Research: Oceans*, 24633-24642.

Godin, G. (1973). *The analysis of tides.* Toronto: University of Toronto.

Gregory, J. M., Griffies, S. M., Hughes, C. W., Lowe, J. A., Church, J. A., Fukimori, I., . . . van de Wal, R. S. (2019, April 29). Concepts and Terminology for Sea Level: Mean, Variability and Change, Both Local and Global. *Surveys in Geophysics*, 1251-1289.

Hamon, B. V. (1966, June 15). Continental shelf waves and the effects of atmospheric pressure and wind stress on sea level. *Journal of Geophysical Research, 71*(12), 2883-2893. doi:10.1029/JZ071i012p02883

Hersbach, H., Bell, B., Berrisford, P., Biavati, G., Horányi, A., Muñoz Sabater, J., . . . Thépaut, J.-N. (2018). *ERA5 hourly data on single levels from 1979 to present*. Retrieved March 25, 2020, from Copernicus Climate Change Service (C3S) Climate Data Store (CDS): https://cds.climate.copernicus.eu/cdsapp#!/dataset/reanalysis-era5-single-levels?tab=form

Hersbach, H., Bell, B., Berrisford, P., Horányi, A., Sabater, J. M., Nicolas, J., . . . Dee, D. (2019, April). *Global reanalysis: goodbye ERA-Interim, hello ERA5.* Retrieved from ECMWF: https://www.ecmwf.int/en/newsletter/159/meteorology/global-reanalysis-goodbye-era-interim-hello-era5

Hibbert, A., Royston, S. J., Horsburgh, K. J., Leach, H., & Hisscott, A. (2015). An empirical approach to improving tidal predictions using recent real-time tide gauge data. *Journal of Operational Oceanography, 8*(1), 40-51. doi:10.1080/1755876X.2015.1014641

International Hydrographic Organization. (2018, January). *International Hydrographic Organization ENC Creation.* Retrieved from Intarnational Hydrographic Organization: https://iho.int/iho_pubs/standard/S-57Ed3.1/S-57%20Appendix%20B.1%20Annex%20A%20UOC%20Edition%204.1.0_Jan18_EN.pdf

International Hydrographic Organization. (2020, September). *S-44 Standards for Hydrographic Surveys ed. 6.0.0.* Retrieved from International Hydrographic Organization: https://iho.int/uploads/user/pubs/standards/s-44/S-44_Edition_6.0.0_EN.pdf

International Hydrographic Organization. (2020, September). *Standards and Specificaitons: S-67.* Retrieved from International Hydrographic Organization: https://iho.int/uploads/user/pubs/standards/S-67/S-67%20Ed%201.0.0%20Mariners%20Guide%20to%20Accuracy%20of%20Depth%20Information%20in%20an%20ENC_EN.pdf

IPCC. (2019). *IPCC Special Report on the Ocean and Cryosphere in a Changing Climate.* In Press: Intergovernmental Panel on Climate Change.

Kurapov, A. L., Allen, J. S., & Egbert, G. D. (2010, April). Combined Effects of Wind-Driven Upwelling and Internal Tide on the Continental Shelf. *American Meteorolgical Society, 40*, 737-756. doi:10.1175/2009JPO4183.1

LINZ. (2015, December 21). *Meteorological effects on tides*. Retrieved from Land Information New Zealand: https://www.linz.govt.nz/sea/tides/introduction-tides/meteorological-effects-tides

MacGougan, G., Lachapelle, G., & Nayak, R. (2001). Overview of GNSS signal degradation phenomena. *e International Symposium on Kinematic Systems in Geodesy*, (pp. 87-100). Banff, Canada.

Miller, A. R. (1958, January). The effects of winds on water levels on the New England Coast. *Limnology and Oceanography, 3*(1), 1-14.

Moore, G. W., & McNeil, K. (2018, August 13). The Early Collapse of the 2017 Lincoln Sea Ice Arch in Response to Anomalous Sea Ice and Wind Forcing. *Geophysical Research Letters, 45*(16), 8343-8351. doi:10.1029/2018GL078428

Mudryk, L. R., Dawson, J., Howell, S. E., Derksen, C., Zagon, T. A., & Brady, M. (2021, July 8). Impact of 1, 2 and 4 °C of global warming on ship. *Nature Climate Change, 11*, 673-679. doi:10.1038/s41558-021-01087-6

Nagano, A., & Wakita, M. (2019, August 30). Wind-driven decadal sea surface height and main pycnocline depth changes in the western subarctic North Pacific. *Progress in Earth and Planetary Science, 6*(59). doi:10.1186/s40645-019-0303-0

National Oceanic and Atmospheric Adminsitration. (2017, August 13). *Tides and Water Levels*. Retrieved from National Ocean Service: https://oceanservice.noaa.gov/education/tutorial_tides/tides08_othereffects.html

Natural Resources Canada. (2021, April 9). *About the Canadian Spatial Reference System*. Retrieved from Natural Resources Canada: https://natural-resources.canada.ca/maps-tools-and-publications/tools/geodetic-reference-systems/canadian-spatial-reference-system-csrs/9052

Natural Resources Canada. (2022, November 3). *Spatial reference system updates*. Retrieved from Natural Resources Canada: https://natural-resources.canada.ca/maps-tools-and-publications/geodetic-reference-systems/height-reference-system-modernization/9054

Office of Geomatics. (2023, March 14). *World Geodetic System 1984 (WGS 84)*. Retrieved from Office of Geomatics: https://earth-info.nga.mil/index.php?dir=wgs84&action=wgs84

Pizzolato, L., Howell, S. E., Derkesn, C., Dawson, J., & Copland, L. (2014). Changing sea ice conditions and marine transportation activity in Canadian Arctic waters between 1990 and 2012. *Climatic Change*(123), 161-173. doi:10.1007/s10584-013-1038-3

Planck, C. J., Whitlock, J., Polashenski, C., & Pervovich, D. (2019, September). The evolution of the seasonal ice mass balance buoy. *Cold Regions Science and Technology, 165*. doi:10.1016/j.coldregions.2019.102792

Ponte, R. M. (1994, April 15). Understanding the relation between wind- and pressure-driven sea level variability. *Journal of Geophyscial Research: Oceans, 99*(C4), 8033-8039. doi:10.1029/94JC00217

Ponte, R. M., & Joël, D. (2003, February 01). Uncertainties in ECMWF Surface Pressure Fields over the Ocean in Relation to Sea Level Analysis and Modeling. *Journal of Atmospheric and Oceanic Technology*, 301-307. doi:10.1175/1520-0426(2003)020<0301:UIESPF>2.0.CO;2

Postlethwaite, C. F., Morales Maqueda, M. A., le Fouest, V., Tattersall, G. R., Holt, J., & Willmott, A. J. (2011). The effect of tides on dense water formation in Arctic shelf seas. *Ocean Science, 7*, 203-217. doi:10.5194/os-7-203-2011

Robin, C., Nudds, S., MacAulay, P., Godin, A., De Lang Boom, B., & Bartlett, J. (2016). Hydrographic Vertical Separation Surfaces (HyVSEPs) for the Tidal Waters of Canada. *Marine Geodesy*, *39*(2). doi:10.1080/01490419.2016.1160011

Robin, C., Nudds, S., MacAulay, P., Godin, A., De Lange Boom, B., & Bartlett, J. (2016). Hydrographic Vertical Separation Surfaces (HyVSEPs) for the Tidal Waters of Canada. *Marine Geodesy, 39*(2), 195-222. doi:10.1080/01490419.2016.1160011

Roquet, F., Madec, G., McDougall, T. J., & Barker, P. M. (2015). Accurate polynomial expressions for the density and specific volume ofseawater using the TEOS-10 standard. *Ocean Modelling*, 29-43.

Rusu, L., & Soares, C. G. (2015, December). Impact of assimilating altimeter data on wave predictions in the western Iberian coast. *Ocean Modelling, 96*(1), 126-135. doi:10.1016/j.ocemod.2015.07.016

Saha, S., Moorthi, S., Wu, X., Wang, J., Nadiga, S., Tripp, P., . . . Becker, E. (2014). The NCEP Climate Forecast System Version 2. *Journal of Climate, 27*, 2185-2208.

Schädel, C. (2022, February 14). Arctic Coasts Predicted to Erode. *Nature Climate Change, 12*, 224-225.

Smith, S. M. (2016, November). Contributions of recent barometric pressure trends to rates of sea level rise in southeastern Massachusetts (USA). *Reginal Studies in Marine Science, 8*(1), 41-50. doi:10.1016.j.rsma.2016.09.005

Tulaktarvik Inc. (2014, May 14). *Tulaktarvik: Submission to the Tanker Safety Expert Panel (Phase II - 'North of 60').* Retrieved from Transport Canada: https://www.tc.gc.ca/media/documents/mosprr/Tulaktarvik_and_Ocean_Group.pdf

USACE. (1984). *Shore protection manual.* Vicksburg, Mississipi: Coastal Engineering Research Cener. Retrieved from http://ft-sipil.unila.ac.id/dbooks/S%20P%20M%201984%20volume%201-1.pdf

Vandam, T. M., & Wahr, J. (1993, April 1). The Atmospheric Load Response of the Ocean Determined Using Geosat Altimeter Data. *Geophysical Journal International, 113*(1), 1-16.

Vivier, F., Kelly, K. A., & Thompson, L. (1999, September 15). Contributions of wind forcing, waves, and surface heating to sea surface height observations in the Pacific Ocean. *Journal of Geophysical Research, 104*(C9). doi:10.1029/1999JC900096

Wolski, T., Wiśniewski, B., Giza, A., Kowalewska-Kalkowska, H., Boman, H., Grabbi-Kaiv, S., . . . Lydeikaitė, Ž. (2014). Extreme sea levels at selected stations on the Baltic Sea coas. *Oceanologia, 56*(2), 259-290. doi:10.5697/oc.56-2.259

Wunsch, C., & Stammer, D. (1997, February). Atmospheric loading adn the oceanic "inveted barometer" effect. *Review of Geophysics, 35*(1), 79-107. doi:10.1029/96RG03037

Chapter 4

4 Conclusions

This study has examined the extent of seafloor coverage and bathymetric gaps within Canada's exclusive economic zone, setting a baseline for future reporting on the progress toward complete seafloor coverage. Additionally, this study examined the influence of applying mean sea level pressure (barometric pressure) from ERA5 reanalysis dataset on harmonic analysis predicted tide to the vertical reduction of hydrographic surveys. Overall, findings on both topics are promising. Continued work will be greatly facilitated by in-situ barometric pressure data during hydrographic survey operations to validate and verify ERA5 reanalysis data. Further oceanographic and environmental variables should be considered, which can be extracted from ERA5 reanalysis data.

Firstly, this work developed a method to assess, classify and quantify bathymetric gaps from the full catalogue of the Canadian Hydrographic Service's digital bathymetric inventory. Previous methods from both global (Weatherall, et al., 2015) (Mayer, et al., 2018) and national (Westington, et al., 2018) (Dias, 2021) scales were examined to ensure reporting terminology and cohesion with neighboring nations could be achieved. Applying sounding density methods to align with the United States of America's National Oceanographic and Atmospheric Administration's analysis will allow for ease of bi-national reporting in shared marine areas such as the Great Lakes and St. Lawrence River as well as the eastern and western seaboards.

The establishment of the raster-based Canadian Bathymetric Gap Analysis epoch 2023 (CBGAe2023) will allow for year-over-year comparisons to show progress in seafloor coverage in Canadian waters and act as an additional layer of information to assist in hydrographic survey planning if ingested into the CHS's priority planning tool (Chénier et al., 2018). The results of CBGAe2023 highlighted massive gaps in seafloor coverage in all regions; however, this was amplified in the Canadian Arctic, particularly the Western Arctic due to the transiting route of the Canadian Coast Guard icebreaker program. CBGAe2023 results showed that Canada has 15.11% of its seafloor containing at least a single depth measurement at a 100 m resolution. Furthermore,

results showed that 13.45% (790,690 km^2) was classified as full bottom coverage, largely due to modern technological advancements such as multibeam echo sounders and Light Detection and Ranging (LiDAR) technologies.

This study's methodology also improved seafloor coverage reporting highlighting the overestimation by the Department of Fisheries and Oceans Canada within its predefined low impact shipping corridor by 14.77% (89,880 km^2). Furthermore, the results highlighted implications for Lakebed 2030 initiative, showing large gaps in the Great Lakes region as well. The GBGAe2023 results demonstrate 25.69% (23,332 km^2) of Canadian waters in the Great Lakes contain a sounding at a 100-metre resolution. Assuming a similar rate to NOAA's seafloor coverage acquisition efforts of 1.5% (74,873 km^2) increase per year, we can predict that Canada will exceed both Seabed 2030 and Lakebed 2030 target to acquire 100% coverage, whereby Canada can expect to acquire 100% coverage by 2079.

Chapter 3 investigated the potential enhancement of predicted tides by incorporating mean sea level pressure (barometric pressure) data from the ERA5 dataset. We found that including barometric pressure in the prediction models significantly improved the agreement with ellipsoid referenced surveys (ERS) vertical reduction technique solutions in 7 out of 12 test sites. This suggests that external environmental variables, such as barometric pressure, can be valuable considerations during hydrographic surveying, particularly in high latitude regions where GPS signals may degrade or drop out.

The impact of barometric pressure on tidal height was found to be significant in regions with relatively small tidal signatures (less than 2 meters), while in large tidal regions, it did not make a notable difference. However, in areas with shallow waters, such as ports or navigational channels, and combined with small tidal ranges, the impact of barometric pressure corrections became increasingly critical for under keel clearance.

Our study highlights that relying solely on predicted tides without considering in-situ environmental or oceanographic conditions can lead to inaccuracies. Harmonic analysis of sinusoidal tidal signatures may not account for these factors, and tidal predictions are only valid at the specific survey location, degrading in accuracy further away from the observation point.

Incorporating barometric pressure in the tidal prediction models improved accuracy at 58% of the test sites, but the effectiveness varied across locations. Specific characteristics of each site need to be considered when developing tide prediction models that include barometric pressure.

Furthermore, we acknowledge some limitations in our work, such as using ERS reduced surveys as the baseline of comparison, which may not fully represent real-time scenarios. Additionally, the study focused on a limited number of test sites with various conditions, and future research should encompass a wider range of locations and conditions. Moreover, using gridded time-series ERA5 data covering the entire survey site, not just a single node, would be more comprehensive.

Future research should investigate other variables such as sea water density and wind setup, as they can also influence tidal behavior and contribute to more precise tide predictions. Combining multiple variables in predictive models may lead to further improvements. Recommendations for future research include investigating the influence of wind set and sea water density on water column height in comparison to predicted tides, and continuing to record real-time heave data to improve GPS tide solutions. Near shore and open ocean sites should be compared, with special attention to areas where under keel clearance is critical. In-situ tidal observations coupled with barometric pressure measurements aboard the acquisition vessel can provide validation for the ERA5 mean sea level pressure dataset.

4.1 References

Chénier, R., Abado, L., & Martin, H. (2018). CHS Priortiy Planning Tool (CPPT) - A GIS Model for Defining Hydrographic Survey and Charting Priorities. *International Journal of Geo-Information, 7*(240). doi:https://doi.org/10.3390/ijgi7070240

Dias, T. G. (2021, May 31). Program Seamap 2030 - 100% of the Portuguese maritime spaces mapped by 2030. *International Hydrographic Review, 27*. Retrieved from https://ihr.iho.int/articles/program-seamap-2030-100-of-the-portuguese-maritime-spaces-mapof-the-portuguese-maritime-spaces-mapped-by-2030/

Mayer, L., Jakobsson, M., Allen, G., Dorschel, B., Falconer, R., Ferrini, V., . . . Weatherall, P. (2018, February 8). The Nippon Foundation - GEBCO Seabed 2030 Project: The Quest to See the World's Oceans Completely Mapped by 2030. *Geosciences*, *8*(2). doi:10.3390/geosciences8020063

Weatherall, P., Marks, K. M., Jakobsson, M., Schmitt, T., Tani, S., Arndt, E., . . . Wigley, R. (2015, June 29). A new digital bathymetric model of the world's oceans. *Earth and Space Science*. doi:https://doi.org/10.1002/2015EA000107

Westington, M., Varner, J., Johnson, P., Sutherland, M., Armstrong, A., & Jencks, J. (2018). Assessing Sounding Density for a Seabed 2030 Initiative. *2018 Joint Canadian Hydrographic and National Surveyors' Conference.* Victoria, British Columbia. Retrieved from https://www.eiseverywhere.com/ehome/chc-nsc2018/711593/

Appendices

Appendix 1 – List of Acronyms

BDB	Bathymetric Database
BT	Barometric pressure enhanced predicted Tide
CAEAC	Canada Albers Equal Area Conic
CATZOC	Category Zone of Confidence
CBGAe2023	Canadian Bathymetric Gap Analysis epoch 2023
CD	Chart Datum
CFSRv2	Climate Forecast System Reanalysis version 2
CGG	Canadian Coast Guard
CHS	Canadian Hydrographic Service
CM	Continuous Maintenance
CPPT	Canadian Hydrographic Service's Priority Planning Tool
CSAR	CARIS Spatial Archive Raster
CUBE	Combined Uncertainty and Bathymetric Estimator
CV	Comparative Validation
DEM	Digital Elevation Model
DEW	Distant Early Warning System
DFO	Department of Fisheries and Oceans Canada
ECCC	Environment and Climate Change Canada
ECWMF	European Center for Medium-Range Weather Forecasts
EEZ	Exclusive Economic Zone
ERA5	European Center for Medium-Range Weather Forecasts Reanalysis v5 dataset
ERS	Ellipsoidal Referenced Survey
FIG	Federation of International Surveyors
GEBCO	General Bathymetric Chart of the Oceans
GIS	Geographic Information System
GLOS	Great Lakes Observing System
GNSS	Global Navigation Satellite System
GPS	Global Positioning System
GPS Tide	Global Positioning System tide reduction method
GRS80	Geodetic Reference System of 1980
HyVSEP	Hydrographic Vertical Separation Model
IBCAO	International Bathymetric Chart of the Arctic Ocean
IBE	Inverse Barometer Effect
IH	Instituto Hidrográfico (Portuguese Hydrographic Office)
IHO	International Hydrographic Organization
IMU	Inertial Motion Unit
ITRF08	International Reference Frame of 2008
LiDAR	Light Detection and Ranging
LISC	Low Impact Shipping Corridor

LLT	Larger Large Tide
LLWLT	Lower Low Water Large Tide
LTR	Large Tide Range
MBES	Multibeam Echosounder
MLV	Multibeam, LiDAR, Vertically sweep system
M-QUAL	Metadata on the quality of the data
NAD83	North American Datum of 1983
NAD83(CSRS)	North American Datum of 1983 - Canadian Spatial Reference Frame
NCEP	National Climate Environmental Prediction
NMTC	Northern Marine Transportation Corridor
NOAA	National Oceanic and Atmospheric Administration
OAT	Other Acquisition Techniques
OPP	Oceans Protection Plan
PT	Predicted Tide
RP	Reference Point
RSME	Root Square Mean Error
SBES	Singlebeam Echosounder
SRTM	Satellite Radar Topography Mission
SSH	Sea Surface Height
SWAN	Simulating Waves Nearshore model
TECSOU	Technique of Soundings Acquisition
TPU	Total Propagated Uncertainty
VR	Variable Resolution
WGS84	World Geodetic System of 1984